Microalgal wastewater treatment, enhanced biomass productivity, and biofuel conversion under a biorefinery approach

A Thesis

Submitted in Partial Fulfillment of the Requirements for the Degree of

DOCTOR OF PHILOSOPHY

by

Sanjeev Mishra

(146151004)

School of Energy Science and Engineering

Indian Institute of Technology Guwahati

Guwahati - 781039, Assam (India)

June 2021

This thesis is dedicated to my Parents who have inspired me and made me strong enough to achieve my goal

School of Energy Science and Engineering

INDIAN INSTITUTE OF TECHNOLOGY GUWAHATI

STATEMENT

I do hereby declare that the content embodied in this thesis entitled *"**Microalgal wastewater treatment, enhanced biomass productivity, and biofuel conversion under a biorefinery approach**"* is the result of investigations carried out by me at the School of Energy Science and Engineering, Indian Institute of Technology Guwahati, Guwahati, India, under the guidance of **Prof. Kaustubha Mohanty**.

In keeping with the general practice of reporting scientific observations, due acknowledgements have been made wherever the work described is based on the findings of other investigators.

Sanjeev Mishra

13 July, 2021 **Sanjeev Mishra**

School of Energy Science and Engineering

INDIAN INSTITUTE OF TECHNOLOGY GUWAHATI

CERTIFICATE

This is to certify that **Mr. Sanjeev Mishra** has been working under my supervision since July 2014. I hereby forward his thesis entitled ***"Microalgal wastewater treatment, enhanced biomass productivity, and biofuel conversion under a biorefinery approach"*** to be submitted for the award of the degree of Doctor of Philosophy to IIT Guwahati. I certify that he has fulfilled all the requirements according to the rules of this institute and the investigations embodied in his thesis have not been submitted elsewhere for a degree or diploma.

Dr. Kaustubha Mohanty

Date: 14.07.2021

Professor of Chemical Engineering and Head,
School of Energy Science and Engineering,
Indian Institute of Technology Guwahati

Acknowledgement

I would like to take this opportunity to express my heart-felt gratitude to them, whose contribution has made this thesis possible.

In particular, the foremost appreciation goes to my supervisor Prof. Kaustubha Mohanty for his consistent guidance throughout the research work that had enabled to pursue my academic skills under his precious supervision and expertise. I thank him along with his family members for their encouragements and moral supports throughout my research tenure at IIT Guwahati.

I would like to acknowledge my sincere gratitude to my doctoral committee members, Prof. Arun Goyal, Prof. Niranjan Sahoo, and Prof. Chandan Das, for their insightful advices and suggestions throughout the research.

My sincere thanks to Prof. Pranab Goswami and Prof. Vijay S. Moholkar, former Head, Centre for Energy, for their moral support and inspiration. I would also like to convey my sincere thanks to the Head of Central Instruments Facility (CIF), IIT Guwahati, for providing me the analytical facilities of CIF. I am also grateful to Dr. Pankaj Kalita and all the staff members of Centre for Energy and Department of Chemical Engineering.

I would also like to thank my teachers and former research guides, Dr. S. Anbuselvi and L. Jeyanthi Rebecca (Bharath University), Dr. Sudhamoy Mandal (ICAR-NRRI), Mr. Lala Behari Sukla (CSIR-IMMT), Dr. Prasanna Kumar Panda (CSIR-IMMT), Dr. M. T. Arasu (CSIR-IMMT), Dr. Anil Kumar Sarma and Dr. Sachin Kumar (SSS-NIBE) for their consistent support throughout my research carrier.

I am indebted to the selfless help and co-operation of my Research group members Dr. Krushna Prasad Shadangi, Dr. Himadri Sahu, Dr. Sanjukta Bhoi, Dr. Madhusmita Dash, Proloy Das, Dr. Kulbhushan Samal, Dr. Ranjeet Kumar Mishra, Dr. Rahul Maurya, Dr. Saran Sarangapany, Dr. Sounak Bera, Bikashbindu Das, Naveenkumar A Yaranal, Aanisha Akhtar, Harsh Vardhan, Om Prakash, Ananya Bardhan, Janaki Komandur, Santosh Kumar Hotta, Barasa Malakar, Pranab Jyoti Sarma, Sachankar Buragohain, Madonna Roy, Munmi Bhattacharya, Deepesh Singh Chohan, Saptaswa

Biswas, Ankit Agarwal, Bibek Mishra, Madhurima Nandi, and Maskura Hasin. I would also like to acknowledge the support and encouragement of Dr. Muthusivaramapandian Muthuraj, Dr. Pyarimohan Dehury. I am also thankful to all my seniors and friends Paddu, Bidhu, Sushil, Shweta, Naresh, Sikha, Aslam Bhaijan, Balwant Ji, Neetu, Shuvashish bhai, Paul Ji, Nilesh, Richa, and Mani for their constant help and motivation in each and every stage of the work.

I would also like to thank Ministry of Human Resource Development (MHRD) for providing fellowship and Council of Scientific and Industrial Research (CSIR), Indo-German Centre for Sustainability (IGCS), German Academic Exchange Service (DAAD), Science and Engineering Research Board (SERB), The Biotech Research Society (BRSI) for providing financial assistance for national and international training and conference.

Last but not the least, I express my deepest sense of gratitude to my parents and wife, for their patience, endless support and inspiration towards the completion of my Ph.D thesis. I extend my sincere thanks to all my dear friends and well-wishers who had consistently supported and encouraged me, without which this work would have never been completed. My sincere apology goes to them whom I forget to mention but helped me at any part of the research work.

Thank you all!!

Sanjeev Mishra

ABSTRACT

In view of globalization and energy consumption, an economic and sustainable biorefinery model is essential to address energy security and climate change. From this perspective, renewable biofuel production from microalgae, along with a wide range of value-added co-products, defines its potential as a biorefinery feedstock. However, the economic viability of microalgal biorefinery at its current state is not considered sustainable. To address this challenge, the present study aims to develop a sustainable biorefinery model that includes the production of microalgal biomass using wastewater, conversion of biomass to biofuel via chemical and thermochemical process, and valorization of waste to produce co-products. In the present study, domestic sewage wastewater (DSW) was used as microalgal growth media. From DSW, eight native microalgal strains were isolated, and their screening study was performed using raw DSW (RDSW) and autoclaved DSW (ADSW). The study confirmed RDSW as a potential growth medium while *Monoraphidium* sp. KMC4 showed superior biomass (1.47 ± 0.08 g L^{-1}) and lipid (436 ± 0.06 mg L^{-1}) yield. The corresponding values for bioremediation of ammonia, nitrate, phosphate, and COD remained within 88-100%. The CHNS, biochemical, TGA, FTIR, FAME analysis of

KMC4 confirmed its potential as a bioenergy feedstock. Microalgal growth factors were optimized in flask and scaled-up in 25 L flat-panel indoor photobioreactor to enhance the biomass yield. The study showed the optimal culture condition of KMC4 in PBR includes a supplement of 1.25 g L^{-1} nitrate, 30 mg L^{-1} phosphate, and 25 ℃ culture temperature, 15% inoculum, and a combination of 250-500 µmol m^{-2} s^{-1} and 2-4% of light intensity and CO_2, respectively. At optimized conditions, KMC4 resulted in 2.49 ± 0.07 g L^{-1} of biomass yield, which was ~44.97% superior to the unoptimized PBR and 8% superior to the optimized flask study. Considering the scalability potential of KMC4, the batch study was further optimized under fed-batch and semi-continuous mode of cultivation in PBR. The obtained biomass at the end of both processes was 3.62 ± 0.1 g L^{-1} and 6.14 g L^{-1} in fed-batch and semi-continuous mode, respectively.

The availability of microalgal biomass feedstock in all seasons is a significant challenge that affects the sustainability of the biorefinery. Addressing this challenge, the present study developed co-hydrothermal liquefaction (Co-HTL) process using two different feedstocks, such as KMC4 biomass and domestic sewage sludge (DSS). During this, reaction parameters were optimized, and comprehensive characterization of biocrude was performed. The study showed that Co-HTL at optimum operating conditions of 325 °C, 75:25 wt% (KMC4:DSS), and 45 min resulted in 39.38 wt% biocrude yield at a conversion of 83.96 wt%. The optimum biocrude yield was 16% and 79% higher than the individual HTL of KMC4 and DSS, respectively. The comprehensive characterizations of Co-HTL biocrude showed 76.77%, 10.6%, 8.85%, 3.38% of C, H, N, O, and 39.47 MJ Kg^{-1} HHV with an energy recovery rate of 77.53%. Meanwhile, Co-HTL enhanced the distillation profile of biocrude, which had 10.13% of heavy naphtha, 23.92% of kerosene, and 27.09% of gas oil. The FTIR and GC-MS analysis confirmed that the Co-HTL biocrude had superior hydrocarbons such as alcohols and esters with limited nitrogen and oxygen heterocyclic compounds. Besides, ICP-AES demonstrated a significant decrease in the transfer of mineral elements from the Co-HTL feedstock to biocrude.

The last study was focused on valorizing solid residue and liquid effluent erived from the biofuel conversion process under the circular bioeconomy model. The lipid-extracted microalgal biomass (LEMB) was processed for hydrochar production

via hydrothermal carbonization (HTC). At optimal reaction conditions (temp 225 ℃ and time 60 min), 55 ± 2 wt% hydrochar yield was estimated that had a HHV of 29.77 MJ Kg^{-1} with an energy densification ratio of 1.53. Similarly, a comprehensive characterization of solid residue and liquid effluent of the Co-HTL process was performed, which showed its potential application to produce value-added co-products.

CONTENTS

LIST OF TABLES

LIST OF FIGURES

Chapter 1

Introduction

1.1. Background

1.1.1. Current world energy scenario

Growing population and urbanization in the recent past has resulted in substantial consumption of carbon-emitting fossil fuels, which are the primary sources of greenhouse gases, and its increased production has significantly affected the environment [1]. Presently, oil, coal, and natural gas derived from the fossil fuels represent the primary energy sources in the world that contribute nearly 80% of the total energy used per year (~570 EJ) (Fig. 1.1a). The consumption of primary energy since 1970 has significantly increased with an approximate from 5-13 billion toe (tonne of oil equivalent) and reached a growth rate of 2.9% last year, which was fastest since 2010 (Fig. 1.1a). Among all, the industrial sector (including the non-combusted use of fuels) currently found consuming around half of all the global energy, whereas the rest being consumed by residential and commercial buildings (29%) and transport (21%). That has further resulted in about 35 Gt global carbon dioxide (CO_2) emission, which has grown at a rate of 2% (British Petroleum (BP) Statistical Review of World Energy 2019).

According to a report by the Ministry of Statistics and Program Implementation (MSPI) GoI, coal and oil are India's primary sources of energy that accounted for 62.92% and 31.26% share of the total energy supply (8,37,370 Kilo Tonne of Oil Equivalent) in 2017-18. As of March 2018, the estimated reserves of coal and crude oil in India were 319.04 billion tonnes (BTs) and 594.49 million tonnes (MTs). Being a developing nation with more than 1.3 billion population, the consumption of coal and oil in 2017-18 has increased at a Compound Annual Growth Rate (CAGR) of 5.01% (896.34 MT) and 4.59% (251.93 MMT), respectively. Besides, India imported

208.27 MTs of coal and 220.43 MTs of crude oil (2017-18) due to a significant depletion of fossil fuel reserves and high ash content in Indian coal. However, the primary energy consumption per capita for the year 2018 was limited to 25 GJ, which is significantly less as compared to the developed countries (120-390 GJ).

The above data suggests that there is a significant need for primary energy sources for the socio-economic development of a nation. This has resulted in the depletion of fossil fuel reservoirs worldwide [3]. More importantly, its substantial consumption is affecting humanity and also the environment through global warming, acid rain, and urban smog [4]. Thus, there is an urgent need to find alternate sources, which will deliver clean, green, and renewable energy.

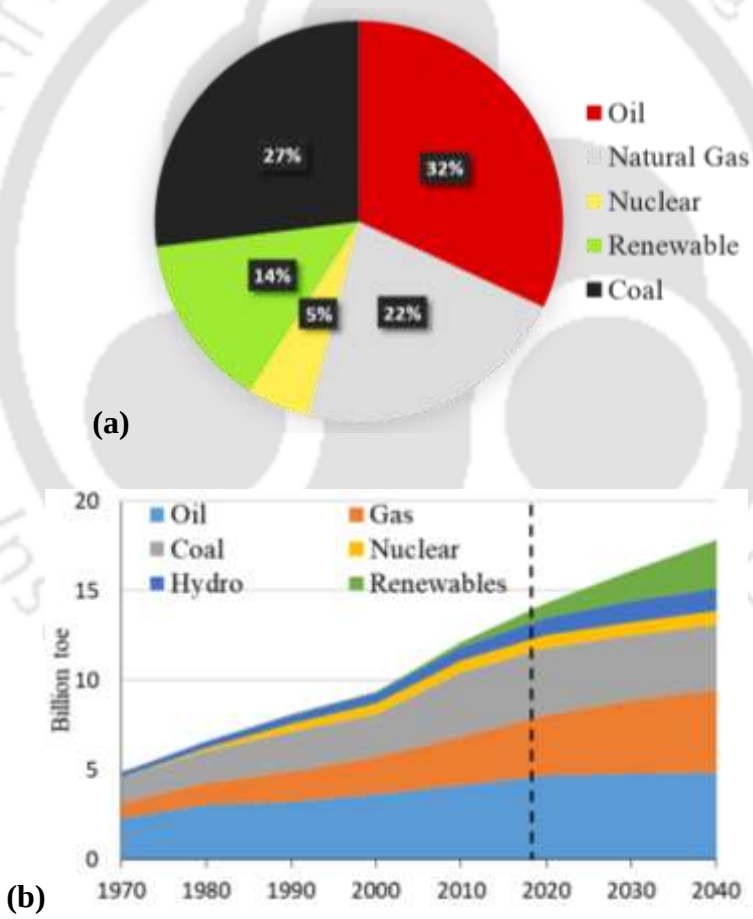

Fig. 1.1. (a) Total energy supply globally in 2016 (Global Bioenergy Statistics reports, 2018), (b) Primary energy consumption by fuel (British Petroleum (BP) Statistical Review of World Energy, 2019).

1.1.2. Renewable energy and its advantages

Renewable energy is collected from renewable sources such as sunlight, wind, geothermal, ocean, and biomass. Due to the replenished nature of renewable sources, it is considered as a sustainable, cost-effective, and environment-friendly alternative that has the potential to replace conventional energy sources in a greater context [2]. Additionally, harvesting energy from renewable sources has almost zero-emissions of both air pollutants and greenhouse gases (GHG). Recently a significant increase in renewable energy production is observed throughout the world. According to the BP Statistical Review of World Energy 2019, renewable energy has grown by 14.5% and currently contributes 14% of the total energy sources (Fig. 1.1b). The growth in renewable energy is dominated by the developing world that includes China, India, and Other Asian countries, accounting for almost half of the growth in global renewable power generation. A recent report addressed the key advantages of a developed renewable energy system that includes [3]:

- Improves energy supply reliability and organic fuel economy.
- Solves problems of local energy and water supply.
- Increases the standard of living and level of employment of the local population.
- Ensures sustainable development of the remote regions in the desert and mountain zones.
- Implementations of the obligations of the countries about fulfilling the international agreements relating to environmental protection.

Besides several advantages and sustainable applications, renewable energy has quite a few challenges and limitations. The technologies are more expensive than the traditional energy systems for which certain tax credits and rebates are provided to alleviate the initial cost. The energy production is not uniform throughout the years due to the non-availability of these renewable energy resources year-around (sunlight, wind, and tides are season-specific). Thus, the solution to the intermittency of energy resources is to use large-scale storage facilities and maintain a consistent energy supply. However, storage technologies are expensive and have limited self-lifespan. Additionally, it also has geographic limitations such as the geothermal reservoirs that

are location-specific; solar energy production requires adequate direct sunlight; wind turbines need 26 mph to 55 mph of wind flow. Thus, there is a need to address all these challenges to make the commercial renewable energy plant sustainable.

1.1.3. Potential of bioenergy

Bioenergy is renewable energy produced from biological sources, and it is considered to be carbon neutral [4]. It is obtained from solid biomass and liquid biofuels, which are called bioenergy feedstock. In the last few decades, technological developments and commercial productions of bioenergy have shown rapid growth compared to other renewable energy sources. According to the International Energy Agency (IEA), the global supply of bioenergy reached 1381 Million tonnes of oil equivalent (Mtoe) in 2013, ranking fourth after traditional fossil fuels, such as crude oil (4211 Mtoe), coal (3913 Mtoe) and natural gas (2898 Mtoe). This proves the importance of bioenergy as the leading renewable energy [5].

According to the World Biomass Association (WBA), biomass is a major source of bioenergy, currently being used by foremost developing countries for heating, lighting, and cooking [5]. The advantage of biomass is its stored energy, whereas energy storage is a major challenge for other renewable technologies such as solar and wind [6]. Recent advances in the field of physical, chemical, and biological biomass conversion technologies have supported the production of various biofuels such as biogas, liquid fuels, and electricity [5]. However, the combustion of biomass has been the primary source of biofuel generation [6].

In general, biofuels are classified as (i) primary biofuels such as firewood, wood chips, pellets, animal waste, forest and crop residues, landfill gas, and (ii) secondary biofuels comprising bioethanol, butanol, biodiesel, and hydrogen. Further, biofuels such as bioethanol, butanol, biodiesel production from edible biomass feedstocks are considered as first-generation biofuels. Whereas, biofuels production from the non-edible biomass feedstocks such as *Jatropha*, cassava, *Miscanthus*, and other lignocellulosic sources (straw, wood, and grass) are considered as second-generation biofuels [7].

However, the need for abundant cropland, food vs. fuel challenge, regional and seasonal availability, feedstock unavailability in the long term, transportation of feedstock, process scale-up, and energy-intensive technology are among the critical challenges associated with the 1st and 2nd generation biofuels. Therefore, there is a pressing challenge to develop renewable and sustainable energy sources and technologies around the globe [7,8].

1.2. Microalgae as 3rd generation bioenergy feedstock

1.2.1. Potential of microalgae

Microalgae are sunlight-driven photosynthetic microorganisms typically found in fresh and marine water with relatively simple requirements for growth when compared to other sources of biomass [9]. Recently, Wijffels and Barbosa [10] reported in *Science* about the broad prospects of microalgal biofuels over terrestrial crop-based biofuels (2nd generation). In their report, they also highlighted how a 50-year-old concept of microalgal cultivation came into focus during the oil crisis of the 1970s. Since then, over thousands of algal species have been isolated, identified, and studied towards its potential for biofuel and value-added products. Following are a few advantages of microalgal biomass that validate its potential as a 3rd generation biofuel feedstock [11–14]:

- Microalgae has the potential to grow throughout the year with an annual oil yield of between 58,700 L ha^{-1} (30% oil) to 136,900 L ha^{-1} (70% oil), which is far superior to any oilseed crops.
- It has superior growth rate with a cell doubling time as short as 3.4 h.
- It has less water footprint compared to the terrestrial crops.
- It requires less nutrients and can grow in non-arable lands and, therefore, may not incur any change in land-use, minimizing associated environmental impacts.
- Microalgae cultivation does not require herbicides or pesticides application.
- Besides lipids for biodiesel production, microalgal biomass contains carbohydrates, proteins, and pigments that make de-oiled biomass as a potential feedstock for the production of biofuels and value-added products.

- The CO_2 sequestration potential of a microalgal culture is about 8.3%, while the maximum attainable photosynthetic efficiency of C3 plants cannot exceed 2.4% annually (1 kg of dry algal biomass utilize about 1.83 kg of CO_2).
- Wastewater with adequate nitrogen and phosphorus is a suitable growth medium for microalgae that is often considered for bioremediation.
- Thus, integrating wastewater treatment with CO_2 sequestration and production of biofuels and co-products signifies the potential of microalgae under the biorefinery approach.

1.2.2. Challenges in microalgal biofuel production

Despite several advantages, commercial microalgal biorefinery plant operation deals with several challenges [11–14]. They include:

- Isolation/selection of a potential strain with an inherent adaptability to the local climate and sustainable biomass production.
- Development of techniques for single species cultivation, reduction in evaporation, and CO_2 diffusion losses.
- Dependent on high volume water for microalgal cultivation (0.001-0.11 m^3 of water per Kg biomass).
- Installation of cultivation systems with easy access to freshwater/ wastewater for a continuous cultivation process throughout the year.
- Development of energy-efficient, large-scale cultivation systems is needed to achieve higher photosynthetic efficiency at a continuous mode of operation.
- Sustain superior biomass productivity in winter and rainy season.
- Development of a sustainable harvesting technique.
- Potential for negative energy balance after accounting for requirements in water pumping, CO_2 transfer, harvesting, and extraction.
- Limited large-scale cultivation plants are in operation; therefore, there is a lack of data for the design of commercial plants.
- Energy-efficient biomass to biofuel conversion technique with feasibility towards the production of other value-added co-products.

1.3. Microalgal wastewater treatment and biomass production

In the recent past, growing population, urbanization, and industrialization have resulted in the production of a considerable amount of domestic, agricultural, and industrial wastewater that contains various organic and inorganic contaminants [15]. Conventionally, the treatment of wastewater is done in three steps. Initially, the primary treatment process is followed by physicochemical methods to remove the larger solid particles by filtration and auto-sedimentation. Effluent from primary clarifier flows into large, rectangular aerated tanks called Aeration Basins, where activated sludge (single-celled microorganisms, mostly bacteria, and protozoa) performs the secondary treatment. These microorganisms are further removed by physical methods and treated effluents are released to rivers, lakes, or other aquatic environments. However, several municipal and industrial treatment systems follow the tertiary treatment process to improve wastewater quality before its reuse, recycle, or discharge to the environment that removes remaining inorganic compounds, microorganisms, and substances, such as nitrogen and phosphorus [16,17].

Besides several advantages, the treatment process has several challenges that include energy consumption, requires skilled operational and maintenance teams, overheating of blowers and lack of air in the system, insufficient nitrification and COD removal, sludge leakage from the settling tank etc. Often inefficient disposal of these wastewaters would inevitably cause eutrophication phenomena (enrichment of nitrogen and phosphorus in water). That leads to increased production of algae and aquatic plants, depletion of oxygen affects aquatic animals, general deterioration of water quality, and complete degradation of freshwater ecosystems [18].

1.3.1. Microalgal wastewater treatment and bioenergy production

Wastewater with substantial pollutants such as nitrogen, phosphorous, and organic carbon is considered as a significant growth medium for microalgae. Cultivation of microalgae in wastewater results in simultaneous wastewater treatment, CO_2 sequestration, and generation of high-value biomass feedstock. Additionally, the microalgae-based wastewater treatment system has several advantages over the traditional treatment process. It can be integrated with the existing treatment systems that requires low maintenance and does not depend on skilled labor, which makes the

process economical. The energy requirement during microalgal wastewater treatment is less compared to the conventional activated sludge process. Assimilatory mechanisms of nutrient removal by microalgae result in the production of high-value biomass feedstock. Whereas, the traditional method follows dissimilatory mechanisms that dissipate components such as N and C to the atmosphere. Microalgae have a higher bioremediation efficiency for nitrogen and phosphorous rich wastewaters (such as cattle, swine, and poultry) and a potential for CO_2 sequestration that significantly reduces GHG emissions compared to the conventional method [12]. Recently, several studies performed treatment of domestic, municipal, agricultural, and industrial wastewater using microalgal strains in both lab-scale and pilot-scale. Additionally, an optimized process with selective strains had shown significant removal of micropollutants such as heavy metals, pharmaceutical contaminants, and other toxic and carcinogenic pollutants that cannot be eliminated with traditional wastewater treatment methods [19–22].

Wastewater treated derived microalgal biomass has proven its potential for sustainable biofuel production. The harvested biomass is often found rich in biomolecules (lipid, carbohydrate, and protein) and used as a feedstock for biofuel generation [16]. A study suggests that nutrient stress conditions in wastewater supports the accumulation of a higher lipid content in microalgae, which is further used for biodiesel production [1]. Additionally, a combination of carbohydrates, proteins, and lipids makes an optimal N/P balance for anaerobic digestion. The methane produced can be used to run various on-site processes that assist in maintaining the energy balance and make the process self-sustainable. Moreover, microalgal biomass is also used as feedstock for the production of other biofuels (biohydrogen, bioethanol, and biocrude), which is discussed in the following sections. [1].

1.3.2. Challenges with microalgal growth in wastewater

Nutrient composition (N, P, and COD) in wastewater is often at the extreme range that significantly hinders optimal biomass productivity. The COD/BOD levels, N and P present in anaerobic digestates, and agro-industrial wastewaters are in the order of 3000-16,000 mg L^{-1}, 30-9000 mg L^{-1}, and 10-500 mg L^{-1}, respectively [12]. Whereas, it is 734-13251 mg L^{-1}, 2-267 mg L^{-1}, and 5-56 mg L^{-1} in industrial

wastewaters such as a slaughterhouse, soybean-processing plant, digested starch, molasses, and brewery plant [16]. In this context, the selection of potential native strain is essential to achieve sustainable biomass productivity. Studies suggest dilution of wastewater has resulted in attaining the optimal biomass yield. However, that persists the freshwater dependence challenge [1]. Turbidity in wastewater due to the suspended solids lessen the penetration of light into the wastewater and interfere with microalgae growth. The presence of sludge in wastewater also adds to harvested biomass and alters its biochemical composition. Sand and the presence of other inorganic solid particles increase the overall ash content in the biomass and affects its energy value [23]. Transportation of wastewater from the industries located at a remote place adds cost to the overall process [24].

1.3.3. Advantages of microalgal growth in sewage wastewater

Supplementation of an optimal nutrient to the low-nutrient containing wastewater is a promising alternative for microalgal cultivation, thereby making the process less dependent on freshwater. Moreover, it makes the commercialization process sustainable, especially where the availability of freshwater is of great concern. In this regard, sewage wastewater is widely considered for microalgal growth as the nitrate, phosphate, and COD content is comparatively less than other industrial and agricultural wastewaters [1]. Sewage wastewater in all rural and urban places releases a definite volume of wastewater at regular intervals. This helps to retain the cultivation volume and supports for fed-batch, semi-continuous, and continuous mode of operations. Whereas, the volumetric discharge of wastewater is not directly affected by the seasonal and other factors as compared to the agricultural and industrial effluents. A recent study has shown that microalgae belonging to the genus *Chlorella* and *Scenedesmus* were able to grow effectively in sewage wastewater, and their harvested biomass had the potential for biofuel production [25]. Sewage sludge is also a potential bioenergy feedstock that has a superior volatile matter along with energy value. Additionally, the integration of microalgal biomass and sludge can be further explored for the production of biofuels via biochemical and thermochemical conversion processes [26].

1.4. Microalgal biomass to biofuels conversion

Bioenergy derived from microalgae is considered as one of the clean, green, and sustainable energy resources and can be integrated into the biorefinery process [27]. The conversion of microalgal biomass to biofuels is carried out using three different conversion processes, namely biochemical, thermochemical, and chemical (Fig. 1.2) [28]. Feedstock composition, reaction conditions, biofuel yield, and energy efficiency are among the key factors that play a vital role in the sustainable biofuel conversion process. Among several, biodiesel, biocrude, and hydrochar are major biofuels that are gaining wide attention. Considering all these aspects, the present study was focused on the production of these biofuels through their respective conversion process.

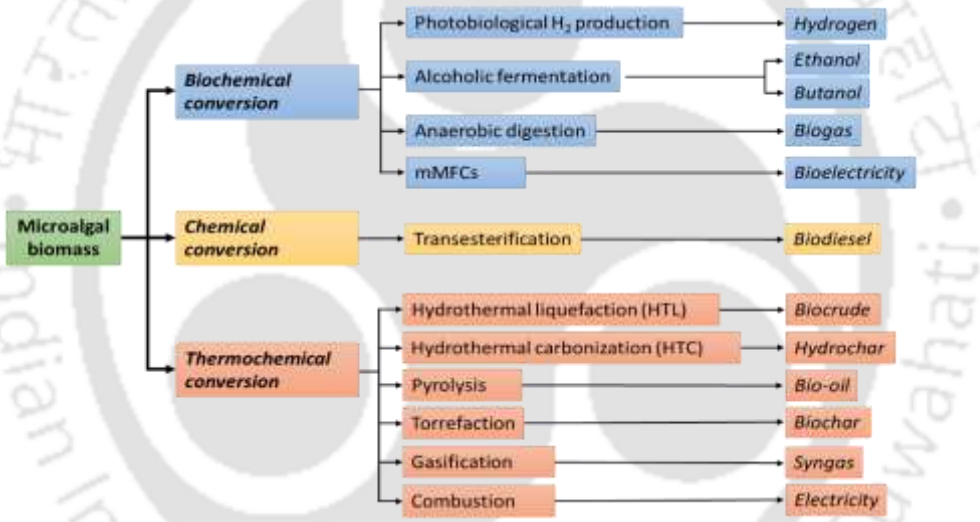

Fig. 1.2. A schematic of microalgal biomass to biofuel conversion techniques.

1.4.1. Transesterification

The transesterification reaction is a process that converts the triglycerides (TGs) into long chain fatty acid methyl esters (FAME) in the presence of methanol and catalyst (NaOH) (Fig. 1.3). FAME is also known as biodiesel, and its conventional production method from microalgae is followed by lipid extraction and conversion to FAME and glycerol [28]. However, the presence of high free fatty acid (FFA) in microalgal lipid is highly reactive with alkali catalyst resulting in an unfavorable saponification process. This leads to the formation of by-products, such as soaps and

gels. To overcome this, a two-step catalytic process is followed. In the first step, esterification is followed by acid-pretreatment using an acid catalyst that reduces the FFA content (<1%) in lipid and converts FFA into esters. Whereas in the second step (transesterification), an alkali catalyst is employed to turn the TGs into FAME [29]. During this, alcohols break down TGs into FAMEs and glycerol. There are three reversible steps involved in the transesterification process, where TGs are converted to diglycerides, then diglycerides are converted to monoglycerides, and monoglycerides are then converted to esters (biodiesel) and glycerol [14]. Factors such as reaction temperature, retention time, lipid-alcohol ratio, and catalyst loading are considered to optimize the process for the significant FAME conversion [28,30,31]. Mata et al. [14] reported the relationship between the feedstock mass input and biodiesel mass output is about 1:1, which means that theoretically, 1 kg of oil results in about 1 kg of biodiesel. However, the biodiesel yield significantly depends on the feedstock composition, catalyst and reaction conditions.

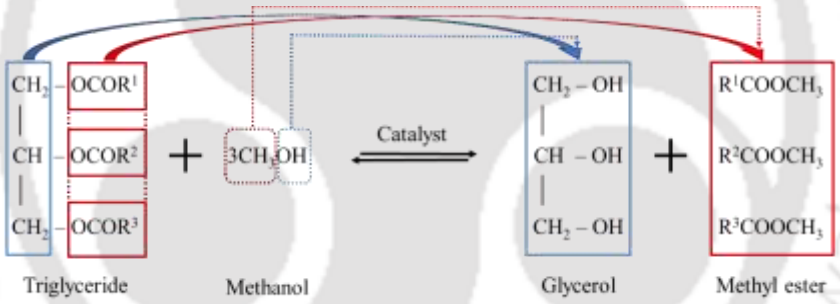

Fig. 1.3. Transesterification of triglyceride into FAME and Glycerol.

1.4.2. Hydrothermal liquefaction (HTL)

Hydrothermal liquefaction (HTL) is a thermochemical conversion process that converts wet microalgal biomass into biocrude that has properties comparable to crude petroleum oils [32,33]. HTL is operated at near supercritical state (temperature 250-370 °C), where water acts as an acid and base catalyst. That triggers isomerization, depolymerization, and repolymerization resulting in the conversion of biomolecules (e.g., proteins, polysaccharides, lipids, chlorophyll) into biocrude. The key factors that influence the optimal conversion are biomass composition, reaction temperature, retention time, and feedstock loading [34]. However, the efficiency and sustainability

of catalytic HTL has been shown to enhance biofuel yield. The elemental composition of the biocrude includes carbon (60-78 wt%), hydrogen (7-11 wt%), and HHV (25-38 MJ Kg^{-1}). Whereas, chemically it is comprised of acids, alkenes, ketones, esters, and nitrogen-containing heterocycles, which is comparable to the petroleum crude-oil [35,36].

1.4.3. Hydrothermal carbonization (HTC)

Conversion of dry biomass into carbon or carbon-rich residue (biochar) at temperatures above 300 ℃ is achieved by carbonization. Recently, hydrothermal carbonization is gaining wide attention due to its potential to convert wet biomass into high-energy-density solid fuels (hydrochar) [37]. The process is similar to HTL; however, the reaction temperature is limited to 180-250 ℃ and the pressure between 2MPa to 10 MPa. Additionally, the residence time of hydrothermal carbonization is preferably > 1 h [37,38]. The primary hydrochar formation mechanism focuses on solid-solid conversion that follows hydrolysis, condensation, decarboxylation, thus converting microalgal biomass into hydrochar [39]. Besides biofuel, hydrochar also has applications in wastewater treatment, soil remediation, and other carbonaceous materials [8].

1.5. Biorefinery approach

According to the US Department of Energy, a biorefinery is an overall concept of a processing plant where biomass feedstock is converted and extracted into a spectrum of variable products [40]. Recently several literatures had discussed on the spectrum of microalgal mainstream products that are integrated with microalgal biorefinery [40–42]. In the context to microalgal biofuel, reduce, recycle, and reuse of bioenergy wastes (liquid waste and solid residues) is essential for a sustainable zero-waste biorefinery [40]. Fig. 1.4 shows detail applications of liquid effluents and solid residues for a zero-waste microalgal biorefinery approach.

1.5.1. Processing of liquid waste streams

The two primary sources of bioenergy conversion process derived liquid waste streams are the harvested medium from the microalgal cultivation process and the liquid waste from the biofuel conversion process. It is estimated that the production of

1.0 kg microalgal biomass and 1.0 L of biodiesel requires approximately 997 kg and 3000 L of water, respectively [43,44]. Recycling and processing of this liquid waste is necessary for the reduction of water footprint and the production of sustainable biofuel. Separation methods such as flocculation, filtration, and centrifugation play a vital role in the final effluent property and its subsequent valorization [45]. Thus, the use of microalgal strains with auto-sedimentation features can significantly reduce the use of chemical flocculants and subsequently enhance reusability prospects [45]. Moreover, bioenergy derived effluents that are rich in nutrients can be incorporated for microalgal cultivation. That will further address the zero-waste biorefinery under a circular biorefinery approach [15].

1.5.2. Processing of solid residue

Bioenergy production through biochemical, thermochemical, and chemical conversion of microalgal biomass generates a considerable amount of solid residues in the form of fermentation residue, anaerobic digestate, biochar, fly ash, bottom ash, and de-oiled biomass. Among these, the generation of lipid-extracted microalgal biomass (LEMB) is estimated to be three times the amount of biodiesel produced, assuming 25% lipid is extracted from microalgae biomass [24]. This contains leftover lipid, carbohydrate, protein, nitrogen, phosphorous, and other micronutrients in substantial quantities, which makes it a potential biofuel feedstock [1,46]. Studies have shown, LEMB with high carbohydrate content is a potential feedstock for the production of bioethanol, biomethane, and biohydrogen through various biochemical conversion processes [41]. LEMB is also considered for multiple thermochemical conversion process is due to the presence of superior volatile compounds and limited ash content. However, the yield of solid residue obtained from an optimal HTL process is limited to < 10 wt% of the feedstock. It has a high ash content and limited hydrogen, nitrogen, and sulfur. The solid residue also contains several mineral elements such as Si, Fe, Al, Ca, Mg, K, Zn, Ti, Mn, Na, Ba, Sr, Ag, and Pb, which are transferred from the feedstocks [47]. Due to an adequate presence of nutrients and minerals, the solid residues are potential candidates as fertilizers for soil amendment. The solid residues are also used for the treatment of various wastewaters as activated biochar [48].

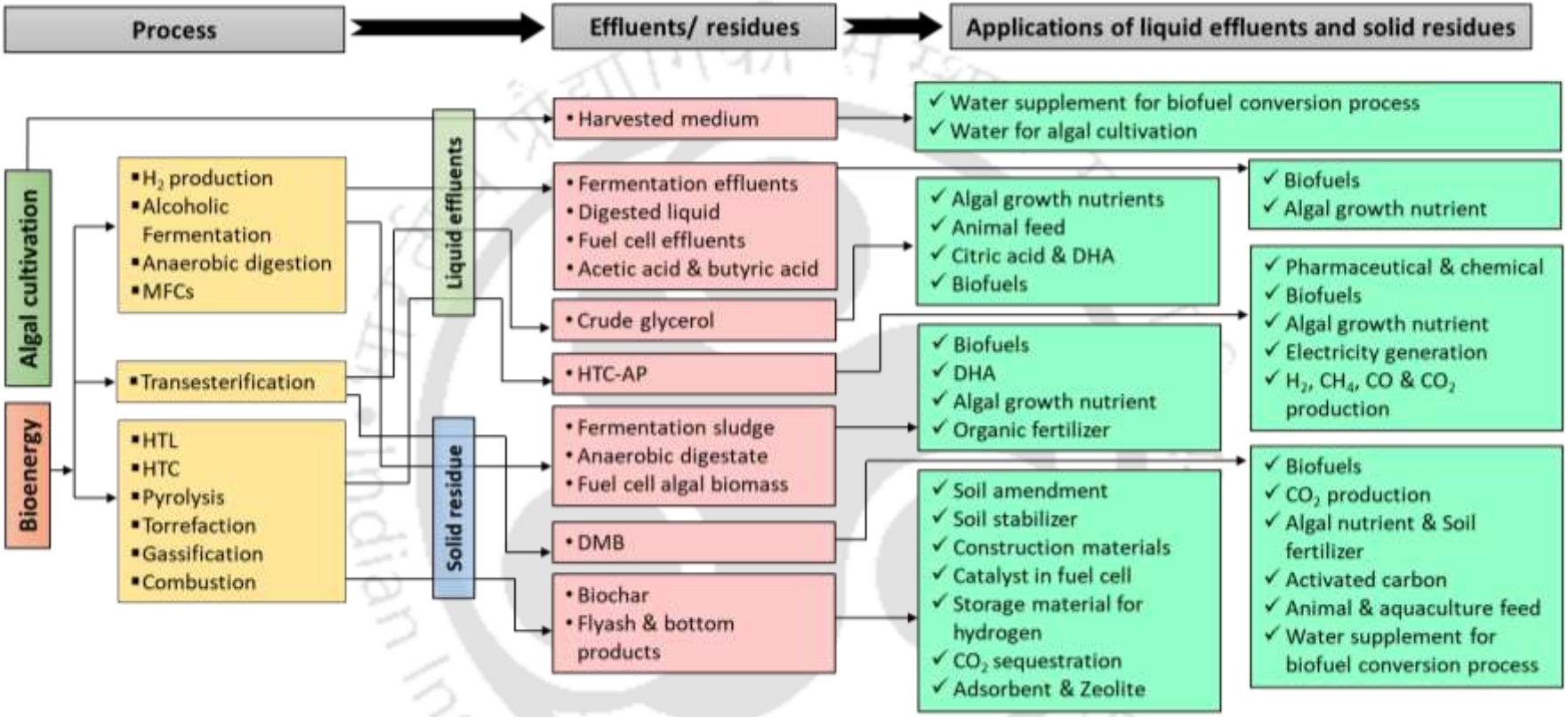

Fig. 1.4. Applications of liquid effluents and solid residues for a zero-waste microalgal biorefinery approach

Chapter 2

Literature Review and Objectives

2.1 Microalgal culture in conventional medium and wastewater

Ever-escalating global energy demand and global warming due to the burning of fossil fuels encourage the necessity for exploring and implementing alternate clean, green, and sustainable energy resources. Among several other renewable energy alternatives, bioenergy production from microalgae has acquired wide recognition since the last few years [10]. However, their water and nutrient dependence has been a vital challenge for researchers to make the process sustainable [1,49]. Additionally, the commercialization of the process is a challenge considering current capital costs per unit of fuel production [40]. Hence, to bring a solution to this problem is to make use of wastewater as they contain various essential nutrients necessary for microalgae cultivation (e.g., carbon, nitrogen, phosphorus, and micronutrients) [50–52]. Literature also suggests that microalgal cultivation can be the best approach to minimize the cost as it also supports biological wastewater treatment [1,53,54].

2.1.1 Microalgal growth in conventional medium

Conventional lab-grade synthetic media are widely studied at lab-scale or small scale experiments for screening and process optimization of various algal strains [55]. During the culture process, nitrate and phosphate play a central role in microalgal cell physiology and growth, where the optimum concentration enhances the growth rate of microalgal cultures [56]. In addition to nutrients, CO_2 improves the algal photosynthetic efficiency leading to an uplifting algal growth rate [57]. In a recent study, Basu et al. [58] grew indigenous *Scenedesmus obliquus* SA-1 in BG11 medium and studied its growth characteristics. The study reported a higher biomass productivity of 4.86 g L^{-1} at 13.8 ± 1.5% CO_2 supply. Whereas, to study the nitrogen and phosphorous effect on algal growth, the CO_2 concentration was increased, which resulted in achieving higher biomass concentrations of 4.975 ± 0.003 g L^{-1}. As algae

are known to have a specific nutrient requirement for their growth, their growth characteristics vary for different media. This was observed in an experiment where Chaichalerm et al. [59] grew six algal strain (*Chlorococcum humicola, Didymocystis bicellularis*, *Monoraphidium contortum*, *Oocystis parva*, *Sphaerocystis* sp., and *Scenedesmus acutus)* in 4 different growth media (3NBBM, BG-11, Kuhl, and N-8). The growth effect was observed by varying nutrient composition. A significant difference in their growth characteristic and lipid productivity to its growth medium was observed for all the six strains. Among all, *C. humicola* had the highest biomass yield of 0.113 g L^{-1} d^{-1} (in Kuhl medium), the highest lipid content of 45.94% (in BG-11 medium), and the highest lipid yield of 0.033 g L^{-1} d^{-1} (in 3NBBM medium). The 3NBBM medium, which has the lowest nitrogen concentration among the four culture media, was considered the optimal culture medium for *C. humicola* for lipid production. This is due to the fact that nitrogen limitation does not inhibit algal growth and creates a stress environment to cells which enhances synthesis of membrane and storage of lipid [60]. Some potential algal strains and their growth characteristics are presented in Table 2.1.

Table 2.1. Growth characteristics of different algal strains grown in synthetic media.

Algal Strain	Specific Growth Rate (d^{-1})	Biomass Productivity (g L^{-1})	Lipid (%)	References
Nitzschia cf. pusilla YSR02	1.68 ± 0.28	1.37 ± 0.08	48 ± 3.1	[55]
Chlorella ellipsoidea YSR03	1.42 ± 0.02	1.48 ± 0.04	32 ± 5.9	
Micractinium pusillum YSW07	1.19 ± 0.17	2.28 ± 0.16	24 ± 0.5	
Ourococcus multisporus YSW08	0.51 ± 0.14	0.95 ± 0.11	52 ± 8.3	
Scenedesmus obliquus YSR04	1.32 ± 0.05	1.98 ± 0.04	21 ± 1.1	
Scenedesmus obliquus YSR01	2.35 ± 0.55	1.57 ± 0.67	58 ± 1.5	
Scenedesmus obliquus YSR05	1.06 ± 0.03	1.75 ± 0.34	27 ± 1.9	
Scenedesmus obliquus YSW06	0.99 ± 0.02	1.80 ± 0.13	27 ± 5.6	
Scenedesmus obliquus SA-1	-	4.86	33.04 ± 0.4	[58]
Nannochloropsis oculata	0.19-0.57	0.29-0.49 [a]	22.7 - 41.2	[61]
Nannochloropsis sp. F&M-M24	-	0.18 [a]	30.9	[62]
Pavlova salina CS 49	-	0.16 [a]	30.9	
Chlorococcum humicola	-	0.113 [a]	45.94	[59]

[a] (g $L^{-1}d^{-1}$)

2.1.2 Microalgal growth in wastewater

In the past few decades, tremendous efforts have been put into the research of microalgae cultivation in different wastewaters such as domestic wastewater, olive-oil mill wastewater (OMW), urban wastewater, and dairy manure wastewater [63–67]. Among these, availability and volumetric production of domestic and municipal wastewater are to a greater extent. Recently, Cai et al. [63] reported, increasing urbanization and expansion of urban populations has resulted in more significant quantities of municipal wastewater. A city with a population of 5,00,000 and water consumption of 0.2 td^{-1} $capita^{-1}$ would produce approximately 85,000 td^{-1} of wastewater. The primary effect of releasing wastewater rich in organic compounds and inorganic chemicals such as phosphates and nitrates is mainly eutrophication. To overcome this problem, the combination of microalga-based biofuel production and wastewater treatment is a promising solution [68,69]. However, achieving high nutrient removal efficiency and viable biomass yield is somewhat tricky due to the high nutrient load in wastewater, which creates a stressful environment for algal growth. Few algae have inherent adaptability to sustain their growth in a high nutrient load environment. Among them, *Chlorella* sp. is more commonly studied in various types of wastewaters and achieved high nutrient removal efficiency in addition to viable biomass yield [63]. Li et al. [70] isolated *Chlorella sp.* by growing it in municipal wastewater, where a higher growth rate of 0.677 d^{-1} was achieved without any lag phase. During the 14 days of the cultivation period, *Chlorella* could reach more than 80% of nutrient removal (ammonia, total nitrogen, total phosphate) with 0.92 g L^{-1} of feasible biomass productivity. There is also a report which claimed of achieving 9.8 g L^{-1} and 6.3 g L^{-1} biomass from thin stillage and soy while growing *Chlorella vulgaris* at mixotrophic conditions in a bioreactor. Besides high biomass yield, *Chlorella vulgaris* could achieve a high lipid yield of 43 % and 11% (w/w), respectively [71].

As mentioned earlier, the nutritional requirement for algal growth varies from strain to strain, for which different algal strains need to be screened. Sydney et al. [64] conducted a screening experiment over 20 microalgal strains on secondary domestic wastewater treated effluents. Three strains, such as unknown LEM-IM 11, *Botryococcus braunii*, and *Chlorella vulgaris* have shown higher growth rates and

high nutrient removal. During the 2 L photobioreactor study, unknown LEM-IM 11 has shown a growth rate of 0.19 d^{-1}, whereas 0.11 d^{-1} was observed in *Botryococcus braunii* and *C. vulgaris*. But more significant nutrient removal was achieved by *Botryococcus braunii* with 79% nitrate and 100% phosphate and higher biomass productivity of 0.68 g L^{-1} containing over 36.14% lipid. There are also reports where two different wastewaters were mixed in different proportions to achieve higher algal growth and nutrient removal. In one such study, *Scenedesmus obliquus* CCAP 276/3A reported a maximum specific growth rate of 0.074 h^{-1}, volumetric biomass productivity of 4 mg dm^{-3} h^{-1}, and net biomass generation 0.28 g dm^{-3} when grown in a culture blend of 25% (v/v) of urban wastewater from secondary treatment added to 5% (v/v) olive-oil mill wastewater [66]. *Chlamydomonas reinhardtii* was grown in wastewater, shown biomass productivity of 0.82 ± 0.04 g L^{-1} d^{-1} [72]. *Tetraselmis indica* cultivated in secondary treated domestic sewage achieved 0.88 ± 0.04 g L^{-1} biomass yield along with 60.93% phosphate, 78.46% nitrate, 72.94% chemical oxygen demand (COD) [73]. *Chlorella* sp. was grown in two different types of wastewater (kitchen wastewater (KWW) and sewage wastewater (SWW)), the maximum biomass productivity of 0.6 g L^{-1} was obtained from SWW [74]. Table 2.2 represents various algal strains grown in different wastewater and their biomass and lipid productivity. This suggests algal strains represent variable growth characteristics for which the screening process is highly essential to select potential algal strain to achieve high biomass yield with simultaneous nutrient removal.

Table 2.2. Biomass and lipid productivity of different algal strains studied in different wastewater.

Species	Source of wastewater	Biomass (g L^{-1})	Lipid Content (%)	Reference
Chlorella sp.	Thin stillage	9.8 ± 0.3	43	[71]
	Soy whey	6.3 ± 0.1	11.1 ± 1.1	
	Domestic secondary effluent	0.42	43	[68]
	Brewery wastewater	2.28 ± 0.09	220 ± 0.02 (mg g^{-1})	[75]
	Municipal wastewater	1.75	-	[76]
	Carpet industry wastewaters	0.016± 0.003 (g L^{-1} d^{-1})	17.00 ± 2.89	[77]

Scenedesmus obliquus CCAP 276/3A	Blend of 25% urban wastewater & 5% olive-oil mill wastewater	0.28 (g dm^{-3})	33.2	[66]
Dunaliella tertiolecta	carpet mill untreated wastewater	28 (mg L^{-1} d^{-1})	15.20	[77]
Botryococcus braunii	Treated domestic sewage	0.68	36.14	[64]
Chlamydomonas reinhardtii	Municipal wastewater	2000 (mg L^{-1} d^{-1})	25.25	[72]
Chlamydomonas sp. TAI-2	Industrial wastewater	1.8	18	[78]

2.2 Factors affecting microalgal growth and optimization

2.2.1 Strain selection

Achieving high nutrient removal and viable biomass yield is rather difficult from nutrient-laden wastewater as it creates a stressful environment for microalgal growth [79]. In such cases, isolation and screening of native and novel strains are considered the groundwork for superior wastewater treatment [50,80,81]. Native strains carry an inherent ability to acclimatize and results in superior growth in untreated wastewater [82]. In a recent study, 20 microalgae strains were isolated and screened, which resulted in selecting a model strain for optimal wastewater treatment and biodiesel production [83]. A screening study showed 1.07 g L^{-1} biomass yield with nitrate (90 %) and phosphate (97.8 %) removal from a native filamentous microalgal strain (MC2) [84]. In another study, native strain *Chlorella vulgaris* isolated from swine wastewater was able to remove 90.51% and 91.54% of total nitrogen (TN) and total phosphorus (TP) in 12 days of the culture period [82]. Similarly, Ferro et al. [85] isolated 62 strains and performed a screening study to select a potential strain for optimum nutrient removal, which simultaneously increased biomass and lipid yield favoring biofuel production.

2.2.2 Nutrient supplement

Studies indicate that nutrient-laden wastewater needs to be diluted to bring down the nutrient concentration to favor microalgal growth [79,86]. This makes commercialization of the process unsustainable, especially where the availability of

fresh-water is a key issue. In this regard, low nutrient containing wastewater supplemented with optimal nutrients is a more promising alternative for microalgal cultivation, thereby making the process less dependent on fresh-water [27]. A recent study discussed that depending on the algal lipid content and other parameters, nitrogen and phosphorous of 0.33-1.5 and 0.071-0.21 kg is required to produce one gallon of microalgal lipid [87]. However, supplementation of other nutrients also shown enhanced biomass yield. In a recent study, total phosphorus and $FeCl_3.6H_2O$ content of 4.41 mg L^{-1} and 6.48 mg L^{-1} resulted in biomass, lipid content, and TN/TP removal efficiency of 1.46 g L^{-1}, 36.26%, and >99%, respectively [51]. In another study, palm oil mill effluent (POME) was supplemented with an optimal concentration of glucose, urea, and glycerol. This resulted in *Chlorella sorokiniana* CY-1 with a biomass yield of 1.68 g L^{-1} followed by pollutant remediation efficiencies of 63.85% COD, 91.54% TN, 83.25% TP [79]. Multi-objective optimization of media nutrients found 16.8 mM $NaNO_3$, 300.9 µM K_2HPO_4, and 2.6% (w/v) glucose supplement resulted in *Chlorella pyrenoidosa* with 34.8% (w/w), 1464.3 mg $L^{-1,}$ and 93.4% of lipid, biomass, and carbohydrate, respectively [88]. Thus, the above study suggests that the supplement of nutrients at an optimal concentration significantly impacted enhanced biomass feedstock production. Thus, the above study suggests that the supplement of nutrients at an optimal concentration significantly impacted enhanced biomass feedstock production.

2.2.3 Inoculum concentration

Besides nutrients, microalgal growth depends on several physical factors such as light, temperature, and abiotic factors. One such abiotic factor is initial cell density that can be decided with inoculum concentration. The study suggests, a higher initial inoculum helps to gain maximum growth rate and nutrient removal efficiency. This is because the high density of inoculums could minimize the initial lag phase resulting in the rapid exponential growth of microalgae. However, high cell density would lead to self-shading, an accumulation of auto-inhibitors, and a reduction in photosynthetic efficiency [89]. Recently, several studies on microalgal wastewater treatment had considered 5-10% (v/v) of inoculum as optimal [90–92]. Beyond its optimal range, cells had shown photoinhibition, resulting in a reduced growth rate [93].

2.2.4 Light intensity

Microalgae are a photosynthetic organism that utilizes light energy to perform photosynthesis and maintain its growth metabolism. Blue and red light have shown better results to microalgal growth as it contains chlorophyll a and b, which are primary light-harvesting pigments and sensitive to these wavelengths [94]. Whereas, the light intensity is directly proportional to the culture volume. A recent study reported nitrogen and phosphorus are consumed in the production of nitrogen and phosphorous-containing compounds, such as adenosine triphosphate (ATP) and nicotinamide adenine dinucleotide phosphate (NADPH) for photosynthetic metabolism, but only when microalgae are illuminated. When the illumination intensity and photoperiod are insufficient, microalgae cannot generate enough energy via photosynthesis to fulfill their metabolic requirements, resulting in low nitrogen and phosphorous removal rates [92].

Meanwhile, auto-shading caused by microalgal cells that inhibit the growth of others by reducing light availability significantly affects light delivery efficiency. Thus, some microalgal cells inhibit the growth of others by decreasing light availability. However, this limitation could be overcome by air delivery systems such as sparging air bubbles, which increases Brownian motion uniformity of light delivery to the cells [95]. In another study, light intensity from 0.3-538 μEm^{-2} s^{-1} was studied using *Botryococcus braunii* KMITL 2 that had shown 200 μEm^{-2} s^{-1} was optimal to produce biomass with 54.69 ± 3.13% lipid content. Beyond its optimal illumination, a reduced microalgal growth profile was recorded [96]. This was also comparable to the study done by Binnal and Babu [92], where Light intensity of 6 Klux was found optimal for *Chlorella protothecoides* while grown between 4-8 Klux.

2.2.5 Culture temperature

Temperature is one of the essential physical parameters that significantly controls cell metabolism, morphology, and physiology [96]. The low temperature of the culture medium is unfavorable for the enzyme activity of ribulose biphosphate carboxylase oxygenase (RuBisCO), leading to a reduction in the rate of photosynthesis. In contrast, high temperature inhibits microalgal metabolic rate and reduces CO_2 solubility. Low CO_2 solubility causes photorespiration, whereby

RuBisCO binds to O_2 rather than CO_2, thereby reducing carbon bioconversion by 20-30% [97,98]. Additionally, in a recent report, Juneja et al. [99] highlighted several mechanisms of temperature-dependent photoinhibition. These include mechanisms under which: (i) low-temperature results in reduced electron transport at a given photon flux rate due to slower rate of CO_2 fixation; (ii) low temperature inhibits the active oxygen species, which results in reducing photoinhibition by protecting PSII; and (iii) low temperature inhibits the synthesis of the D1 protein degraded during photoinhibition, consequently impeding the PSII repair cycle.

The optimal culture temperature is microalgal species-specific, and it varies from 20-30 ℃. However, an optimal culture temperature also depends on other factors such as light intensity, medium composition, reactor type [94]. Recently, Salama et al. [50] reported, 25 ℃ was found optimal for various microalgal strains that had shown the highest biomass yield during cultivation in wastewaters.

2.2.6 CO_2 supplement

Microalgae utilize atmospheric CO_2 for its growth via photosynthesis. Several studies shown, additional input of CO_2 to culture media through aeration had significantly enhanced biomass yield [50,58,100,101]. This is because high CO_2 induced low pH in the culture medium and reduces the activity of extracellular carbonic anhydrase of microalgae, responsible for the carbon concentration mechanism [97]. Recently several studies reported enhanced biomass yield with optimized CO_2 supply [90,98]. Additionally, to support CO_2 sequestration, flue gas of optimal concentration was supplied to the microalgal culture that had shown positive growth and enhanced lipid yield [98,101].

2.3 Biofuel from microalgae

2.3.1 Chemical conversion

The chemical conversion route of microalgal biomass to biodiesel is performed via transesterification reaction. The reactions of triglycerides to FAME and glycerol are usually catalyzed by an acid or base, using either a homogeneous or heterogeneous catalytic process [40]. During this process, reaction conditions such as temperature, time, catalyst play a significant role that determines biodiesel property [28]. The

property of biodiesel obtained from an optimized process is further compared with the International Biodiesel Standard for Vehicles (EN14214) that defines its potential to be accepted as a substitution for fossil fuels. [11]. Table 2.3 represents the microalgal biomass to biofuel conversion at its optimal operating conditions.

Biodiesel derived from microalgae is currently being recognized as a green and alternative renewable diesel fuel that has gained vast attention. The key advantages of using biodiesel instead of fossil diesel are that it is a non-toxic fuel, is biodegradable, and has lower emission of GHG when burned in diesel engines [102]. Another significant advantage of algal biodiesel is reduced CO_2 emissions of up to 78% compared to emissions from petroleum diesel [11].

Table 2.3. Operating parameters and biodiesel profiles obtained from various microalgal biomass via transesterification.

Feedstock	Reaction temp. (°C)	Residence time (min)	Catalyst	HHV ($MJ \cdot kg^{-1}$)	Bioenergy production	Reference
Nannochloropsis gaditana	113.6	2 h	H_2SO_4	-	97.8%	[103]
Chlorella sp. FC2 IITG	90	40	NaOH and H_2SO_4	-	65-85 % (C16-C18)	[104]
*Chlorella*sp. FC2 IITG	255	25	-	39.4 MJ kg^{-1}	96.9%	[105]
Chlorella sp. FC2 IITG	90	40	NaOH and H_2SO_4	-	98.96%	[30]
Nannochloropsis sp.	80	3 h	Nano $Ca(OCH_3)_2$	-	99.0%	[106]

2.3.2 Thermochemical conversion

Under the thermochemical conversion process, thermal decomposition of biomass is followed to extract various fuel products. The advantage of thermochemical conversion is its short reaction time. Additionally, it can convert a variety of biomass feedstocks and utilize the entire biomass feedstock without any pretreatment process.

The products of thermochemical conversion processes include solid, liquid, and gas biofuels [36]. Examples of thermochemical conversion processes include gasification, thermal liquefaction, pyrolysis, and direct combustion [40]. Table 2.4 represents recent reports on converting various microalgal biomass to biofuel through the thermochemical conversion process.

Recent studies suggest, among several energy-intensive thermochemical conversion processes, biocrude production through hydrothermal liquefaction (HTL) of wet microalgae slurry has significant potential towards sustainable liquid biofuels [32,33,107]. The biocrude comprises acids, alkenes, ketones, esters, and nitrogen-containing heterocycles with properties comparable to the petroleum crude-oil [108]. Although the microalgal HTL process has several advantages, the availability of feedstock in all seasons (comparatively less productivity in winter) is one of the major challenges for commercial HTL plant operation [109]. In this context, Co-HTL of microalgal biomass and various waste-derived biomass (lignocellulosic and food waste) feedstocks were studied that shown superior biocrude yield along with enhanced fuel property [32,110,111]. Co-liquefaction of microalgae and sweet potato waste (4:1 wt%) resulted in ~40% of biocrude yield and promoted energy recovery with high ester contents [112]. Another study achieved the maximum biocrude yield of ~34wt% while the ratio was 5:1 wt% [113]. However, the above studies [112,113], along with a few more reports on non-catalytic Co-HTL had also shown relatively less synergistic effects on biocrude yield [114,115]. Additionally, these feedstocks may also bring logistic costs associated with collection and transportation that should be considered while selecting a source of co-feedstocks to make the process cost-effective.

Table 2.4. Thermochemical conversion of various microalgal biomass to biofuels and its operating conditions.

Process	Feedstock	Product	Reaction temperature (°C)	Residence time (min)	Catalyst	HHV ($MJ \cdot kg^{-1}$)	Bioenergy production	Reference
HTL	sewage sludge (SS): *Chlorella* sp. = 1:1	Bio-oil	340	30	-	*Chlorella* sp. =17.31, SS=16.14	57.87% energy recovery	[26]
	Nannochloropsis sp.	Bio-oil	250	60	Nano-Ni/SiO_2	23.11 $MJ\ kg^{-1}$	30.0 wt%	[116]
PYL	*Chlorella vulgaris*	Bio-oil	500	30	Ni loaded zeolite	-	10.4 wt%	[117]
	Microcystis sp.	Bio-oil	500	15	-	-	54.97 wt%	[118]
GAS	*Chlorella vulgaris*	Combustible gas	800	-	-	-	1.05 $Nm^3\ kg^{-1}$	[119]
	Chlorella vulgaris	Syngas	800	20	Oxygen carrier	-	93.92 wt%	[120]
HTC	Microalgal biomass	Hydrochar	210	60	-	12.1 $MJ\ kg^{-1}$	~37 wt%	[38]
	Sludge of wastewater treatment plant and *Chlorella* sp.	Hydrochar	210	30	-	5810 $kcal\ kg^{-1}$	87.68 wt%	[121]
TOR	*Nannochloropsis Oceanica*	Biochar	200	15	-	21.016 $MJ\ kg^{-1}$	99.82 wt%	[122]

HTL: Hydrothermal Liquefaction; PYL: Pyrolysis; GAS: Gasification; TOR: Torrefaction; HHV: Higher heating value; HTC: Hydrothermal carbonization

2.4 Zero-waste biorefinery approach

The waste-derived from a microalgal bioenergy production system can be broadly categorized as liquid waste streams and solid residues (Fig. 1.4). A sustainable process that can reduce, recycle, and reuse these wastes is essential for an energy-efficient biorefinery. Recently several literatures have discussed the production of food, pharmaceuticals, and other value-added products that defines microalgal biorefinery zero-waste [15,40,123]. However, recycle and reuse of these solid and liquid waste for bioenergy production can make commercial biofuel production sustainable. Table 2.5 summarizes all the solid residues and liquid effluents used to produce bioenergy and value-added products.

2.4.1 Liquid effluents from thermochemical conversion

Thermochemical conversion technology, such as hydrothermal conversion (HT), transfers around 20%-50% of the organics into the aqueous phase (HT-AP) during the process [124,125]. Recovery of resources from aqueous co-products produced during HT of microalgal biomass is necessary because they contain high concentrations of organics, including nitrogen, phosphate, polysaccharides, proteins, phenolic compounds, and organic acids [126]. Moreover, these organic compounds can pollute the environment if not treated properly.

Phenol and the carboxylic acid-rich HT-AP was reported to find its application in the pharmaceutical and chemical industries [127]. Whereas, monosaccharide rich HT-AP serves as a potential feedstock for bioethanol production. Many researchers have carried out anaerobic digestion of the HT-AP for reducing its COD to ~ 44%-61% and converting it to biogas such as methane. HT-AP accumulates a considerable amount of N, P, K that can be utilized as a nutrient source for algal growth. *Chlorella vulgaris* removed 45.5%-59.9% of total nitrogen, 85.8%-94.6% of total phosphorus, and 50.0%-60.9% of COD on differently diluted HT-AP [128]. Moreover, a microbial fuel cell can be employed for the production of energy from HTC-AP. Recently, catalytic hydrothermal gasification is being applied to convert the organic compounds present in the HT-AP to gas consisting of H_2, CH_4, CO, and CO_2 [129,130].

2.4.2 Solid residues from thermochemical conversion

The solid residue yield obtained from an optimal HTL process is limited to <10 wt% of the feedstock. It has high ash content and limited hydrogen, nitrogen, and sulfur. The solid residue also contains several mineral elements such as Si, Fe, Al, Ca, Mg, K, Zn, Ti, Mn, Na, Ba, Sr, Ag, Pb, etc are transferred from the feedstocks. Due to an adequate presence of nutrients and minerals, the solid residues are potential candidates as fertilizers for soil amendment. Additionally, thermochemical processes are also recommended for the production of other energy carriers [131]. Mineral elements such as Al, Si, P, Fe, Na, etc., and carbon in the solid residue in substantial quantities may express catalytic properties for an enhanced reaction mechanism [26]. However, the shift of trace amounts of mineral elements into the biocrude could reduce its quality, causing interferences in the subsequent downstream process [132]. Solid residues are also used for the treatment of various wastewaters as activated biochar [48]. However, future studies are recommended to explore the possible application of HTL solid residue as a high-value co-product.

Biochar is a solid residue of the pyrolysis process. Traditionally, biochar is produced from lignocellulosic biomass and is considered as black carbon. It is commonly used for soil amendment, construction materials, catalyst in fuel cell and other bioenergy conversion processes, storage material for hydrogen, and CO_2 sequestration [133,134]. Recent studies reported that enlarged pore size and surface area of biochar enhances adsorption potential. Mitigation of substrate-induced instability by biochar can significantly improve anaerobic digestion, followed by reduced greenhouse gas emission [135,136].

2.4.3 De-oiled microalgal biomass (DMB)

High carbon: nitrogen (C/N) ratio of DMB indicates high carbon content, which favors the biochemical conversion of DMB to bioethanol, biomethane, and biohydrogen [41]. Bioethanol can be produced from carbohydrate-rich DMB through saccharification and microbial fermentation after an appropriate pretreatment process. Chng et al. reported 0.26 g of bioethanol from one gram DMB of *Scenedesmus dimorphus* without pretreatment [137]. Moreover, biogas consisting of methane and carbon dioxide can be produced through anaerobic digestion of DMB. The de-oiled

biomass of marine microalgae is not suitable for biogas production as a high concentration of sodium salts may inhibit the anaerobic digestion process [138]. The DMB was found to serve as a potential feedstock for biohydrogen production after thermo-alkaline pretreatment [139].

Biofuels can also be recovered through the thermochemical conversion of DMB, although the process is energy-intensive compared to biochemical conversion. Bio-oil with 24-45% yield was procured from DMB of *Nannochloropsis oceanica*, *Scenedesmus* sp., and *Spirulina* sp. through HTL [140,141]. The volatile matter of DMB is re-condensed to obtain pyrolytic bio-oil. In fact, the pyrolysis of DMB requires less energy in comparison to fresh microalgae [41]. The DMB, being rich in carbon, can produce syngas through the gasification of carbonaceous materials. Biofuels like hydrogen and methane can also be obtained from syngas along with some chemical intermediates.

Besides, DMB also serves as a nutrient-rich growth medium for microalgae, bacteria, and yeast [24]. Biomass and lipid content of *C. vulgaris*, *Chlorella* sp., and *Scenedesmus acutus* were increased when DMB was utilized as a sole nitrogen source [142]. DMB can be used as a potential feedstock for the preparation of activated carbon. DMB also functions as an active biosorbent for removing dyes and heavy metals from industrial effluents. It has been observed that when compared to raw biomass, DMB has more surface area, as algal cells are ruptured during the lipid extraction process resulting in exposure of more active sites for biosorption [143]. The protein-rich DMB can also be utilized as an animal and aquaculture feed supplement. The DMB has the ability to substitute chemical fertilizers as it contains nitrogen, phosphorus, and several other minerals that are the primary constituents of a soil fertilizer [41].

Table 2.5. Recycle of solid residues and liquid effluents for production of bioenergy and value-added products

Source of residue	Microalgal species	Application	Features	References
Liquid residue				
Thermochemical	*C. sorokiniana*	Nutrient recycling	Contains high concentration of phosphate, organic nitrogen and polysaccharides	[126]
Transesterification	-	Hydrogen, syngas, butanol	Releases high amount of crude glycerol	[144]
	Chlorella minutissima	Microalgal biomass and lipid production	Glycerol is a rich source of carbon	[145]
Solid residue				
Thermochemical	*Chlorella vulgaris*	Wastewater treatment	COD, NO_3, NH_3 and PO_4 was reduced by 53.3%, 58.6%, 94.7%, 59.7%	[48]
	Spirulina sp.	soil amendment	Contains 11.82% C, 1.81% H, 1.41% N and 0.61% S	[131]
Transesterification	*Scenedesmus dimorphus*	Bioethanol	Fermentation of DMB produced 0.26 g g^{-1} of bioethanol	[137]
	Chlorella sp.	Activated carbon	Activated carbon with 840 m^2 g^{-1} and 0.46 cm^2 g^{-1} surface area and total pore volume respectively	[146]
	Botryococcus braunii	Biogas	AD of glycerol:DMB = 10:90 produced 448 mL CH_4 g^{-1} VS	[147]
	Nannochloropsis oceanica, *Desmodesmus* sp.	Dietary source	DMB of these two species served as an iron and protein source for an anemic pig	[148]
	Chlorella pyrenoidosa	Methane	28.38% energy recovered as methane from DMB	[149]

2.5 Knowledge gaps and objectives

The literature survey was motivated to grab the particular node, which was a significant lacuna in the earlier work published. Based on the knowledge gaps, the major five objectives of the current research were decided and planned accordingly.

2.5.1 Knowledge gaps

The above literature survey showed significant reports on the potential of microalgal wastewater treatment and biofuel production. However, limited studies are focused on developing a sustainable biorefinery model to integrate microalgal based domestic sewage wastewater treatment, biofuel production, and production of value-added co-products from the residues. Additionally, no significant studies explored the feasibility of co-feedstocks, such as microalgal biomass and sewage sludge for biocrude production.

Hence, to develop one such biorefinery model, a study is required to carry out from the very beginning that includes isolation and screening of potential microalgal strains, process optimization on wastewater treatment, process scale-up, conversion of biomass to biofuel, and valorization of residues.

2.5.2 Objectives:

With an aim to develop a sustainable microalgal biorefinery model, the following objectives are selected, and an extensive study was carried out.

1 Isolation, identification, and screening of native microalgal strains from domestic sewage wastewater (DSW) for biofuel production.

2 Optimization and process development for enhanced biomass production in flat-panel photobioreactor.

3 Process optimization for fed-batch mode of biofuel feedstock production in flat-panel photobioreactor.

4 Process development for biocrude production via Co-HTL of microalgal biomass and domestic sewage sludge.

5 Valorization of bioenergy residues for biorefinery applications.

Chapter 3

Materials and Experimental Methods

3.1. Wastewater collection and microalgae isolation

The domestic sewage wastewater (DSW) (Table 3.1) samples were collected from the primary settler of the sewage treatment plant, located at the Indian Institute of Technology Guwahati, India (Fig. 3.1). Initially, solid particles present in collected DSW were allowed to settle, and then it was filtered using Whatman® filter paper 42. Then spread plate and streak plate culturing were carried out on BG11 agar plates (1.5% agar (w/v)) followed by serial dilutions to isolate native microalgal strains [82]. The purity and morphological identification of the axenic microalgal strains were confirmed by microscopic observation (Axio Scope.A1, Zeiss, USA). Genetic identification was carried out using 18S rRNA gene partial sequencing method using forward primer ITS1 (5′-TCCGTAGGTGAACCTGCGG-3′) and reverse primer as ITS4 (5′-TCCTCCGCTTATTGATATGC-3′). The obtained sequences were subjected to nucleotide BLAST search at the National Centre for Biotechnology Information (NCBI) database to identify species that were closest to these strains. Further, a phylogenetic tree of isolates was constructed using the Neighbour-Joining algorithm by using MEGA 7.0 software [150]. The obtained sequences were later submitted in GeneBank, NCBI, and respective accession numbers were obtained for future references.

Table 3.1. Characteristics of collected DSW effluent before supplementation of NO_3^- and PO_4^{3-}

Components	RDSW	ADSW
pH	7.81 ± 0.38	7.92 ± 0.11
COD (mg L^{-1})	166 ± 12.77	143.7 ± 9.52
NO_3^- (mg L^{-1})	8.3 ± 0.48	5.88 ± 0.2
PO_4^{3-} (mg L^{-1})	10.7 ± 0.42	7.3 ± 0.48
NH_4^+ (mg L^{-1})	44.7 ± 1.92	38.4 ± 3.68

Fig. 3.1. Sewage treatment plant, located at the Indian Institute of Technology Guwahati, India.

3.2. Experimental design

3.2.1. Screening of wastewater and microalgal strain

An equimolar nitrate and phosphate of BG11 were added to the DSW to support microalgal growth that had a low-nutrient content. After supplementing nutrients, growth studies of all isolated strains were performed in raw DSW (RDSW), autoclaved DSW (ADSW), and BG11 medium as control. All batch experiments were conducted in 500 mL Erlenmeyer flasks containing 250 mL of growth medium (Fig. 3.2) with an initial biomass of 0.02 g L^{-1}. Light intensity of 100 µmol $m^{-2}s^{-1}$ was provided using fluorescent tubes with 16:08 h of light and dark period. The experiments were performed at 25 ± 2 °C, with continuous aeration of atmospheric air (0.5 vvm) for uniform culture mixing. The culture pH was maintained at 7-8 with an external supply of CO_2 at a regular interval. During the culture period, samples were collected every alternate day to estimate the growth and nutrient removal rate of the isolates. At stationary phase, all culture flasks were harvested by centrifugation (Harmle Z300, Hettich, Germany) at 6000 rpm for 15 min, and wet biomass was oven-dried at 80 °C until constant weight (DCW) was achieved. Further, an extensive study of biomass feedstock was carried out to evaluate its feasibility for bioenergy production.

Fig. 3.2. Screening study of wastewater and microalgal strains in flasks.

3.2.2. Batch optimization of growth parameters

The batch optimization of *Monoraphidium* sp. KMC4 (potential strain identified from screening study) growth in RDSW medium was performed in two phases. In the first phase of studies, optimization was performed in 500 mL flasks containing 250 mL of culture volume. In the second phase, scaled-up studies were performed in 25 L flat-panel indoor photobioreactor (PBR) with a culture volume of 20 L (Fig. 3.3).

During optimization in flasks, several growth parameters were studied for maximum biomass yield that includes nitrate (0.5-1.75 g L^{-1}), phosphate (10-60 mg L^{-1}), temperature (20-35 ℃), inoculum volume (5-25% v/v), and light intensities (70-130 PPFD). The initial biomass was 0.02 g $L^{-1,}$ and light intensity was 100 µmol $m^{-2}s^{-1}$ (fluorescent tubes) with 16:08 h of light and dark period for these experiments. The culture temperature was maintained at 25 ± 2 °C, with continuous aeration of atmospheric air (0.5 vvm). The culture pH was maintained at 7-8 with an external supply of CO_2 at a regular interval. Further, the optimal growth parameters from the flask studies were used for the scaled-up studies in PBR. However, to enhance biomass yield at scaled-up conditions, the effect of inoculum, light, and CO_2 concentrations were also studied. All PBR experiments were performed at 25 ± 2 °C, 16:08 h of light and dark period, and with a continuous aeration at 0.5 vvm. Samples were collected on alternate days to estimate growth and nutrient removal profiles until cells reached the stationary phase. After completion of experiments, biomass was allowed for auto-sedimentation overnight (media pH at 9) and stored at 4 °C for further studies.

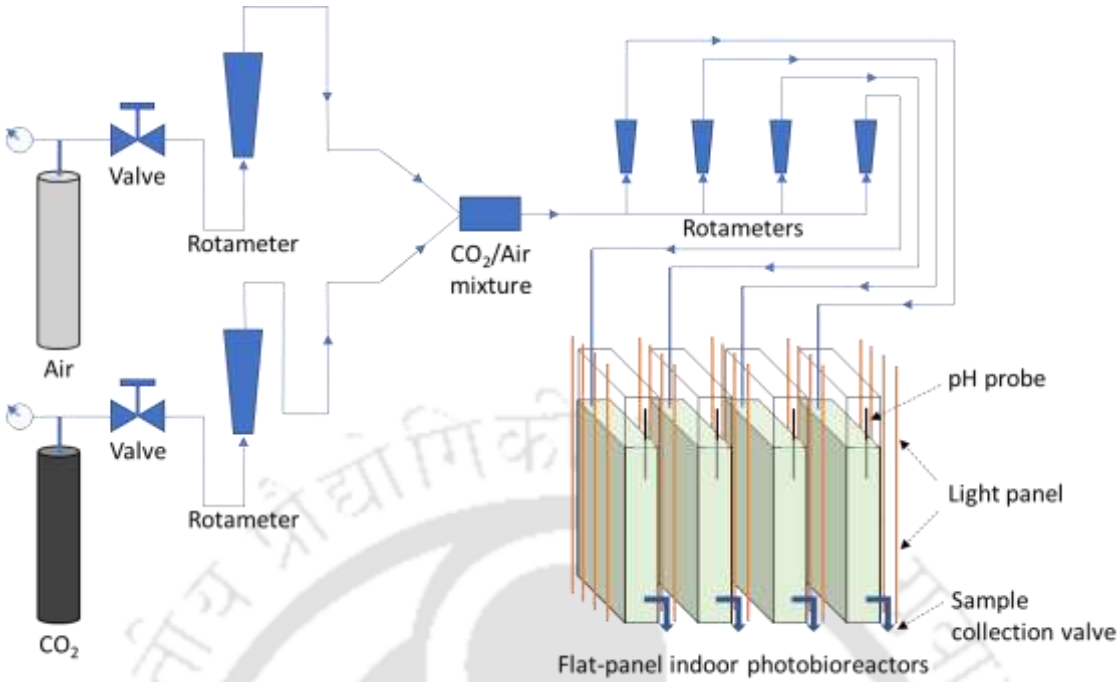

(a)

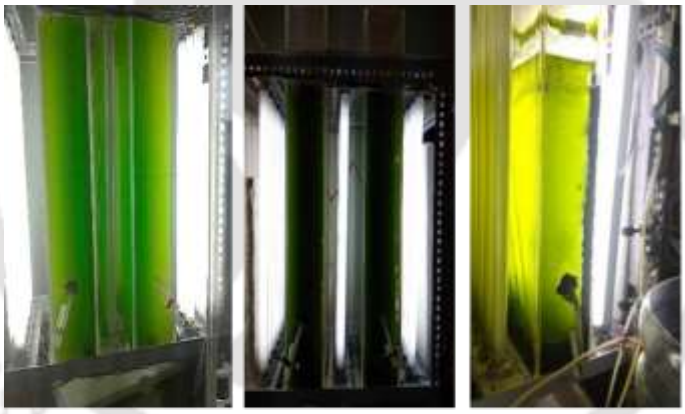

(b)

Fig. 3.3. (a) Schematic of photobioreactor experimental setup, (b) Different phases of KMC4 culture in photobioreactor.

3.2.3. Fed-batch and semi-continuous in PBR

Both these experiments were performed in 25 L flat-panel indoor photobioreactor (PBR) with a culture volume of 20 L using *Monoraphidium* sp. KMC4 as the potential strain. During the fixed volume fed-batch study, an intermittent feeding

of nitrate and phosphate was done to maintain the nutrients at its optimal concentration. In semi-continuous mode of operation, after reaching the maximum specific growth rate, 10% (v/v) of culture was periodically harvested, and to retain final culture volume fresh RDSW medium was added into the reactor. Other culture conditions such as temperature, pH, light, and photoperiod were maintained as per the optimal batch study. During the culture period, growth, pH, and nutrient consumption (nitrate, phosphate, ammonia, COD) were periodically observed. Further, biomass was harvested from the PBR as per the batch process and stored at 4 °C for further studies.

3.2.4. Transesterification

A two-step based transesterification process was followed to study the feasibility of biodiesel production [31]. In brief, neutral lipid extracted from harvested biomass was endured for esterification, and then transesterification was followed to obtain fatty acid methyl esters (FAME). Esterification was done using sulphuric acid as the catalyst to reduce the acid value of the lipid [151]. Initially, 250 mg of neutral lipid was placed in a 25 mL two necked round-bottom flask. In its first step, H_2SO_4 (1.5 wt. % of lipid) was used as an acid catalyst for the esterification step. In the second step, NaOH (1.5 wt. % of lipid) was used as the base catalyst towards transesterification process. During both these steps lipid: methanol of 1: 20 (molar ratio), reaction time three hour and reaction temperature 70 ± 2 °C was maintained. On completion of each step, the product was transferred to separating funnel where water was added to separate glycerol and catalyst from FAME. The reaction conditions (concentrations of H_2SO_4, NaOH, methanol to oil ratio, duration of reaction, temperature) are obtained after series of optimization performed on microalgal lipids to achieve maximum FAME yield.

3.2.5. Hydrothermal liquefaction (HTL) and product separation

The HTL studies were done in two-phase (i) HTL of *Monoraphidium* sp. KMC4, then (ii) Co-HTL of KMC4 and domestic sewage sludge (DSS). The slurry of KMC4 biomass was obtained after RDSW treatment in a 25 L flat-panel indoor photobioreactor. DSS was collected from the primary settler of the sewage treatment plant, located at the Indian Institute of Technology Guwahati campus, India. To reduce ash content, the collected DSS was well stirred and then kept undisturbed overnight at

4 °C. This allowed the larger solid particle to settle, and the upper slurry was used as feedstock. The proximate and ultimate analyses and biochemical composition of the feedstocks are presented in (Table 3.2).

Table 3.2. Physicochemical characteristics of KMC4 and DSS.

Components	KMC4	DSS
Proximate composition		
Moisture (wt%)	4 ± 0.5	4.6 ± 0.8
Volatile matter (wt%)[a]	74 ± 0.8	56 ± 1.1
Fixed carbon (wt%)[a]	15.26 ± 0.2	8.4 ± 0.21
Ash (wt%)[a]	6.74 ± 0.1	31 ± 0.26
Ultimate composition		
C (wt%)[a]	47.91 ± 0.11	35 ± 0.13
H (wt%)[a]	7.83 ± 0.05	6.52 ± 0.08
N (wt%)[a]	6.8 ± 0.1	8.3 ± 0.08
S (wt%)[a]	0.17 ± 0.01	1.68 ± 0.06
O (wt%)[b]	30.55 ± 0.13	17.5 ± 0.11
HHV (MJ Kg^{-1})[a]	21.38 ± 0.33	18 ± 0.27
Biochemical composition [a]		
Carbohydrate (wt%)	27.4 ± 2.2	-
Protein (wt%)	39.7 ± 1.07	-
Lipid (wt%)	28.86 ± 2.9	-

[a]Dry basis
[b]By difference

The HTL experiments were performed in a 100 mL high-temperature high-pressure stirred autoclave reactor (4598 Micro Bench Top Reactor, Parr, USA). In a typical experiment, 40 mL of aqueous slurry (10 wt% dry solid content) was fed into the reactor. Pure nitrogen gas was purged three times to create an inert atmosphere and then pressurized up to 2 MPa as an initial pressure [152]. Initial HTL experiments were performed using individual feedstocks at four different temperatures and its corresponding pressure (275 °C (~6 MPa), 300 °C (~8.5 MPa), 325 °C (~12 MPa), and 350 °C (~16.5 MPa)) (heating rate ~5 °C min^{-1}) at a residence time of 30 min and continuous agitation of 400 rpm. The reaction pressure was not controlled and maintained as it was auto-generated to its reaction temperature. During the Co-HTL, the effect of temperatures (275 °C-350 °C), feedstock ratio (25:75, 50:50, and 75:25 wt% of KMC4:DSS) and residence time (15 min, 30 min, 45 min, and 60 min) on

biocrude yield was studied. In all such experiments, the residence time did not include the preheating time.

After completion of each batch study, the reactor was quenched in a room temperature water bath (~25 °C) and depressurized by releasing the gas. Subsequently, dichloromethane (DCM) of 10 mL was added to the reactor to extract the organic components from both liquid and solid products. The product mixture (containing aqueous phase, biocrude, and solid residue) was transferred to centrifuge tubes and centrifuged at 4500 rpm for 15 min to separate each phase. Then, it was filtered using Whatman® filter paper 42. The total solid residue was rinsed repeatedly with DCM to extract any residual biocrude. The remaining solids were oven-dried at 105 °C overnight to determine the solid residue yield. DCM was separated from the biocrude using a rotary evaporator (Rotavapor® R-210, Buchi, Switzerland) under a vacuum of about 1 kPa at 35 °C for 20 min and the moisture-free biocrude was quantified gravimetrically. The biocrude samples were stored at -20 °C for further analysis. Accurate collection and quantification of gas volume in our present setup was impeded due to low gas yield from limited feedstock loading. Therefore, the present study did not focus on analyzing gaseous products. The detailed experimental procedures and product separation is described in Fig. 3.4.

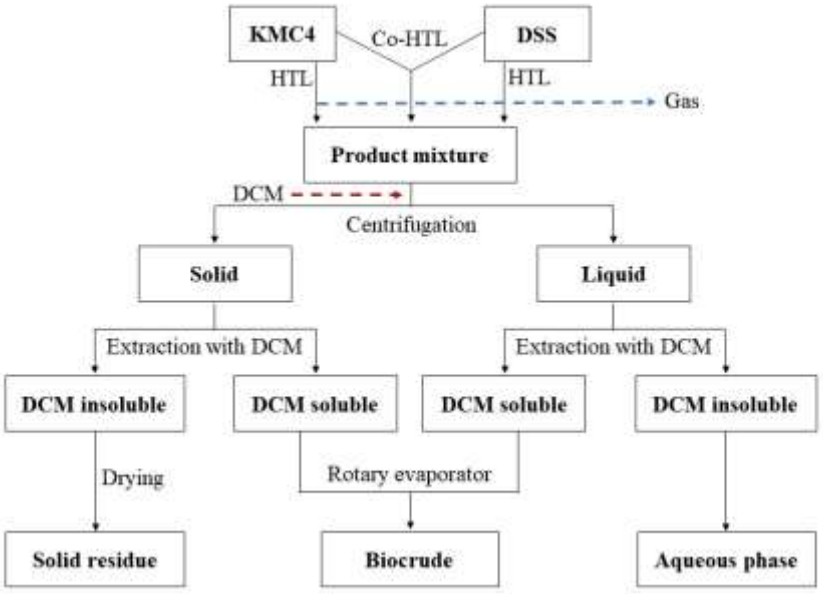

Fig. 3.4. Experimental flowchart for separation of HTL and Co-HTL products

3.2.6. Hydrothermal carbonization (HTC) and product separation

After lipid extraction, the residual lipid-extracted microalgal biomass (LEMB) was studied as a feedstock for bioenergy production via hydrothermal carbonization (HTC). During this, 40 mL of LEMB aqueous slurry (10 wt.% dry LEMB powder) was loaded into an autoclave reactor (4598 Micro Bench Top Reactor, Parr, USA). To create an inert atmosphere, pure nitrogen gas was purged three times and pressurized up to 2 MPa as an initial pressure. To optimize the reaction conditions, HTC experiments were performed at three different temperatures of 200 °C, 225 °C, 250 °C (heating rate ~5 °C min^{-1}), two different residence time (30 min and 60 min) and with continuous agitation of 400 rpm.

At the end of each batch experiment, the reactor was quenched and depressurized as per the HTL experiments. The slurry was centrifuged at 400 rpm to separate the solid (hydrochar) and aqueous phase. Further, hydrochar was oven-dried at 105 °C for overnight, and product yield was estimated gravimetrically. The comprehensive characterization of hydrochar was followed to explore its bioenergy potential.

3.3. Analytical methods

3.3.1. Microalgal growth and biomass estimation

The spectrophotometric method of microalgal growth estimation was followed every alternate day by taking optical density (OD) of cultures at 680 nm (Thermo Fisher Scientific, USA) until cells reached the stationary phase. Dry cell weight (DCW) was estimated using respective standard curves that were prepared for each strain and culture medium (R^2 greater than 0.98). At the stationary phase, cultures were harvested by centrifugation (Harmle Z300, Hettich, Germany) at 6000 rpm for 15 min, followed by oven drying at 80 °C until constant weight (DCW) was achieved. Overall biomass productivity (Pb, mg L^{-1} d^{-1}), specific growth rate (μ, d^{-1}), and cell doubling time (TD, d^{-1}) were calculated using equations 3.1-3.3 [31,81,97].

3.3.2. Nutrient composition

The nutrient composition of wastewater samples, culture medium, and HTL aqueous phase was estimated. Ammonia, nitrate, and phosphate concentration were

estimated by protocols prescribed by APHA (APHA, 1998). COD was estimated using HACH COD reagents and quantified in the DR900 calorimeter (Hach, USA), whereas, total organic carbon (TOC) was measured using a TOC analyzer (model no. 1030, O-I-Analytical, Aurora, USA). The nutrient removal efficiency (RE %) and removal rates (*RR*, g L^{-1} d^{-1}) were calculated using the following equations (3.4-3.5) [81].

3.3.3. Biochemical composition

Biochemical compositions such as carbohydrate, protein, lipid, and pigments were estimated from the harvested microalgal biomass. The carbohydrate and protein content was estimated by the phenol-sulphuric acid and the Biuret method [153]. Chlorophyll a, b, and carotenoids estimation was done by spectrophotometric based pigment estimation as reported previously [154]. Lipid extraction was performed using Soxhlet extraction setup. Powered dried microalgal biomass was placed in a thimble, and to extract polar and neutral lipids, methanol and n-hexane were used as extracting solvents. The extraction temperature was maintained at 65 ± 2 °C until completion of the process. Extracted lipid-solvent mixtures were further separated using a rotary evaporator (Rotavapor® R-300, Buchi, Switzerland), and moisture-free lipids were quantified gravimetrically.

3.3.4. Proximate and ultimate analysis

Proximate composition (moisture, volatile matter, fixed carbon, and ash) of feedstocks (microalgal biomass and sewage sludge) were estimated by the ASTM standards (E-871, D1102-84) as reported earlier [155]. Briefly, the moisture content (MC) was estimated by placing the samples in a hot air oven (Optics Technology Delhi, India) at 105 °C for 1 h. The volatile matter (VM) was estimated after moisture free samples were kept in a muffle furnace (Optics Technology, Delhi India) for 7 min at 925 ± 10 °C. Then, the Ash content was determined after VM free samples kept at 575 ± 10 °C for 4 h. Before the estimation of weight difference, samples were placed in a desiccator for isothermal cooling. The fixed carbon (FC) was calculated by using the equation (3.6). For ultimate analysis, elemental compositions (C, H, N, S) of moisture and solvent-free samples were estimated in a CHNS analyzer (Flash EA 1112 series, Thermo Finnigan, Italy). The oxygen content was estimated by difference.

3.3.5. TGA, FTIR, and ICP-AES analysis

The pyrolysis and combustion property of biomass and hydrochar samples were studied using a thermogravimetric analyzer (TGA) (STA7200, Hitachi, Japan) in an atmosphere of air and nitrogen (50 mL min^{-1}). Dry samples of 8-10 mg was loaded into a platinum crucible and temperature was programmed from room temperature to 900 °C at a heating rate of 20 °C min^{-1}. The sample weight loss with effect to rise in temperature was recorded, and then TGA data were collected. Additionally, TGA was also followed for the distillation profile of biocrude (moisture and solvent-free sample) using the aforementioned procedure under nitrogen atmosphere.

To understand the presence of various functional groups in biomass and biocrude, Fourier transform infrared spectroscopy (FTIR) analysis was conducted using IRAffinity-1 (Shimadzu, Japan). The IR range used was between 400 cm^{-1} and 4000 cm^{-1} at a scan rate of 20 and a step size of 4 cm^{-1}.

Mineral elements present in the optimal Co-HTL feedstock (75:25 wt%; KMC4:DSS) and biocrude were analyzed using ICP-AES (ARCOS, Simultaneous ICP Spectrometer, SPECTRO Analytical Instruments GmbH, Germany).

3.3.6. GC and GC-MS analysis

The FAME and biocrude compositional analysis was done using the gas chromatographic method. The FAME samples were analyzed in gas chromatography (7890 A GC System, Agilent Technology) equipped with an FID detector with the support of AOCS official method 1998, Ce 1-62, and Ce 2-26. Further, FAME conversion was estimated as reported previously [156].

The chemical composition of biocrude was analyzed with a gas chromatography-mass spectrometry (GC-MS) (450-GC, 240-MS, Varian, USA). The GC-MS was equipped with a column Agilent VF-5ms (30m×0.25mm×0.25 μm), and helium was the carrier gas at a flow rate of 1 mL min^{-1}. Biocrude was diluted 100 times in DCM and filtered by 0.2 μm PTFE membrane filters before injection. An injection volume of 1 μL was used, and the injector temperature was maintained at 300 °C at a split ratio of 1:10. The column temperature was set at 80 °C for 2 min, then ramped up at a rate of 8 °C min^{-1} to 140 °C and then at 4 °C min^{-1} to 280 °C and was kept isothermal for 2 min. The mass spectrometer was set to an ionizing voltage of 70 eV with a scan range of 50 to 1000 m/z. The compounds were identified by comparing

the spectra of the samples with the electron impact mass spectrum from NIST Database.

3.4. Mathematical equations

Biomass productivity (Pb, mg L^{-1} d^{-1}), specific growth rate (μ, d^{-1}), and cell doubling time (TD, d^{-1}) were calculated using the following equations [31,81,97].

$$P_b = \Delta X / \Delta t \quad \textbf{(3.1)}$$

$$\mu = ln\,(W_1/ W_0)/\Delta t \quad \textbf{(3.2)}$$

$$T_D = ln2/\mu \quad \textbf{(3.3)}$$

where, "ΔX" is the variation of biomass concentration (mg L^{-1}) within a cultivation time of "Δt" (d), "W_1" and "W_0" are the biomass concentration (g L^{-1}) at the end and the beginning of a batch run.

The nutrient removal efficiency (RE %) and removal rates (*RR*, g L^{-1} d^{-1}) were calculated using the following equations [81].

$$RE = ((S_0 - S_t)/ S_0)\ X\ 100 \quad \textbf{(3.4)}$$

$$RR = (S_0 - S_t)/(t_t - t_0) \quad \textbf{(3.5)}$$

where, "S_0" and "S_t" are the initial and final concentrations (in mg L^{-1}) of the pollutant at initial "t_0" and final "t_t" time (days), respectively.

The fixed carbon (FC) was calculated by using the following formula:

$$FC(\%) = 100 - (MC\ (\%) + VM\ (\%) + Ash\ content\ (\%)) \quad \textbf{(3.6)}$$

where, "*MC*" is moisture content and "*VM*" is volatile matters.

HTL and Co-HTL product quantification and estimation of energy values were quantified with the following equations (dry feedstock), as reported earlier [32,152].

$$\text{Biocrude yield (wt.\%)} = m_{\text{dry biocrude}}/m_{\text{dry feedstock}} \times 100\% \quad \textbf{(3.7)}$$

Solid residue yield (wt.%) = $m_{dry\ residue}/m_{dry\ feedstock} \times 100\%$ **(3.8)**

Aqueous phase yield (wt.%) = $m_{aqueous\ product}/m_{dry\ feedstock} \times 100\%$ **(3.9)**

Conversion (wt.%) = $100\% - Y_{dry\ solid\ residue}$ **(3.10)**

Energy recovery (ER%) = $HHV_{biocrude} \times Y_{biocrude}/HHV_{dry\ feedstock} \times 100\%$ **(3.11)**

High heating value (HHV) = 0.3383C + 1.422 (H-O/8) **(3.12)**

where, C, H, and O are the mass percentages of carbon, hydrogen, and oxygen, respectively [152].

Chapter 4

Results and Discussion

4.1. Isolation, identification, and screening of microalgal strains and growth medium

4.1.1. Morphological and genetic identification of microalgal strains

In the present study, eight native microalgal strains were isolated from DSW to develop a sustainable process for microalgal based wastewater treatment coupled with biofuel production under the biorefinery approach. An initial morphological study performed under a microscope showed that all axenic strains were morphologically distinct from each other (Fig. 4.1). Strain KMC1 was found to have spherical cells of three to four clustered together in single mucilage sheath of 4-10 µm cell diameter. Later, three other strains KMC2, KMC4, and KMC7, were found to be from the same genus; however, they had completely distinct morphological features. KMC2 was of lunate shaped unicellular cells with 4-10 µm, KMC4 was among the smallest (2-6 µm) pear and cylindrically shaped cells, and KMC7 having long diameter slender cells (8-20 µm) with few were helically twisted, and few were sigmoidal shaped. The unclustered oblong or ovate shaped KMC3 strains were of 4-10 µm diameter, whereas KMC6 was found to be clustered spindle-shaped cells of 8-20 µm size. Also, spherical shaped KMC5 (2-6 µm) was unicellular, whereas KMC8 (4-10 µm) was colonial chlorophyte, which was not enclosed in a mucilage sheath. Beside morphological study, genetic identification was performed by the sequences obtained after 18S rRNA sequencing and was compared with most similar sequences retrieved from the NCBI database [31,81]. This further revealed that KMC1 had shown 97% similarity to *C. parallestriata* SAG 14.88 (LC086338). KMC2, KMC3, KMC4, KMC5, KMC6, KMC7, and KMC8 had shown above 98% similarity with *M. convolutum* CCAP 202/10C, *D. abundans* CCAP 211/23, *Monoraphidium* sp. HSJA2, *C. sorokiniana* 34-

2, *S. deserticola* BCP-YPGChar, *M. contortum* KMMCC 187, and *M. pusillum* SAG 48.93. In consideration to the higher similarity and clear clusters observed in the phylogenetic study (Fig. 4.2), isolated strains were identified and termed as *Chlamydomonas parallestriata* KMC1, *Monoraphidium convolutum* KMC2, *Desmodesmus abundans* KMC3, *Monoraphidium* sp. KMC4, *Chlorella sorokiniana* KMC5, *Acutodesmus deserticolal* KMC6, *Monoraphidium contortum* KMC7, and *Micractinium pusillum* KMC8 respectively.

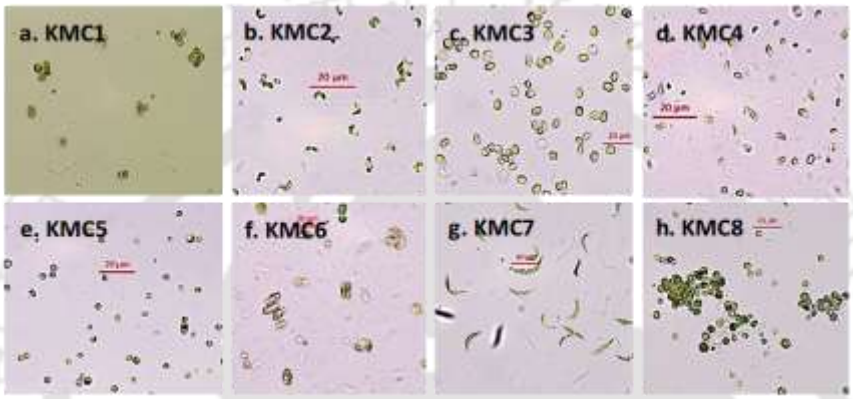

Fig. 4.1. Microscopic image of microalga strains (a) *Chlamydomonas parallestriata*, (b) *Monoraphidium convolutum*, (c) *Desmodesmus abundans*, (d) *Monoraphidium* sp., (e) *Chlorella sorokiniana*, (f) *Scenedesmus deserticolal*, (g) *Monoraphidium contortum*, (h) *Micractinium pusillum*.

Table 4.1. Molecular identification of microalga strains isolated from DSW in this study.

Strain ID	Strain Name	Accession Number	Closest BLAST equivalent and accession number	Similar (%)
KMC1	*Chlamydomonas parallestriata*	MF179625	*Chlamydomonas parallestriata* SAG 14.88 (LC086338)	97
KMC2	*Monoraphidium convolutum*	MG597604	*Monoraphidium convolutum* CCAP 202/10C (MG022710)	99
KMC3	*Desmodesmus abundans*	MG597605	*Desmodesmus abundans* CCAP 211/23 (MG022724)	99
KMC4	*Monoraphidium sp.*	MH183246	*Monoraphidium* sp. HSJA2 (KR061995)	98
KMC5	*Chlorella sorokiniana*	MG597606	*Chlorella sorokiniana* 34-2 (KU948991)	99
KMC6	*Acutodesmus deserticolal*	MG597607	*Scenedesmus deserticola* BCP-YPGChar (AY510463)	99
KMC7	*Monoraphidium contortum*	MG597608	*Monoraphidium contortum* KMMCC 187 (JQ315547)	99
KMC8	*Micractinium pusillum*	MG597609	*Micractinium pusillum* SAG 48.93 (AF364102)	99

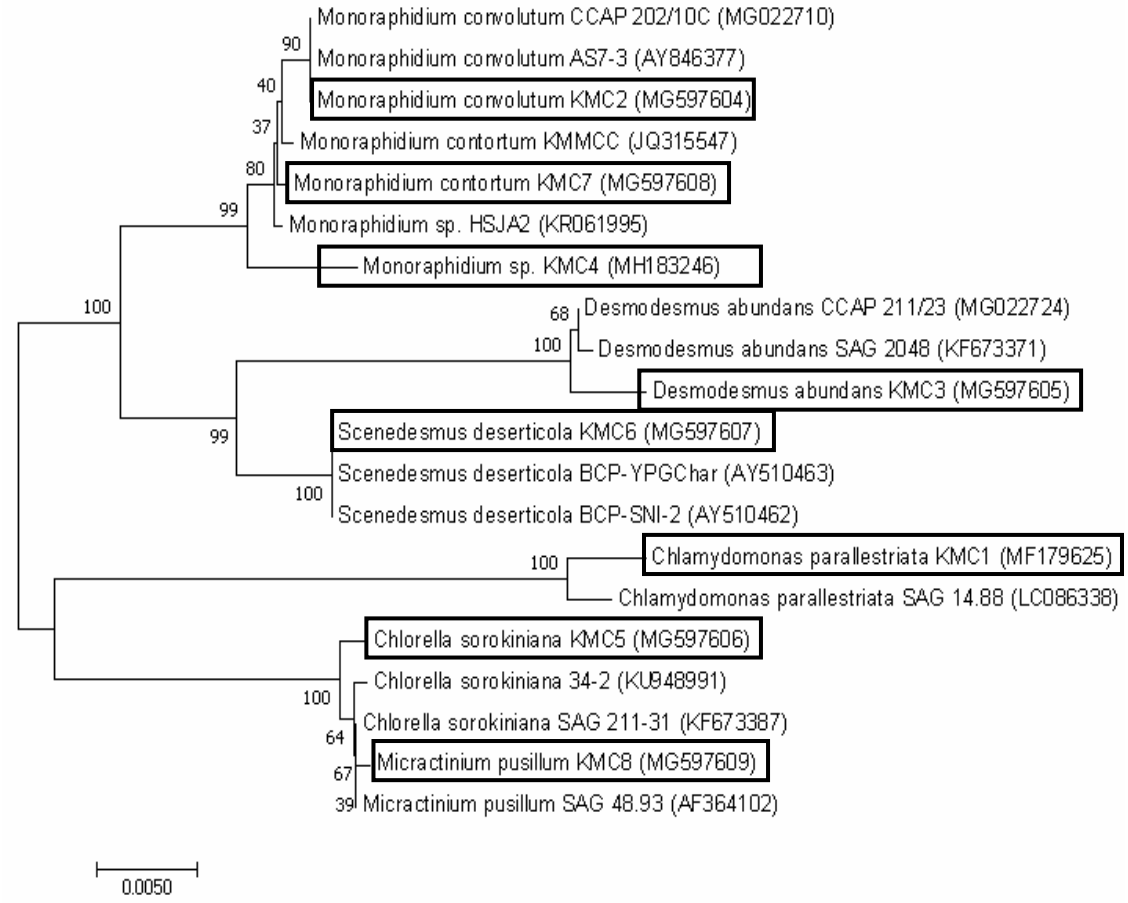

Fig. 4.2. Phylogenetic tree of eight isolated microalgae and the closely related strains from the NCBI nucleotide database.

4.1.2. Screening of potential growth media and microalgal strain

4.1.2.1. Growth study

Isolated native strains were grown in RDSW, ADSW, and control BG11 to select potential microalgal strain and respective DSW growth medium and the results are presented in Fig. 4.3 and Table 4.2. From Fig. 4.3a,b it can be observed that all isolates had shown significant growth in RDSW than the ADSW growth medium, which could be due to the lack of an ideal adaptation phase [82]. Among all, KMC2, KMC3, KMC4, and KMC5 were found to be promising strains in the RDSW medium that expressed an early exponential growth phase with two days of lag phase. The growth phase sustained until the 13th day of culture and later reached an early stationary phase with biomass productivity between 100-123 mg L^{-1} d^{-1}. However, other strains resulted in comparatively less biomass productivity (68-88 mg L^{-1} d^{-1}) in

the RDSW medium (Table 4.2). Recently Shen et al. [81] reported that the autoclaving of real wastewater significantly inhibit the growth of isolated microalgae strains. In agreement with that, the present study also found unfavourable growth of isolates in the ADSW medium (Fig. 4.3b). This resulted in an extended lag phase and significantly affected the native strains growth rate. A recent study suggested that the presence of bacterial community support symbiotic system when co-cultured with native microalgal strain [86]. Thus, the study signifies the use of RDSW as a potential growth medium.

Among all these eight isolates, *Monoraphidium* sp. KMC4 was found to be the potential strain in evidence to its greater adaptability in RDSW medium and higher exponential growth. In consideration to its optimal growth, KMC4 achieved superior growth rate (0.27 ± 0.01 d^{-1}), biomass productivity (122.5 ± 4.3 mg L^{-1} d^{-1}), and lowest doubling time (2.48 ± 0.06 d) (Table 4.2). Additionally, biomass yield of 1.47 ± 0.09 g L^{-1} in the RDSW medium was found relatively higher than other isolates in RDSW and ADSW medium. These results are comparatively higher than previous studies where potential microalgae strains were used for the treatment of different wastewater and biofuel production [81,83,90,157].

Besides the growth study in DSW, the optimal growth potential of all isolates was evaluated in control BG11. From Fig. 4.3c, it can be observed that all native strains had shown enhanced growth profile, though; KMC4 outperformed all others with a maximum biomass yield of 1.57 ± 0.1 g L^{-1} at a biomass productivity of 131.66 ± 4.8 mg L^{-1} d^{-1}. These results are comparable to the previous study, where *Ankistrodesmus falcatus* achieved biomass productivity of 198.46 mg L^{-1} d^{-1} in optimized wastewater. In contrast, higher biomass productivity (211.64 mg L^{-1} d^{-1}) was obtained from the control BG11 medium [158]. Similarly, *Chlorella vulgaris* FACHB-8 resulted in higher biomass yield in control BG11 medium than swine wastewater growth medium [82]. On the other hand, the study also found enhanced biomass productivity from 353.36 mg L^{-1} d^{-1} to 498.12 mg L^{-1} d^{-1} as an effect of optimization on low nutrient strength wastewater [27]. In this context, RDSW supplemented with equimolar nitrate and phosphate of BG11 was found not to be

optimal for KMC4. However, further optimization of the RDSW medium could significantly enhance biomass yield.

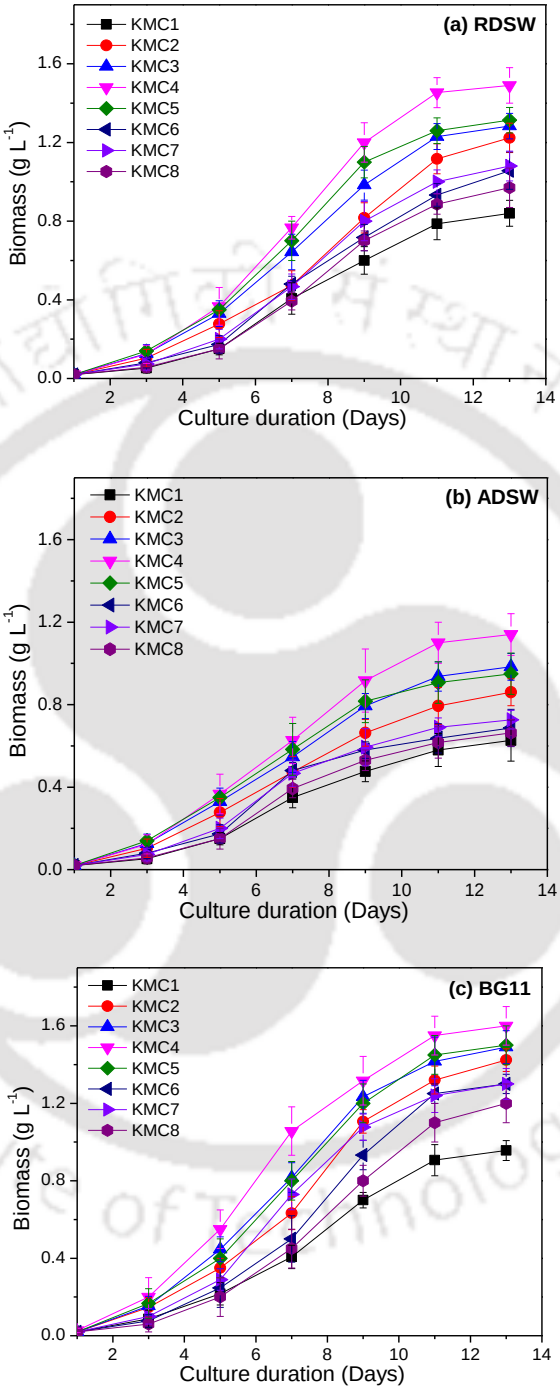

Fig. 4.3. Growth study of microalgal strains in (a) RDSW, (b) ADSW, and in control (c) BG11 medium.

Table 4.2. The growth performance of isolated microalgal strains grown in different growth mediums.

Microalgal strains	Biomass yield (gL^{-1})		P_B ($mgL^{-1}d^{-1}$)		μ (d^{-1})		T_D (d^{-1})	
	RDSW	BG11	RDSW	BG11	RDSW	BG11	RDSW	BG11
KMC1	0.84 ± 0.06	0.93 ± 0.05	68.33 ± 3.15	78.05 ± 2.46	0.16 ± 0.01	0.24 ± 0.02	4.2 ± 0.37	2.89 ± 0.24
KMC2	1.22 ± 0.07	1.4 ± 0.05	100.27 ± 3.61	116.94 ± 2.81	0.21 ± 0.01	0.25 ± 0.01	3.22 ± 0.19	2.5 ± 0.19
KMC3	1.28 ± 0.06	1.47 ± 0.08	105.27 ± 3.13	122.5 ± 4.11	0.24 ± 0.02	0.28 ± 0.01	2.94 ± 0.32	2.47 ± 0.16
KMC4	1.47 ± 0.09	1.57 ± 0.1	122.5 ± 4.33	131.66 ± 4.81	0.27 ± 0.01	0.28 ± 0.02	2.48 ± 0.06	2.42 ± 0.17
KMC5	1.31 ± 0.06	1.48 ± 0.1	107.77 ± 3.13	123.33 ± 4.81	0.23 ± 0.03	0.27 ± 0.02	3.05 ± 0.47	2.53 ± 0.26
KMC6	1.06 ± 0.09	1.28 ± 0.05	86.38 ± 4.57	106.66 ± 2.4	0.21 ± 0.01	0.26 ± 0.02	3.28 ± 0.23	2.7 ± 0.23
KMC7	1.09 ± 0.07	1.28 ± 0.08	88.33 ± 3.63	106.66 ± 3.84	0.2 ± 0.01	0.26 ± 0.01	3.43 ± 0.23	2.64 ± 0.11
KMC8	0.97 ± 0.1	1.18 ± 0.01	79.16 ± 4.81	98.33 ± 4.81	0.18 ± 0.02	0.25 ± 0.01	3.88 ± 0.55	2.69 ± 0.16

4.1.2.2. Nutrient uptake

Considering low-nutrient strength in DSW, nitrate and phosphate were supplemented to support native microalgal growth metabolism and its subsequent bioenergy feedstock production. From Fig. 4.4 to Fig. 4.6, it can be observed that substantial nutrient uptake was achieved concerning an increase in biomass yield. Among all, KMC2, KMC3, KMC4, and KMC5 were successful in significant nutrient removal in the RDSW growth medium (Fig. 4.4). This was due to the excellent adaptability and presence of other microbial community that supports a symbiotic growth system [82,86]. On the other hand, decreased nutrient in ADSW inhibited

native microalgae growth and simultaneously limited nutrients consumption (Fig. 4.5). In a similar study, a decrease in TN, TP, and COD was observed due to autoclaved swine wastewater, which directly affected Chlorella vulgaris biomass yield [82].

A recent study suggested that phosphorous played a significant role in the cellular metabolism process of microalgae [159]. Due to its limited content (21.8 ± 0.04 mg L^{-1}) in all growth mediums, almost 96-100% phosphate was removed by native isolates. Among all, KMC4 was found to be the potential strain that expressed near-complete removal of phosphate at 4.3 ± 0.02 mg L^{-1} d^{-1}, 2.69 ± 0.03 mg L^{-1} d^{-1}, and 5.45 mg L^{-1} d^{-1}, in RDSW, ADSW, and BG11 mediums respectively (Fig. 4.7). However, the lowest consumption of phosphate (1.75 ± 0.04 mg L^{-1} d^{-1}) was achieved by *M. pusillum* KMC8 in the ADSW medium. These results are found comparable to previous studies, where 90-100% phosphate removal was achieved [157,158]. However, few studies also showed comparatively less phosphate removal concerning higher biomass yield [27,79,101].

Nitrogen plays a vital role in the synthesis of protein, nucleic acid, and phospholipid in microalgae, and it was present in the form of ammonia and nitrate in RDSW. The presence of COD in RDSW did support microalgae to enhance growth rate through a photo-heterotrophic mechanism. Besides, total consumption of phosphate, assimilation of ammonia, nitrate, and COD was found to be moderate in respective growth mediums. As mentioned in Table 4.3, the maximum assimilation of ammonia ($99.5 \pm 0.7\%$), nitrate ($89 \pm 2.8\%$), and COD ($88.44 \pm 2.2\%$) was obtained by KMC4 in RDSW medium at a rate of 3.7 ± 0.02 mg L^{-1} d^{-1}, 81.13 ± 2.6 mg L^{-1} d^{-1}, and 12.23 ± 0.3 mg L^{-1} d^{-1}, respectively. These results were found to be in accordance to previous studies where maximum nutrient present in wastewater was consumed by microalgae to augment various growth metabolism and resulted in high-value biomass feedstock production [83,101,157,159]. These findings validated that the RDSW medium enriched with nitrate and phosphate can opt as a promising native microalgal growth medium to generate bioenergy feedstock towards biorefinery applications.

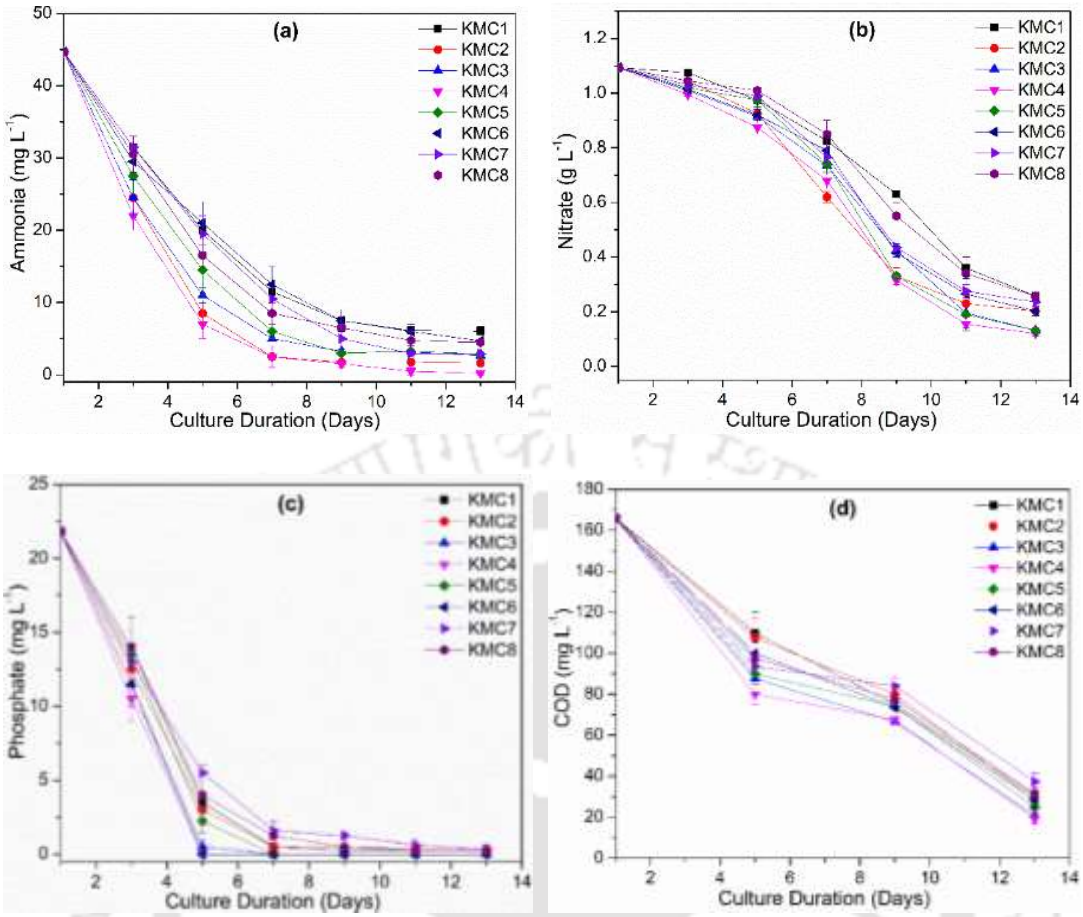

Fig. 4.4. Nutrient removal by isolated microalgae strains in RDSW medium (a) Ammonia removal profile, (b) Nitrate removal profile (c) Phosphate removal profile, and (d) COD removal profile.

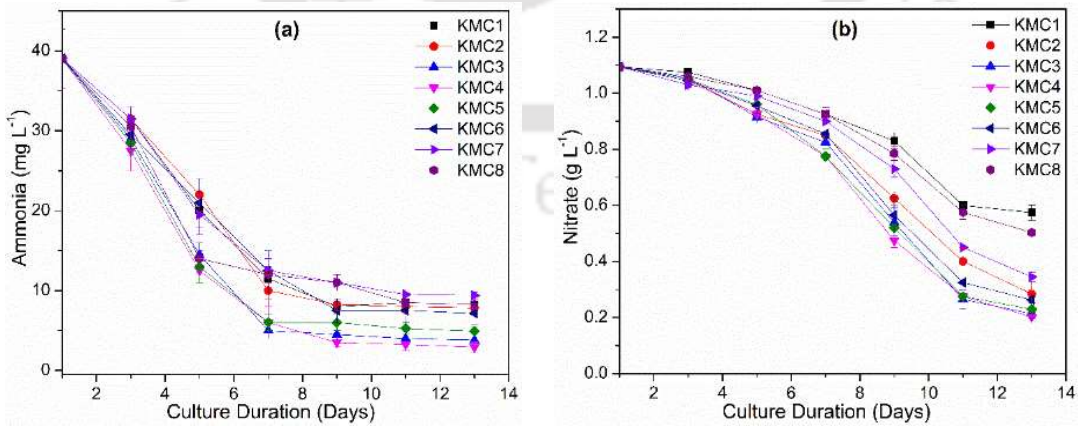

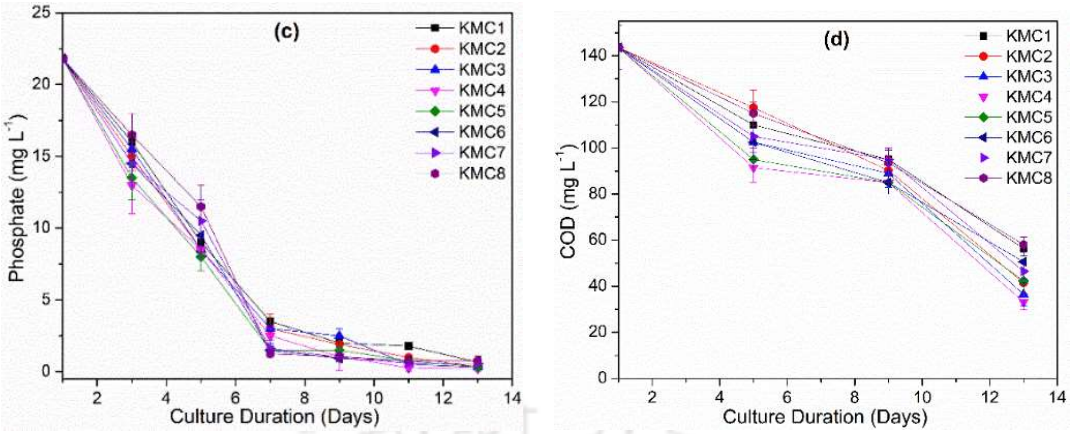

Fig. 4.5. Nutrient removal by isolated microalgae strains in ADSW medium (a) Ammonia removal profile, (b) Nitrate removal profile (c) Phosphate removal profile, and (d) COD removal profile.

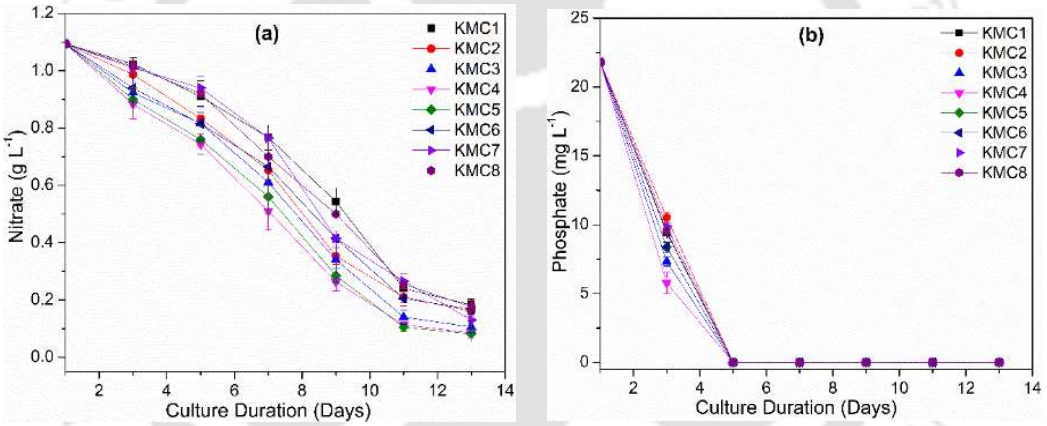

Fig. 4.6. Nutrient removal by isolated microalgae strains in control BG11 medium (a) Nitrate removal profile, and (b) Phosphate removal profile.

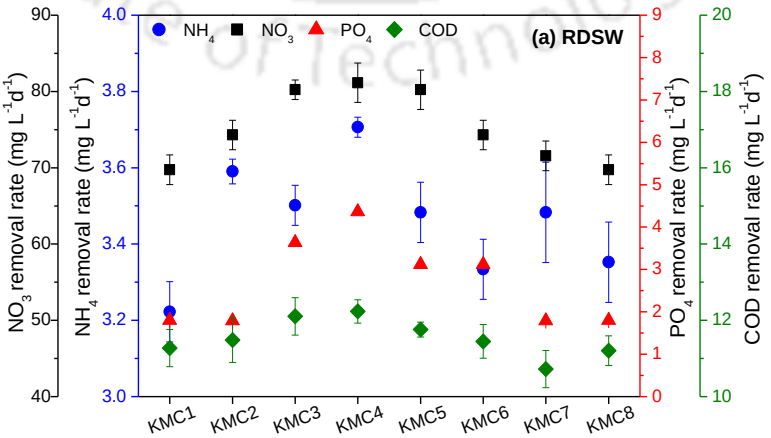

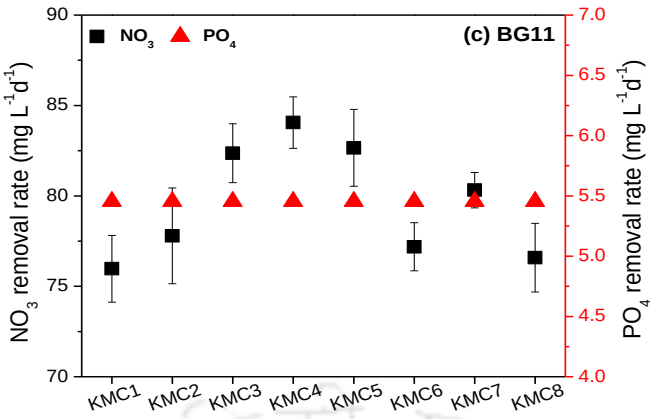

Fig. 4.7. Nutrients removal rate of microalgae strains in (a) RDSW, (b) ADSW, and in control (c) BG11 medium.

Table 4.3. Nutrient removal profile (%) of isolated microalgae in different growth mediums

Microalga	RDSW				ADSW				BG11	
strains	NH_4^+	NO_3^-	PO_4^{3-}	COD	NH_4^+	NO_3^-	PO_4^{3-}	COD	NO_3^-	PO_4^{3-}
KMC1	86.5 ± 2.12	76.5 ± 2.12	99 ± 1.41	81.5 ± 3.53	81.5 ± 2.12	47.5 ± 3.53	97 ± 2.8	66 ± 2.8	83.33± 2.02	100
KMC2	96.38 ± 0.86	81.5 ± 2.12	98.5 ± 2.12	83 ± 4.24	85 ± 7.07	74 ± 5.65	98.5 ± 2.1	75 ± 4.24	85.33± 2.9	100
KMC3	94 ± 1.41	88 ± 1.41	100	87.5 ± 3.53	91.5 ± 2.12	80.5 ± 2.11	98.5 ± 2.1	78 ± 2.2	90.34± 1.78	100
KMC4	99.5 ± 0.7	89 ± 2.82	100	88.44 ± 2.2	93.5 ± 2.12	81.5 ± 2.13	99 ± 1.4	80 ± 2.8	92.2± 1.56	100
KMC5	93.5 ± 2.12	88 ± 2.82	100	85 ± 1.41	89 ± 1.4	79 ± 1.4	98.5 ± 2.12	74.5 ± 3.53	90.66± 2.33	100
KMC6	89.5 ± 2.12	81.5 ± 2.12	100	82.75 ± 3.18	84 ± 4.24	76 ± 1.4	96.5 ± 2.1	69.5 ± 3.5	84.66± 1.45	100
KMC7	93.5 ± 3.53	78.5 ± 2.11	98.5 ± 2.1	77.5 ± 3.53	79 ± 1.41	68.5 ± 2.1	97.5 ± 0.7	72 ± 2.82	88.1± 1.06	100
KMC8	90 ± 2.82	76.5 ± 2.13	99 ± 1.4	81 ± 2.82	81.5 ± 2.1	54 ± 1.4	96.5 ± 2.1	65 ± 2.81	84 ± 2.8	100

4.1.3. Characterization of KMC4 biomass feedstock

4.1.3.1. Biomass composition

The elemental study of KMC4 biomass obtained from RDSW and the BG11 medium were found nearly similar compositions (Table 4.4). Both biomass had carbon

(48-52%) and hydrogen (7.6-8%) as major composition due to the superior lipid content, which makes it a potential feedstock for bio-oil production. The low oxygen content (35-38%) resulted in high HHV (20.33-22.14 MJ kg^{-1}) that was comparable to the previous studies [160,161]. A recent report suggested that high sulfur and nitrogen content in biomass leads to the release of harmful exhaust emission (NOx and SO_2) [31]. However, the sulfur content of the biomass in the present study was 0.08-0.13%, which was much lower as compared to the earlier reports [101,162]. In contrast, nitrogen content (5.5-5.91%) was found to be marginally higher than the previous studies [162,163] that could be due to the presence of a higher amount of nitrogen in the growth medium. Further optimization of the RDSW growth medium will significantly reduce nitrogen content in KMC4 biomass, thus, lead to lower NOx emission.

The biochemical composition of KMC4 biomass derived from two different culture media were found nearly similar as evident from their relatable ultimate compositions. Biochemical compositional study on sewage wastewater treated *Monoraphidium* sp. was not available in the literature; however, the present findings were found to be comparable to microalgal strain *A. falcatus* obtained after supplementation of 400 mg L^{-1} $NaNO_3$ to aquaculture wastewater [158]. Among all biomolecules, 30-31% of carbohydrate content was found in KMC4 biomass, which is considered as a promising substrate for bioethanol production. The protein content of 35.81% in RDSW biomass was found to be higher than the control BG11 biomass (33.7%), which was evident from its increased elemental nitrogen composition in RDSW biomass. Besides, protein content in KMC4 was found to be higher than red algae *Leptotyphlops filiformi* and also to several common vegetable feed proteins such as soybean meal, and peanut meal [157,164]. The total lipid in RDSW and BG11 was 30.07% and 31.4%, respectively, found to be significantly higher than previous reports [157,159,164]. Change in growth medium had no adverse effect on KMC4 lipid content, whereas a decrease in lipid content in the control medium was observed in *Chlorella vulgaris* grown in a mixture of pulp and aquaculture wastewater [159]. These findings confirmed that RDSW can be used as a growth medium for sustainable biofuel feedstock production. Besides these, reasonable quantities of pigments

obtained from KMC4 biomass will have several applications in food, health products, and cosmetic industry [1].

Table 4.4. Biochemical and elemental composition (%) of different microalgal biomass.

Microalgae	*Nannochloropsis oculata* [160]	*Acutodesmus dimorphus* [157]	*Scenedesmus* sp. was [101]	*Ankistrodesmus falcatus* [158]	*Monoraphidium* sp. (Present study)	
Growth medium	CP	DWW	DW	AWW	BG11	RDSW
Carb.	9	29.64 ± 0.99	-	33.88	31.04	30.37
Protein	62	38.69 ± 1.04	-	30.59	33.7	35.81
Lipid	18	25.05 ± 0.77	35.6	35.9	31.4	30.07
Ch. a + b	-	-	-	-	3.17	3.08
Car.	-	-	-	-	0.28	0.22
C	35.6	-	52.1	-	51.04	48.22
H	6.7	-	7.2	-	7.94	7.66
N	5.2	-	6.2	-	5.5	5.91
S	0.5	-	0.4	-	0.08	0.13
O*	47.7	-	34.1	-	35.44	38.08
HHV (MJ kg^{-1})	18	-	-	-	22.14	20.33

* CP: Commercially produced; DWW: Dairy wastewater; DW: Domestic wastewater; AWW: Aquaculture wastewater; Carb.: Carbohydrate; Ch.: Chlorophyll; Car.: Carotenoids; O*: Oxygen (estimated by difference)

4.1.3.2. TGA analysis

In the present study, both pyrolytic (Fig. 4.8a) and combustion properties (Fig. 4.8b) of KMC4 biomass obtained from RDSW and control BG11 medium were evaluated. From Fig. 4.8a, it was noticed that both biomass had three major decomposition stages. During the first stage, mass loss observed up to 150 °C that corresponded to the loss of moisture and light volatile matters. Further, at the second stage (150-500 °C), maximum decomposition occurred, which is known as the active pyrolytic zone. Here, higher molecular weight compounds such as carbohydrate, protein, and lipid in microalgae undergone cracking and depolymerization reactions due to the continuous supply of heat. At the final stage, char formation occurred due to the decomposition of highly thermally stable compounds. From this TGA profile, it

was observed that both biomass decomposed ~4.3% in the first stage, ~73% in the second stage, and 2-3% during the final stage. Additionally, weight loss during the active pyrolytic zone referred to the production of bio-oil that was significantly higher than previous reports [160,161].

Further, Fig. 4.8b demonstrates the combustion profile, where ~4% weight loss up to 150 °C was due to dehydration. In the next stage (150-460 °C), significant mass loss of about 91-93% was noticed due to the devolatilization of higher volatile compounds and their subsequent combustion. At temperature greater than 460 °C, no significant weight loss was observed that primarily appeared due to the presence of inorganic contents in biomass and exothermic char oxidation [165]. However, ~3% ash as estimated was found to be significantly less than other reported studies [161,165]. Thus, significantly high volatile compounds presence followed by limited char and ash formation validated RDSW derived KMC4 biomass as a potential feedstock for pyrolysis and combustion application.

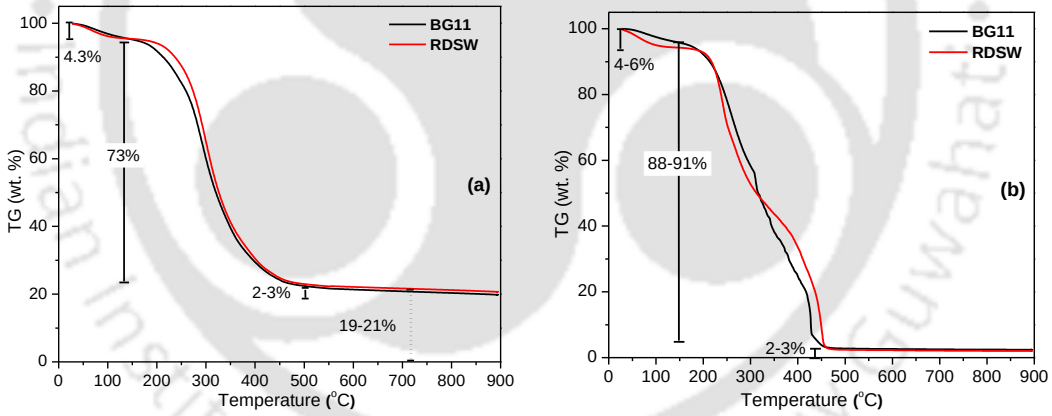

Fig. 4.8. (a) Pyrolysis and (b) combustion profile of KMC4 biomass derived from RDSW and BG11

4.1.3.3. FTIR analysis

The FTIR spectrum of KMC4 biomass with the spectral range of 1700-850 cm^{-1} with the majority of variation denoted the presence of macromolecular groups with respective bands (Fig. 4.9). Strong absorption peaks at 1026 cm^{-1} corresponded to the P = O bond responsible for phospholipids and nucleic acids. The peaks at 1153 cm^{-1}, 1238 cm^{-1}, 1392 cm^{-1}, 1454 cm^{-1} corresponded to C-O-C stretching, CH bending, and

CO stretching, which further denoted the presence of polysaccharides, aliphatic groups, and carbonate ion respectively [97]. Also, major biomolecules such as proteins and lipids were observed at 1705-1460 cm^{-1} and 3000-2800 cm^{-1} [166].

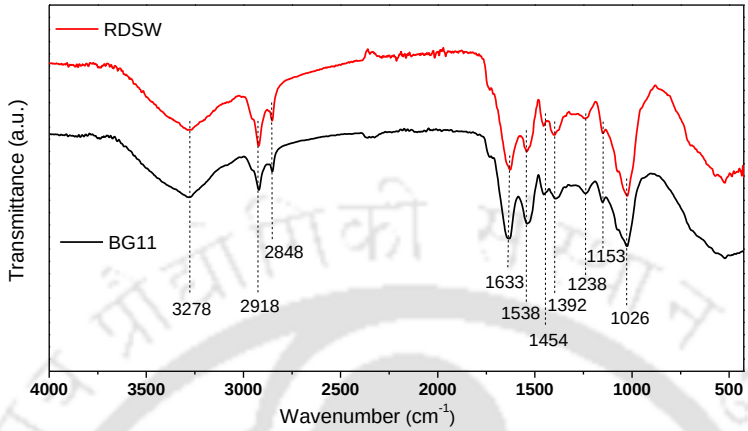

Fig. 4.9. FTIR spectrum of KMC4 biomass derived from RDSW and BG11

4.1.4. FAME analysis

In the present study, the feasibility of KMC4 lipid for biodiesel production was studied by its FAME compositional analysis obtained from GC (Table 4.5). The major fractions that constitute the total fatty acid compositions were palmitic acid (C 16:0), stearic acid (C 18:0), palmitoleic acid (C 16:1), oleic acid (C 18:1), and linoleic acid (C 18:2). The polyunsaturated fatty acids (PUFAs) were found to be less than 14%, whereas C16 and C18 had nearly 78% share in total FAME that was proven to be ideal characteristics of a biodiesel feedstock [79]. These results were found to be in accordance with previous studies [101,164]. Comparatively low oleic acid content in KMC4 lipid will provide improved fuel properties such as ignition quality, combustion heat, cold filter plugging point (CFPP), oxidative stability, and viscosity [31,167]. In the present study, the total saturated fatty acid was found to be higher than the total unsaturated fatty acid that makes biodiesel more suitable for tropical regions [46]. The above analysis suggested that the RDSW growth medium did not alter KMC4 FAME composition in comparison to control. Thus, the above study confirmed that RDSW grown KMC4 biomass is a potential feedstock for biofuel production.

Table 4.5. FAME profile of microalgal biomass derived from differt wastewater.

Microalgae	*Scenedesmus* sp. [101]	*Scenedesmus quadricauda* [164]	*Chlorella zofingiensi* [168]	*Monoraphidium* sp. (Present study)	
Growth medium	Domestic wastewater	Campus sewage	Piggery wastewater	BG-11	RCSTP
C 14:0 (Myristic acid)			-	1.14	0.84
C 16:0 (Palmitic acid)	31.7	54.2	19.73	35.9	36.28
C 18:0 (Stearic acid)	4.3	1.37	17.66	10.3	9.76
C 20:0 (Arachidic acid)	-	-	7.73	7.61	8.44
C 16:1 (Palmitoleic acid)	6.3	3.02	5.42	6.91	6.57
C 18:1 (Oleic acid)	18.7	32.88	-	11.2	12.4
C 20:1 (Eicosenoic acid)	-	-	0.81	4.65	5.2
C 22:1 (Erucic acid)	-	-	-	1.73	0.47
C 24:1 (Nervonic acid)	-	-	5.46	0.5	
C 18:2 (Linoleic acid)	18.9	3.69	26.89	9.77	10.27
C 18:3 (Linolenic acid)	6.9	4.83	14.82	3.5	2.15
C 20:2 (Eicosadienoic acid)	-	-	1.5	-	-
Total Saturated	48.2	55.57	45.11	54.95	55.32
Total unsaturated	51.8	44.43	54.88	38.26	37.06

4.2. Batch optimization of microalgal growth parameters in flasks and PBR

4.2.1. Optimization study in flask

Recently several studies suggested that optimization of wastewater composition by supplementing nutrients and culture conditions had resulted in a significantly improved nutrient removal profile followed by superior biomass yield [27,50,79,158,163]. In consideration of that, the present study was focused on optimizing growth KMC4 in RDSW medium, which was done in two stages. In the first stage, RDSW composition was optimized by supplementing nitrate and phosphate. In the second stage, other growth parameters such as temperature, inoculum concentration, and light intensity were optimized.

4.2.1.1. Nitrate optimization

In the previous chapter, the importance of nitrogen for microalgal growth was discussed, which was present as ammonia and nitrate in RDSW. The initial study showed that the amount of nitrogen was minimal. However, supplementing nitrate equivalent to BG11 significantly improved KMC4 growth (Section 4.1.2.1). In consideration of that, the initial flask optimization was focused on studying the effect of different nitrate concentrations (0.5-1.75 g L^{-1}) on KMC4 growth, and the obtained results are presented in Fig. 4.10a. The study showed an increased nitrate concentration from 0.5 g L^{-1} to 1.25 g L^{-1} resulted in enhanced biomass productivity from 81.06 mg L^{-1} d^{-1} to 140 mg L^{-1} d^{-1}. However, it was later decreased to 109.16 mg L^{-1} d^{-1} as nitrate supplement was increased to 1.75 g L^{-1}. Decreased productivity was because of an increase in nitrate reductase activity at higher nitrate concentration leading to enhanced production of nitrite and ammonia that act as toxins [169].

Thus, the above study found an optimum nitrate concentration of 1.25 g L^{-1} that resulted in maximum biomass yield of 1.7 ± 0.07 g L^{-1}. The optimized nitrate content from the present study was of 155.88 g L^{-1}, which was higher than the previous unoptimized RDSW study that had nitrate equivalent to the BG11 medium (1.09 g L^{-1}). An enhanced biomass yield with nitrate supplement in the present study was found comparable to previous studies [27,158,170–172].

4.2.1.2. Phosphate optimization

During the microalgal growth metabolism, phosphate is incorporated with organic compounds such as ADP through phosphorylation to form ATP [63]. The previous studies on screening of microalgae and wastewater had phosphate content equivalent to BG11 (21.81 mg L^{-1}) that was maintained during the nitrate optimization study. In this study, the effect of different phosphate loading (10-60 mg L^{-1}) in RDSW was evaluated, and its optimal concentration was identified. The study showed that 30 mg L^{-1} and 40 mg L^{-1} of phosphate supplement resulted in higher growth of KMC4 during its early exponential phase (Fig. 4.10b). However, 30 mg L^{-1} had the maximum biomass productivity (149.16 mg L^{-1} d^{-1}) compared to 40 mg L^{-1} of phosphate that had productivity of 140 mg L^{-1} d^{-1}. Beyond these limits, an increase or decrease in the phosphate content resulted in lower KMC4 growth in the RDSW medium. Thus, 30 mg L^{-1} of phosphate was considered optimal, resulting in biomass yield of 1.81 ± 0.05 g L^{-1}, which was 110 mg L^{-1} higher than the unoptimized study (Section 4.2.1.1; nitrate optimization).

The above study found, minimal phosphate supplement (30 mg L^{-1}) optimal for maximum biomass yield, which was comparable to previous studies [22,163]. In contrast to this, a previous study showed increased phosphate loading (444 mg L^{-1}) resulted in the highest biomass yield (1.91 ± 0.03 g L^{-1}) [96]. However, a low phosphate loading in the current batch process had the potential to make scale-up cost-effective.

4.2.1.3. Temperature optimization

The study suggests that photosynthesis and metabolic activity of microalgae are reduced at low temperatures, whereas high temperatures can result in severe oxidative damage [173]. All previous experiments are conducted at a reaction temperature of 25 ℃. To study the effect of reaction temperature, KMC4 was grown at 20-35 ℃ in the RDSW medium with an optimized supplement of nitrate and phosphate. The study showed that an increase in temperature from 20 ℃ to 25 ℃ had resulted in increased biomass productivity from 106.66 ± 4.1 mg L^{-1} d^{-1} to 149.16 ± 4.16 mg L^{-1} d^{-1}. A further increase to 30 ℃ had relatively less effect on the growth of KMC4 during the lag and exponential growth phase (Fig. 4.10c). However, reduced

growth at the late exponential phase resulted in biomass productivity of 131.66 ± 2.5 mg L^{-1} d^{-1}, which was 12% less compared to the 25 ℃ (149.16 ± 4.16 mg L^{-1} d^{-1}). A higher culture temperature at 35 ℃ significantly affected productivity (88.3 ± 2.5 mg L^{-1} d^{-1}) and resulted in the least biomass yield of 1.08 g L^{-1}. This result was similar to a recent study that suggests, microalgal cells undergo significant stress at extreme temperatures (e.g., 20 °C and 35 ℃) and affect its growth rate [174]. Whereas, an optimal temperature enhances microalgal photosynthesis that promotes biomass yield [94].

Thus, the above flask study found that 25 ℃ was optimal for KMC4 growth in the RDSW medium with a maximum biomass yield of 1.81 ± 0.05 g L^{-1}. This suggests that the model strains KMC4 was more suitable for cultivation in a controlled reaction temperature of 25-30 ℃. In addition, KMC4 growth in conventional raceway ponds may require significant structural modification to maintain culture temperature and to achieve optimal growth. However, commercial cultivation in the tropical region of India will be more suitable as its average annual temperature remains between 25-27 ℃.

4.2.1.4. Inoculum optimization

Inoculum volume is related to the initial cell concentrations that reflect on the microalgal growth. The above studies were conducted with 10% (v/v) of inoculum with biomass of 20 mg L^{-1} (DCW). During the optimization, RDSW was inoculated with 5-25% (v/v) of the KMC4 and maintained at the exponential growth phase. The growth profile presented in Fig. 4.10d suggests that 5% and 25% of inoculum had the least biomass yield of 1.5 ± 0.05 g L^{-1} and 1.4 ± 0.06 g L^{-1}, respectively. The study suggests low inoculum leads to low cell density that reduces biomass productivity. In contrast, a higher inoculum attributes to turbidity, a known limiting factor for microalgal growth [175]. The present study found that inoculum of 10-20% (v/v) enhanced KMC4 growth from the lag phase onwards and resulted in a biomass yield of 1.8 g L^{-1} to 1.97 g L^{-1}. Among these, 15% inoculum was found to be optimal that had the maximum biomass yield of 1.97 g L^{-1}. The optimized inoculum had resulted in 160 mg L^{-1} of increased biomass yield than the previous study (Section 4.2.1.3; temperature optimization with 10% v/v of inoculum).

4.2.1.5. Light optimization

Light is an essential growth factor that defines the feasibility of microalgal growth at outdoor conditions in different climatic seasons. During the photoautotrophic growth condition, light energy converts CO_2 present in atmospheric air into biomass [176]. Fig. 4.10e depicts the KMC4 growth profile obtained at a varying light intensity. The study showed that increasing the light intensity from 70 µmol m^{-2} s^{-1} to 130 µmol m^{-2} s^{-1} had reduced the log phase duration, followed by enhanced biomass productivity from 115 mg L^{-1} d^{-1} to 181.66 mg L^{-1} d^{-1}. However, during the late exponential growth phase, KMC4 had shown the maximum biomass productivity of 188.33 mg L^{-1} d^{-1} at 115 µmol m^{-2} s^{-1} of light intensity. Reduced productivity at higher light intensity (130 µmol m^{-2} s^{-1}) could be due to the damage of PSII that leads to photoinhibition [92]. To achieve maximum biomass yield with limiting energy consumption, the present study considered 115 µmol m^{-2} s^{-1} of light intensity optimal for flask based KMC4 growth using RDSW as a growth medium.

Thus, the above optimization study in RDSW with KMC4 concludes with the following culture conditions: supplement of 1.25 g L^{-1} nitrate and 30 mg L^{-1} phosphate followed by culture condition of 25 °C temperature, 15%, v/v inoculum, and 115 µmol m^{-2} s^{-1}light intensity. The optimized study resulted in a significantly improved biomass yield of 2.28 ± 0.07 g L^{-1} compared to the initial unoptimized flask study of 1.47 ± 0.09 g L^{-1}. Enhanced biomass yield of 55.1% validates the significance of optimization in maximizing biomass productivity. The optimized results from the present study were further compared with the previous reports and presented in Table. 4.6.

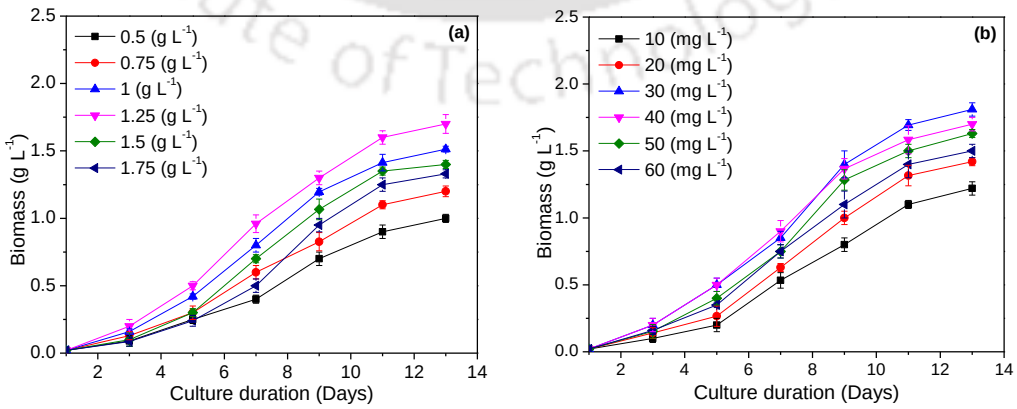

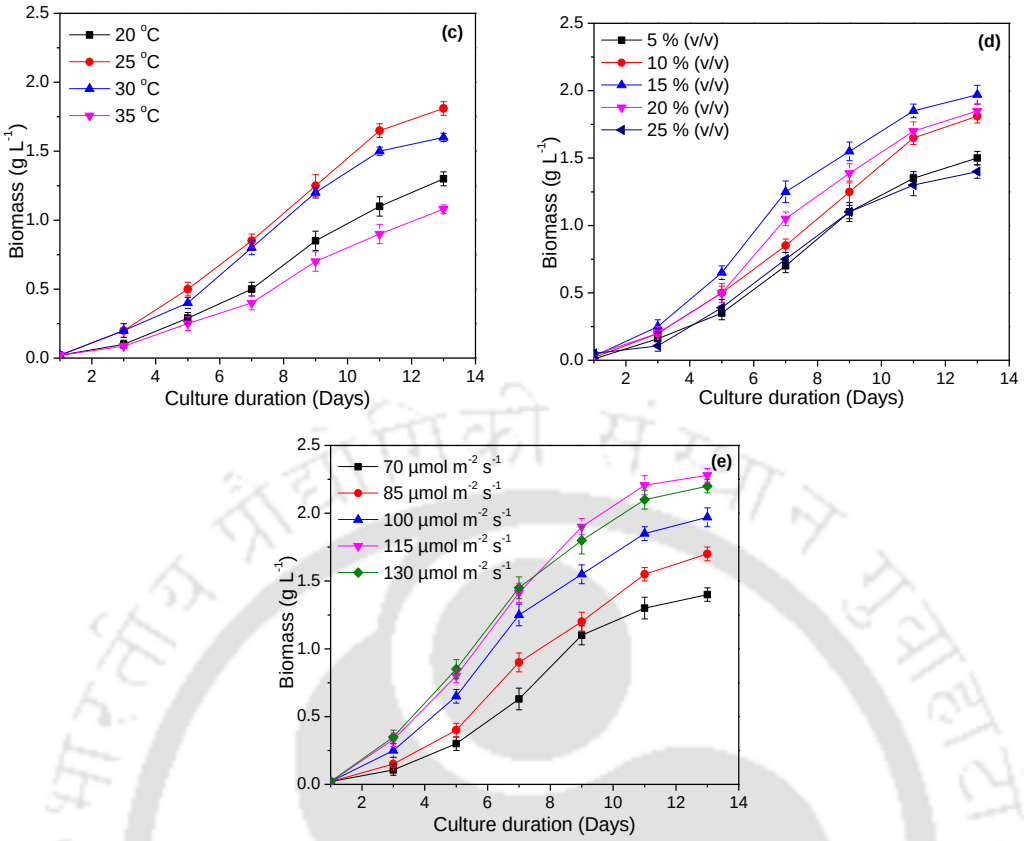

Fig. 4.10. Effect of different (a) nitrate, (b) phosphate, (c) temperature, (d) inoculum volume, and (e) light intensity on biomass yield.

Table 4.6. Effect of optimization on growth profile different microalgal strains.

Microalgal strain	Wastewater source	OP/ UnOP	Culture duration (days)	Biomass yield (gL^{-1})	P_B ($mgL^{-1}d^{-1}$)	µ (d^{-1})	References
Scenedesmus sp.	Domestic wastewater	UnOP	7	0.43 ± 0.01	61.4 ± 1.8	0.44 ± 0.01	[90]
Chlorella sp. ISTLA1	Sewage wastewater	UnOP	14	0.833	-	-	[177]
Scenedesmus obliquus-like microalgae	Municipal wastewater	OP	14	1.46	0.103	-	[51]
Chlorella sorokiniana	Palm oil mill effluent	OP	-	1.68	185	-	[79]
Chlorella vulgaris	Municipal wastewater	OP		1.39	0.13		[178]
Monoraphidium sp. KMC4	RDSW	OP	12	2.28 ± 0.05	188.33 ± 4.16	0.24 ± 0.01	Present study

OP: Process optimized; UnOP: Process unoptimized; *PB*: Biomass productivity; μ: Specific growth rate

4.2.2. Optimization study in PBR

To evaluate the feasibility of scale-up, KMC4 was grown in 25 L flat-panel indoor photobioreactor (PBR) with a culture volume of 20 L of RDSW. The initial growth study showed that increasing the culture volume (from flask to PBR) resulted in reduced biomass productivity. Previous studies reported that optimization of culture conditions such as inoculum, light, temperature, and other factors was essential during the scale-up study to maximize biomass productivity [22,51,173,179]. In this context, the culture conditions in the photobioreactor was optimized for enhanced KMC4 biomass yield. In the present study, the reaction temperature was not optimized, as it was done in indoor PBR at a controlled temperature of 25 ± 2 ℃. Additionally, to limit the cost of nutrient supplement in a batch process, nitrate and phosphate content was kept constant as per the flask optimization. Whereas, the CO_2 concentration supplied through aeration was optimized to maintain pH and enhance biomass productivity.

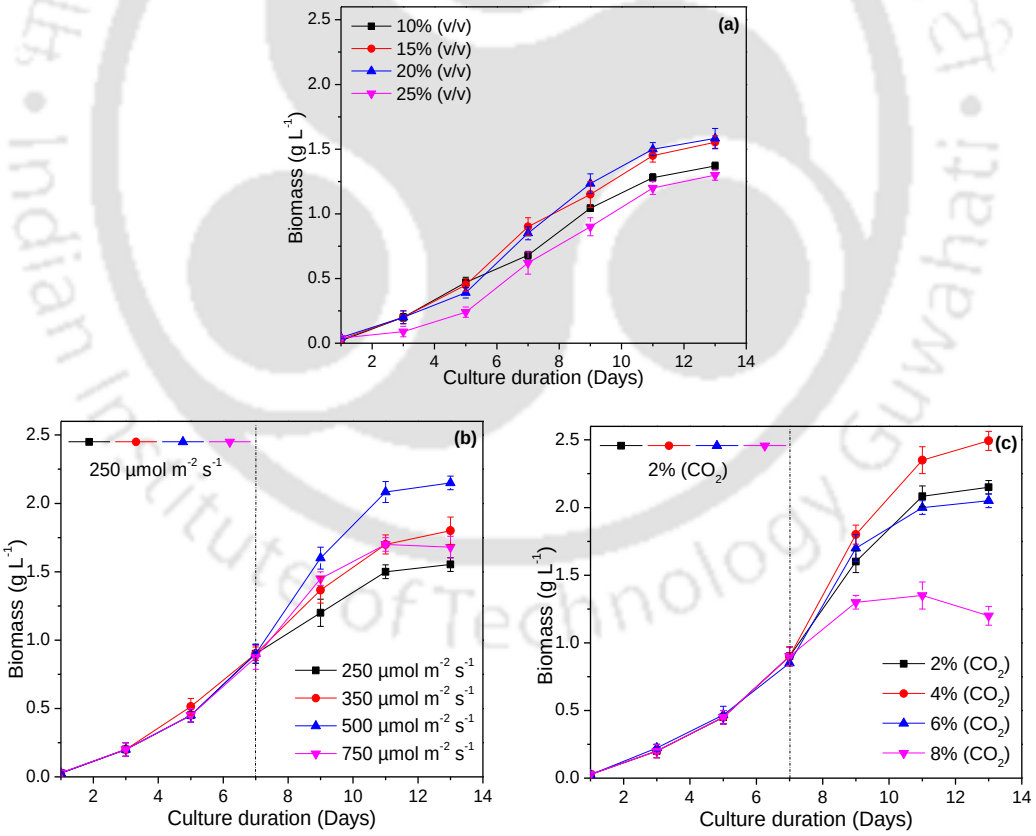

Fig. 4.11. (a) Effect of inoculum volume (light intensity (250 µmol^{-2} s^{-1}), CO_2(2%)); (b) effect of light intensity (on day 7th light intensity was increased, but CO_2 was maintained at 2% throughout); and (c) Effect of CO_2 concentration (day 7th onwards CO_2 concentration was increased from 2% to 8%, whereas from day 1-7 light intensity was at 250 µmol$_{-2}$ s$_{-1}$ then increased to 500 µmol^{-2} s^{-1} on day 7 onwards).

4.2.2.1. Inoculum optimization

Recently several studies showed, increasing the culture volume often requires higher initial biomass loading [22,87]. Since the present scale-up was 80 times higher than the flask study (500 mL flask with 250 mL culture volume), the effect of initial biomass loading on growth and nutrient removal profile was evaluated through optimization of inoculum volume. During this, the culture volume (10%, 15%, 20%, and 25 % (v/v)) was inoculated in PBR, and its effect on KMC4 growth was obtained (Fig. 11a). The results showed that KMC4 had achieved a higher growth rate of 127.77 mg L^{-1} d^{-1} and 130.27 mg L^{-1} d^{-1} with the inoculum loading of 15% and 20%. Whereas, KMC4 expressed a slow growth rate (106-113 mg L^{-1} d^{-1}) with an inoculum of 10% and 25%. This was due to the cells remained in the log phase for four days and later entered an early exponential phase. At the end of the growth phase, it was observed that inoculum loading of 15% and 20% had a comparable biomass yield of 1.55 ± 4.19 g L^{-1} and 1.58 ± 6.36 g L^{-1}, respectively. However, to reduce cultivation cost and to make the scale-up process sustainable, a lower inoculum loading of 15% (v/v) was considered optimum for PBR studies. The biomass yield from this study was found to be 32% less as compared to the optimal flask study. This suggests that the scale-up process in PBR required further optimization to enhance the biomass yield.

4.2.2.2. Light optimization

A low-biomass yield in PBR from the initial study suggested that increased culture volume required a higher light intensity to achieve superior biomass yield. However, providing higher light at the initial stage could create stress and photoinhibition [92]. A recent study reported that light intensity beyond optimal parameter damages cells photosystems and the process of its repair affects microalgal growth [180]. In the present optimization study, the light intensity was maintained at 250 µmol m^{-2} s^{-1} during the initial growth phase, which was increased further after the cells reached the mid-exponential growth phase (7^{th} day) (Fig. 11b). To optimize the process, four different light intensity was considered, and its effect on KMC4 growth was studied. Fig. 11b showed that an increase in light intensity beyond 250 µmol m^{-2} s^{-1} had a positive impact on KMC4 growth. However, increasing beyond 500 µmol m^{-2} s^{-1} resulted in a decreased growth rate. Thus, 500 µmol m^{-2} s^{-1} was considered optimal

that resulted in a biomass yield of 2.15 ± 0.06 g L^{-1} with productivity of 177.5 mg L^{-1} d^{-1}. In addition, the optimization was supported for a 38.7% enhanced biomass yield compared to the previous PBR study (Section 4.2.2.2; inoculum optimization).

4.2.2.3. CO_2 optimization

In this study, continuous CO_2 was provided in PBR to enhance microalgal growth and maintain culture pH. The previous PBR experiments were conducted at 2% CO_2 that was supplied throughout the growth study. During that, an increased pH (9-10) was observed at the late exponential phase. Whereas, in the flasks, the pH was maintained between 7 to 7.5 through periodic purging of CO_2 from an external cylinder. Thus, to study the effect of increased CO_2 concentrations on KMC4 growth in PBR, experiments were conducted at four different CO_2 concentrations. The change in CO_2 concentration was done at the mid-exponential growth phase, and the obtained results are presented in Fig. 11c. The study shown, a small increase in CO_2 from 2% to 4% had improved the biomass productivity (177.5 mg L^{-1} d^{-1} to 206.11 mg L^{-1} d^{-1}). Due to improved productivity, KMC4 biomass yield increased from 2.15 ± 0.06 g L^{-1} to 2. 49 ± 0.07 g L^{-1}, which was the maximum yield in this study. An increased CO_2 loading in culture (4%) helped to maintain the culture pH between 7.5 to 8, which led to an improved KMC4 growth profile. However, with an increased CO_2 concentration to 6%, the biomass productivity was reduced to 169.16 mg L^{-1} d^{-1} and resulted in a biomass yield of 2.05 ± 0.05 g L^{-1}. The reduced output was due to the supply of excess CO_2, which decreased culture pH from 7.8 to 6 on the 10th day. A similar observation was also observed with 8% CO_2 that significantly affected the KMC4 growth as the culture pH was reduced to 5.2 and turned acidic within 24 h of culturing (8th day). Thus, the above study found a combination of 2% and 4% of CO_2 loading optimal for KMC4 growth that had expressed 15.8% improved biomass yield compared to the previous study (Section 4.2.2.3; light optimization).

The above optimization study found 1.25 g L^{-1} (nitrate), 30 mg L^{-1} (phosphate), and 25 ℃ (culture temperature), 15% (inoculum), a combination of 250-500 µmol m^{-2} s^{-1} (light intensity), and a combination of 2-4% of CO_2 optimal for KMC4 growth in indoor-photobioreactor with RDSW as a growth medium. The optimized condition in PBR resulted in 2.49 ± 0.07 g L^{-1} of biomass yield which was ~44.97% superior to the

unoptimized PBR study (Section 4.2.2.1; 10% inoculum). Additionally, the scale-up had an 8% enhanced biomass yield compared to the optimized flask study (Section 4.2.1.5; light optimization). The obtained biomass yield from the present study was further compared to previous reports and presented in Table 4.7.

Table 4.7. The growth and biomass yield profile of microalgal strains grown in PBR.

Microalgal strain	Wastewater source	Culture duration (days)	Biomass yield (gL^{-1})	P_B ($mgL^{-1}d^{-1}$)	μ (d^{-1})	References
Scenedesmus quadricauda SDEC-13	Campus sewage	15	1.09	79.17	0.23	[164]
Scenedesmus sp.	Domestic wastewater	7	1.37 ± 0.04	196 ± 5.1	0.51 ± 0.01	[90]
Scenedesmus sp.	Domestic wastewater	7	1.31 ± 0.12	185.7 ± 7.3	0.5 ± 0.02	[101]
Scenedesmus sp.	Domestic wastewater	4	-	307.5	0.8	[181]
Chlorella protothecoides	Municipal wastewater	10	1.96	-	-	[92]
Chlorella vulgaris	Municipal wastewater	10	941.48 (mgL^{-1})	94.1	0.22	[91]
Scenedesmus obliquus		10	865.44 (mgL^{-1})	86.5	0.21	
Monoraphidium sp. KMC4	RDSW	13	2.49 ± 0.01	206.11 ± 5.85	0.31 ± 0.02	Present study

4.2.3. Nutrient uptake profile in flask and PBR

The flask optimization study showed that 1.25 g L^{-1} (nitrate) and 30 mg L^{-1} (phosphate) supplement to RDSW was optimal for KMC4, which was also maintained in PBR for the batch studies. Besides growth, the present optimization was also focused on evaluating the nutrient consumption profile of KMC4 in flask and PBR. Though nutrient uptake was studied during each growth experiment, a comprehensive study was discussed only for the optimal reaction conditions. The obtained results were further compared with recent reports, and possible improvement to make the process sustainable is proposed.

4.2.3.1. Nutrient uptake in flask

Fig. 12 suggests that nitrogen present in as ammonia and nitrate in RDSW was consumed steadily compared to phosphate. Due to the presence of ammonia at a

limited quantity (44.7 mg L^{-1}) in RDSW, its consumption was faster than nitrate. Fig. 12a shows that change in light intensity had the least effect on the total uptake of ammonia. Whereas, the rate of uptake was found superior with higher light intensity (100-130 µmol m^{-2} s^{-1}) that had resulted in nearly 90% removal within four days of the culture period. At the end of the culture period, among all, 115 µmol m^{-2} s^{-1} found superior in utilized 99.55% of ammonia at 3.7 ± 0.2 mg L^{-1} d^{-1}. This result was found comparable to the unoptimized flask study, also shown near-complete removal of ammonia (99.5%) at the end of the culture period (Table 4.3.).

The culture flasks had around 1.26 g L^{-1} of initial nitrate, and its consumption profile is presented in Fig. 12b. An increase in light intensity from 70-115 µmol m^{-2} s^{-1} resulted in an increased rate of nitrate removal from 82.21 ± 2.8 mg L^{-1} d^{-1} to 98.6 ± 1.2 mg L^{-1} d^{-1}. Further increase in light significantly reduced its rate of nitrate consumption to 90.24 ± 2.1 mg L^{-1} d^{-1}. The study found low-light (70-100 µmol m^{-2} s^{-1}), which inhibits KMC4 growth that resulted in limited nitrate uptake. Whereas, an optimal light 115 µmol m^{-2} s^{-1} resulted in maximum nitrate consumption (94%). The study also showed that due to the optimization, 5.32% enhanced nitrate uptake was achieved by KMC4 in flask compare to the unoptimized study (Table 4.3.).

Fig. 12c depicts the phosphate consumption profile of KMC4 during the flask study. Compared to ammonia and nitrate, phosphate consumption was found directly proportional to the KMC4 growth. Increasing the light intensity from 100-130 µmol m^{-2} s^{-1} had resulted in 95% phosphate consumption by the 5^{th} day of culture. Whereas, due to limited phosphate content (40.7 mg L^{-1}) in RDSW, its near-complete consumption by KMC4 was achieved within six days of the culture period. This result was found comparable to the unoptimized flask study that had also shown complete consumption of phosphate by the end of the culture period (Table 4.3.).

The above study showed that maximum nutrient uptake by KMC4 includes, ammonia 44.5 ± 0.13 mg L^{-1} (99.55%), nitrate 1.18 ± 0.1 g L^{-1} (94%), and phosphate 40.69 ± 0.01 mg L^{-1} (99.9%). Near-complete utilization of nutrients towards KMC4 growth was found comparable to the previous studies [51,180]. This was due to the optimized nutrient in the growth medium supported for enhanced metabolic activity of microalgae [163]. In a recent study, nutrient supplement in wastewater supported

91.54% of total nitrogen and 83.25% of total phosphorus removal by *Chlorella sorokiniana* [79]. However, the study also found a relatively less removal efficiency (65.3% total nitrogen and 71.2% total phosphate) by *Chlorella vulgaris* in glucose-supplemented wastewater [178]. Another study reported, *Chlorella sorokiniana* growth in sodium nitrate supplemented wastewater resulted in maximum nutrient removal of 75.56%, 84.51%, 73.35%, and 71.88% of ammonia, nitrate, phosphate, and COD, respectively [27]. Achieving maximum nutrient uptake in the present study will help biological wastewater treatment [50]. The process was further studied in PBR to validate the concept of integrated biomass production and wastewater treatment under the biorefinery approach.

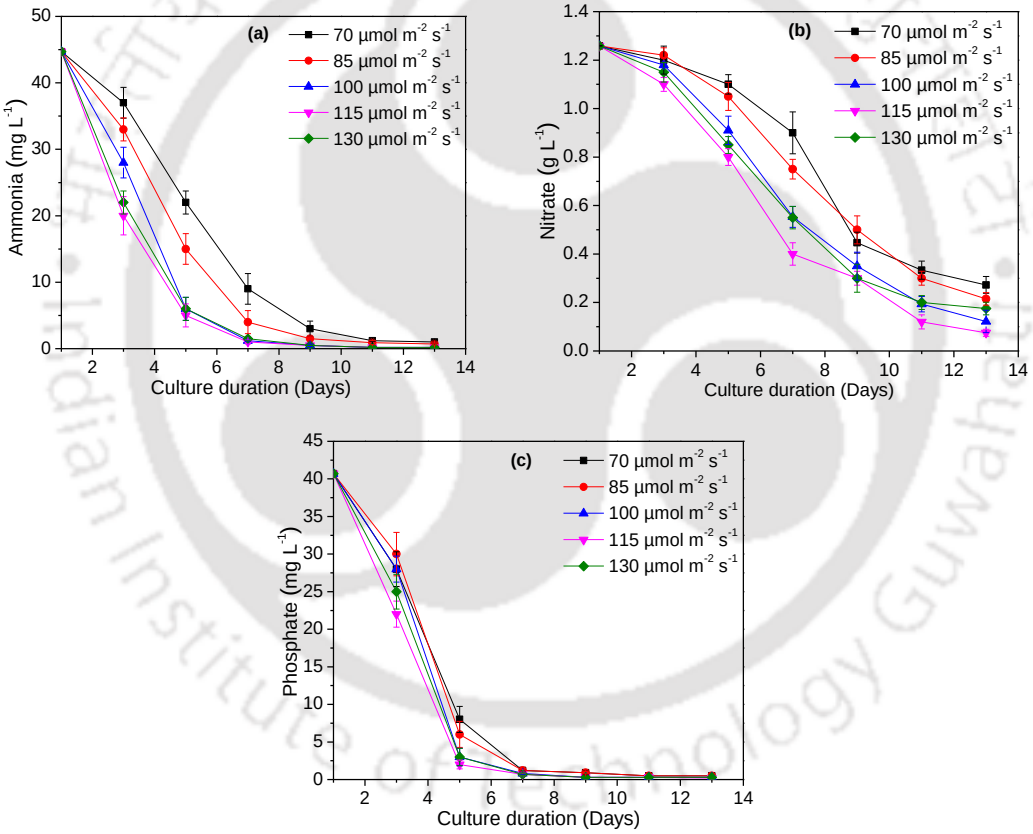

Fig. 4.12. (a) ammonia, (b) nitrate, and (c) phosphate uptake by KMC4 under optimized batch study in the flask.

4.2.3.2. Nutrient uptake in PBR

During the growth optimization, the nutrient supplement was kept constant (1.25 g L^{-1} nitrate and 30 mg L^{-1} phosphate). Fig. 13 shows the nutrient uptake profile

of KMC4 in PBR. The overall consumption of nutrients such as ammonia, nitrate, and phosphate was superior in PBR compared to the flask study. This was due to the enhanced KMC4 growth metabolism achieved under optimized culture conditions.

Fig. 13a shows that the two-stage CO_2 supply had the least effect on the rate of ammonia consumption in PBR. Under the 1st stage of CO_2 supply, all experiments had ~96.64% of ammonia uptake by KMC4. An optimized inoculum and light supply to the PBR resulted in a three-fold increased rate of ammonia uptake (10.94 ± 0.07 mg L^{-1} d^{-1}) compared to the flask experiments. The remaining 2-3% was consumed under the 2nd stage of the CO_2 supply. An exponential growth profile in PBR (Fig. 11c) suggests the absence of ammonia in the 2nd stage of CO_2 supply that had no significant effect on KMC4 growth. However, a superior growth with 4% CO_2 was achieved by assimilating available nitrate in RDSW and a continuous supply of CO_2 (Fig. 13b). In contrast to ammonia, only 54.7% nitrate was consumed (174.57 ± 14.4 mg L^{-1} d^{-1}) under the 1st stage of CO_2 supply. Whereas, 4% CO_2 supply in 2nd stage supported maximum nitrate uptake (36.72%) at 115.5 mg L^{-1} d^{-1}. It was due to superior biomass productivity (88.19 ± 4.8 mg L^{-1} d^{-1}) that resulted in 84.10 ± 4.5% of total nitrate removal from 2%-4% CO_2 supply. Whereas, the least nitrate removal (64.85 ± 2.8%) was achieved from 2%-8% CO_2 supply as it had the lowest biomass productivity (64.85 ± 2.8 mg L^{-1} d^{-1}). Low productivity resulted from the acidic state of RDSW with an excess supply of CO_2.

Compared to ammonia, 98% of phosphate was consumed at 10.15 mg L^{-1} d^{-1} within four days of the culture period (Fig. 13c). The rate of consumption was 57.53% superior to the optimized flask that confirmed optimization had a significant effect on microalgal growth, followed by nutrient removal efficiency. The growth profile in Fig. 11c demonstrates that along with ammonia, the absence of phosphate had the least effect of KMC4 growth during 2nd stage of CO_2 supply. Moreover, nitrate and CO_2 had a significant impact on the growth of KMC4 in PBR. Thus, a combination of 2%-4% CO_2 supply in PBR was established optimal for KMC4 growth that had resulted in complete removal of ammonia, phosphate, and nitrate of 84.10 ± 4.5%.

The obtained result was found comparable to a recent study, where *Chlorella vulgaris* grown in PBR achieved > 99% nitrogen and phosphorous removal, primarily

through biomass assimilation [182]. In another study, complete removal of total nitrogen, total phosphorous was achieved from the tertiary treatment of municipal wastewater by *Chlorella protothecoides* (SAG-211-10C) while grown in a lab-scale externally illuminated photobioreactor [92]. In contrast to the above, comparatively low nutrient uptake (ammonia 93.5 ± 2.9, nitrate 56.7 ± 2.6, phosphate 74.3 ± 2.1) was reported from *Scenedesmus* sp., when it was gown in PBR with domestic wastewater as a growth nutrient [90]. The present study was also found promising than the previous research that had achieved 65.3% total nitrogen and 71.2% total phosphate removal from *Chlorella vulgaris* grown with domestic wastewater with a biomass yield of 1.39 g L^{-1} [178].

The above batch study of microalgal biomass production using RDSW had shown significant biomass yield followed by nutrient removal efficiency, which validates the potential of KMC4 strain for sustainable wastewater treatment under scale-up condition. However, to enhance the biomass productivity, fed-batch and semi-continuous mode of cultivation was proposed.

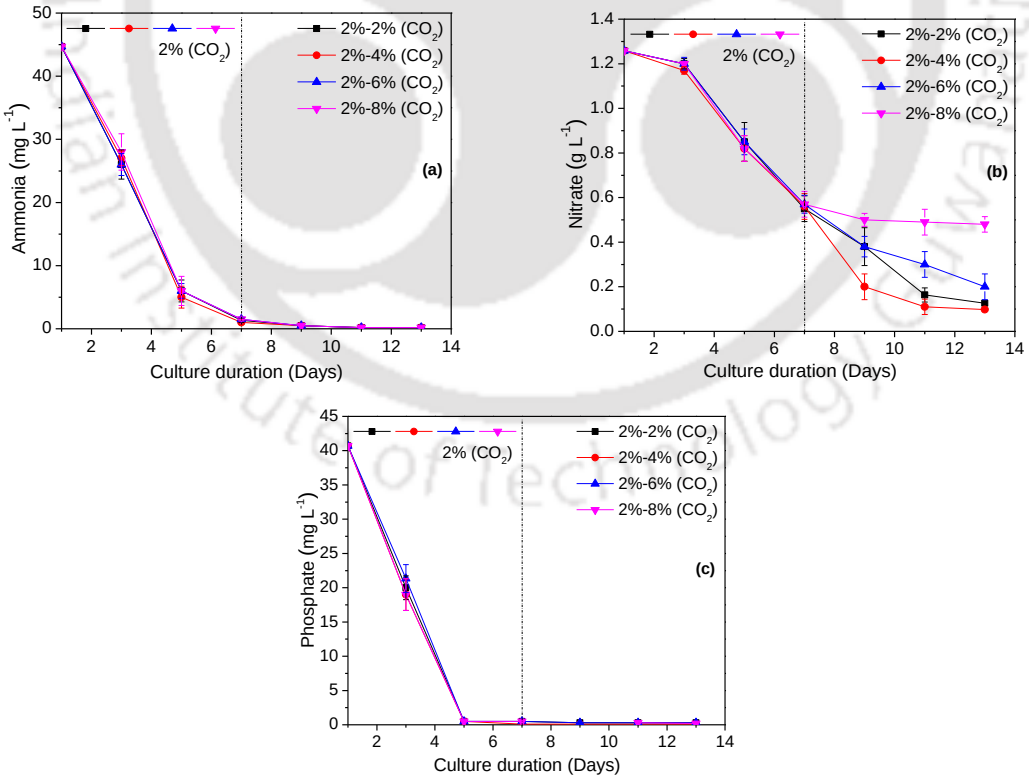

Fig. 4.13. (a) ammonia, (b) nitrate, and (c) phosphate uptake by KMC4 under optimized batch study in PBR.

4.2.4. Characterization of biomass

4.2.4.1. Biomass composition

The compositional analysis was done to evaluate the proximate, ultimate, and biochemical composition of KMC4 biomass derived from the optimal reaction condition from flask and PBR. The proximate analysis (Table. 4.8) suggests that scale-up of RDSW treatment reduced the volatile matter content by 6%, and fixed carbon was increased by 12%. Recently Lee et al. [121] reported, high fixed carbon helped in stable combustion; in contrast, high volatile matters resulted in unstable combustion due to inappropriate heat balance during its combustion. In this context, optimized scale-up had resulted in KMC4 biomass production that can be considered a potential feedstock for bioenergy production. However, scale-up of wastewater treatment had increased ash content, but it was significantly less as compared to previous reports [31,38,121,180].

The ultimate analysis suggests that scale-up followed by optimization had least effect on the elemental composition of KMC4 biomass. The biomass derived from PBR had carbon and hydrogen content of 47.91 ± 0.11% and 7.83 ± 0.05%, which was comparable to the biomass derived from the initial unoptimized flask study (48.22% and 7.66%). Additionally, it was also found equivalent to several biomass feedstocks such as microalgae [121,160,183] and lignocellulosic biomass [155,184], which were study for bioenergy production. The present study had shown that increased nitrogen and sulfur content will lead to the production of SOx and NOx. However, pretreatment of both biomass before the bioenergy production can reduce its effectiveness. Both biomass had HHV of 21.3 MJ Kg^{-1} that was equivalent to the HHV of biomass obtained from the unoptimized flask study. This further defined scale-up, followed by optimization that had the least effect on the energy value of KMC4 biomass. Hence, enhanced biomass yield through the scale-up process resulted in superior bioenergy feedstock production.

The biochemical composition had shown decreased lipid content in PBR biomass (28.86 ± 2.9) in comparison to the flask biomass (31.57 ± 3.4). The lipid content in microalgae increases in a nitrogen-deficient medium. However, the consumption of nitrogen in PBR was less than the flask that had resulted in low lipid

content in the PBR biomass. In this context, two-step cultivation can significantly enhance lipid yield, where harvested biomass from PBR will be transferred to a nitrogen-deficient medium [31]. Both biomass had nearly similar carbohydrate content that can be extracted through hydrolysis for bioenergy production through the fermentation process [15,185]. The protein content in PBR biomass was increased that had resulted in increased elemental nitrogen content. Higher protein content in biomass can be used as a food supplement and add a significant contribution to the biorefinery approach [40].

Table. 4.8. Physicochemical characteristics of KMC4 biomass derived from flask and PBR at the optimized reaction condition.

Components	Flask	PBR
Proximate composition		
Moisture (wt%)	4.05 ± 0.1	4 ± 0.5
Volatile matter (wt%)	78.8 ± 0.7	74 ± 0.8
Fixed carbon (wt%)	16.25 ± 0.2	15.26 ± 0.2
Ash (wt%)	0.9 ± 0.07	3.74 ± 0.1
Ultimate composition		
C (wt%)[a]	49.28 ± 0.08	47.91 ± 0.11
H (wt%)[a]	7.719 ± 0.04	7.83 ± 0.05
N (wt%)[a]	6.202 ± 0.03	6.8 ± 0.1
S (wt%)[a]	0.26 ± 0.01	0.17 ± 0.01
O (wt%)[b]	35.62 ± 0.2	30.55 ± 0.13
HHV (MJ Kg^{-1})[a]	21.32 ± 0.07	21.38 ± 0.33
Biochemical composition[a]		
Carbohydrate (wt%)	28.6 ± 1.8	27.4 ± 2.2
Protein (wt%)	37.1 ± 2.5	39.7 ± 1.07
Lipid (wt%)	31.57 ± 3.4	28.86 ± 2.9

[a]Dry basis
[b]By difference (O = 100 - (C+H+S+N+Ash))

4.2.4.2. Thermal analysis

The KMC4 biomass obtained from flask and PBR at the optimal reaction condition was characterized using TGA to evaluate its thermal decomposition behavior. The TG curves in Fig. 4.14 describes the pyrolytic and combustion profile of both biomass obtained in a nitrogen and air atmosphere at a heating rate of 20 °C

min^{-1}. During the pyrolysis study (Fig. 4.14a), both biomass had three-stage of degradation. The initial weight loss in the first stage (up to 150 °C) was due to moisture removal (4.5%) from the biomass. The second stage (150-500 °C) had a weight loss of 76-79%, due to the devolatilization of organic matters in biomass. In the third stage (> 500 °C), both biomass had a minimal weight loss of 1.4-1.8% and left with char as a residue of 15.5-18%. The pyrolytic study suggests that the presence of a higher volatile matter with low ash content in the KMC4 biomass obtained from flask resulted in a comparatively higher weight loss than the PBR derived biomass. However, the optimization of process parameters significantly improved the TG profile of both biomass compared to the initial unoptimized flask studies. That had less weight loss in the active pyrolytic zone (73%) with high char yield (19-21%). This ascertained that optimization had significantly improved the bioenergy potential of KMC4 biomass.

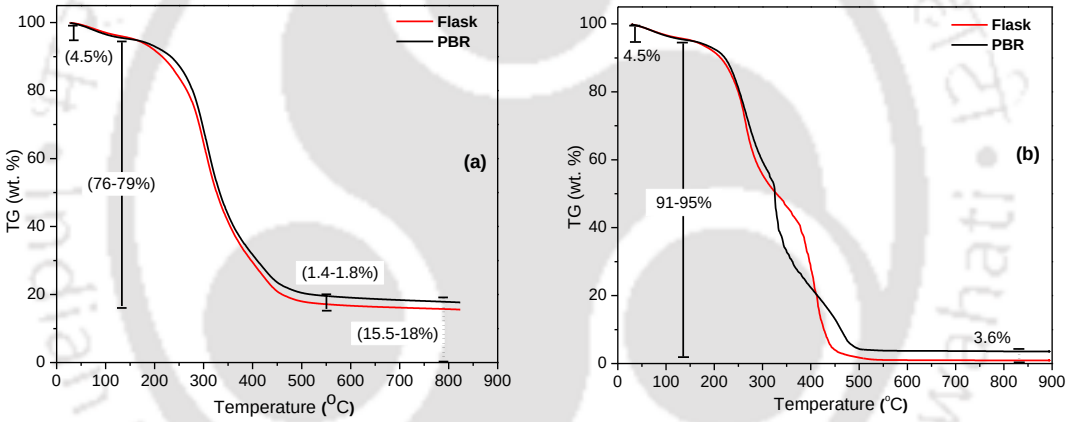

Fig. 4.14 TG profile (a, Pyrolysis; b, combustion) of flask and PBR derived KMC4 biomass.

Fig. 4.14b shows the combustion profile of both biomass that expressed only 4.5% weight loss due to moisture removal (<120 °C) followed by 91-95% of weight loss due to the devolatilization and combustion (120-500 °C). Maximum combustion suggests that both biomass can be considered a feedstock for various thermochemical conversion processes. In comparison to the flask, PBR biomass had a higher residue yield (3.6%) in the form of ash (>500 °C). This was due to the transfer of a higher TDS from wastewater to the biomass and low-volatile compounds in PBR biomass (Table. 4.8). Moreover, recent studies also reported the presence of high ash in biomass, which were obtained from the scale-up process [31,38,121,180]. Nevertheless, 91%

combustion of KMC4 biomass derived from a scale-up study was found comparable to the biomass derived from the initial flask study, which also had 91-93% combustible matter. Hence, the above study ascertained that scale-up of RDSW treatment using KMC4 strain resulted in sustainable biomass production that had feasibility of potential bioenergy production through various thermochemical conversion processes.

4.2.5. FAME analysis

The neutral-lipid extracted using n-hexane was transesterified through a two-step transesterification process, and the obtained FAME profile is presented in Fig. 4.15. The study showed that maximum FAMEs were of saturated fatty acid (SFA) which includes, myristic acid (C 14:0), palmitic acid (C 16:0), stearic acid (C 18:0), arachidic acid (C 20:0). Among both, FAME from PBR had the maximum SFA content (58.95%), and the MUFA and PUFA were comparatively less than the FAME derived from the flask. Additionally, SFA was at a higher range in comparison to the unoptimized flask (55.32%). This property suggests that the PBR biodiesel was more suitable for tropical regions [46]. The present study showed, 77.23% of total FAME content in PBR was of C16 (42.72%) and C18 (34.51%). This includes oleic acid (C 18:1) of 10.6%, which was lesser than the unoptimized flask (12.4%). The above results ascertained that biodiesel derived from PBR had superior biofuel quality. These results were found to be in accordance with previous studies [101,164].

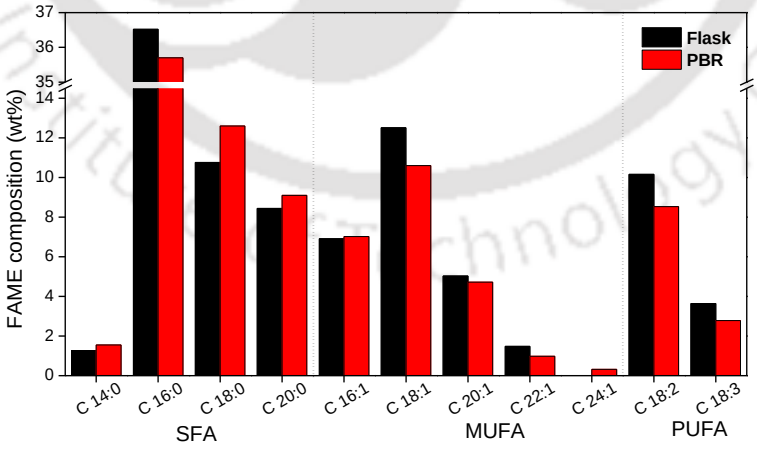

Fig 4.15. FAME profile (SAF: Saturated fatty acid, MUFA: Monounsaturated fatty acid, and PUFA: Polly unsaturated fatty acid) of KMC4 lipid obtained from flask and PBR at optimized reaction conditions.

4.3. Fed-batch and semi-continuous mode of culture in PBR

4.3.1. Fed-batch study

The advantage of fed-batch cultivation is to achieve high cell density compared to batch cultivation that significantly reduces the biomass production cost. Recently several studies are reported on the fed-batch mode of microalgal biomass production and its conversion to biofuel [186–188]. However, limited studies have explored the potential of *Monoraphidium* sp. as a model strain and its scale-up feasibility in large-scale photobioreactors (> 10 L). In the present study, KMC4 was grown in PBR under the fed-batch mode, where RDSW was used as a growth medium. The culture condition optimized for the batch study was followed for fed-batch. To sustain the exponential growth phase, on the 14th day of culture CO_2 supply and light intensity were increased. The obtained biomass was further characterized as a potential feedstock for biofuel production.

4.3.1.1. Growth study

A periodic nutrient feeding during the fed-batch study had significantly improved the KMC4 growth in PBR (Fig. 4.16). During the 1st stage of CO_2 and light supply, KMC4 had achieved 1.03 ± 0.08 g L^{-1} biomass yield that was 12.6% higher than the batch study (0.9 ± 0.07 g L^{-1}). Further increase of CO_2 and light in the 2nd stage enhanced the biomass productivity, and it had reached the maximum on the 9th day of culture (415 ± 21.2 mg L^{-1} d^{-1}). However, an increased cell density in PBR hindered biomass productivity. This was in agreement with a recent study that explains, high cell density during fed-batch may lead to light shading in PBR that has a negative impact on microalgal photosynthesis [186]. To address this challenge, a multi-step increase in light intensity was proposed in a previous study [189]. In consideration to that, the implementation of increased CO_2 and light in the 3rd stage had improved the exponential growth phase of KMC4. It resulted in an overall biomass yield of 3.62 ± 0.1 g L^{-1} at 197.77 ± 3.39 mg L^{-1} d^{-1}. The biomass yield and productivity were found ~45.38% and ~16.91% higher than the batch study. Thus, achieving a higher biomass yield and productivity under scale-up condition validates the potential

of KMC4 for viable biomass production. Whereas, further optimization on fed-batch study can enhance biomass yield.

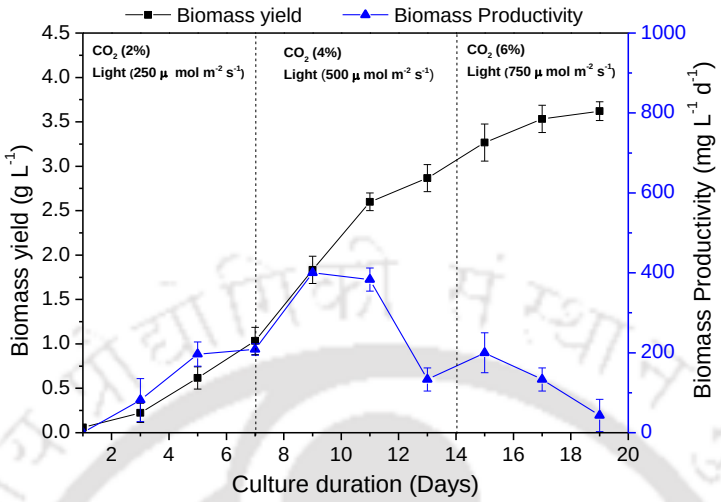

Fig. 4.16. KMC4 growth profile obtained through fed-batch mode of cultivation in PBR.

4.3.1.2. Nutrient uptake

During the fed-batch study, nitrate and phosphate were periodically added to the RDSW for maximizing the KMC4 growth metabolism. Among both, nitrate feeding was done once every three day, whereas the phosphate feeding was done every day considering its higher consumption. Fig. 4.17a shows that maximum nitrate consumption of 27.5% (350 mg L^{-1}) was obtained from the 6th day of culture. This validates that nitrate was used in higher amount for biomass growth compared to phosphate. However, with an increase in culture duration, the consumption of nitrate was reduced. On the 17th day of culture, as microalgal cells reached stationary, nitrate consumption also reduced to ~10%. At the end of the fed-batch process, a substantial nitrate remained unconsumed. However, further optimization of enhancing nutrient uptake is essential to limit nitrate unconsumed.

Fig. 4.17b depicts the phosphate consumption profile of KMC4 obtained from the fed-batch study. In contrast to nitrate, the consumption of phosphate was found increasing gradually along with microalgal growth. This could be due to the low-phosphate content in an optimized RDSW medium. In the 1st stage, maximum

phosphate was consumed 37.5% on the 7th day. With an increased CO_2 and light, maximum consumption of 61.5% was achieved on the 14th day of culture. Later, it was reduced consistently until microalgal cells reached stationary.

The obtained nutrient consumption profile corresponding to biomass yield was found comparable to previous studies. A consortium of microalgae and bacteria studied for wastewater treatment under the fed-batch mode, resulted in ~330 mg L^{-1} of total nitrogen and ~55 mg L^{-1} of total phosphate unconsumed [190].

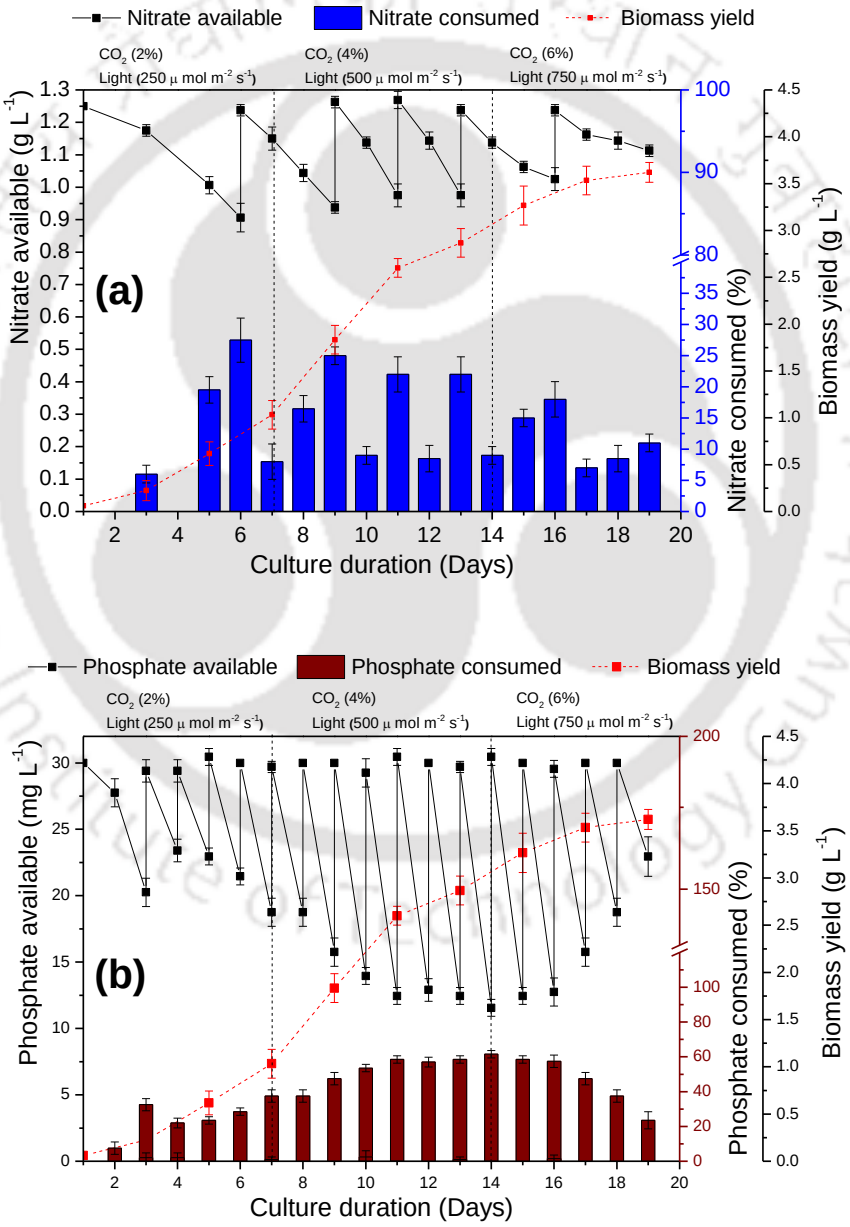

Fig. 4.17. (a) Nitrate and (b) phosphate consumption profile of KMC4 obtained from the fed-batch mode of cultivation.

4.3.2. Semi-continuous study

A semi-continuous mode of microalgal cultivation is preferred to maintain the exponential growth phase of microalgae [186]. In the present study, the 11th day of culture was considered the mid-exponential phase, and on that day fed-batch mode of cultivation was converted into a semi-continuous mode. During semi-continuous mode, 10% of culture was harvested, and a fresh RDSW medium was added into the reactor. To maintain optimal nutrient in the RDSW, periodic feeding of nitrate and phosphate was done.

4.3.2.1. Growth study

Fig. 4.18 shows that KMC4 growth was maintained consistently until the 25th day of culture. To a consistent exponential growth phase, 6% CO_2, and 750 µmol m^{-2} s^{-1} of light intensity was found optimal. The study shown, harvesting 10% of culture from 9th day onwards had resulted in enhanced microalgal growth in comparison to the batch and fed-batch. However, in contrast to biomass yield, the productivity had shown a steady decrease from 410 ± 14.14 mg L^{-1} d^{-1} to 90 ± 13.9 mg L^{-1} d^{-1} (9th day to 29th day). In consideration of that, the periodic harvesting was stopped on the 29th day. The study showed that an overall biomass yield of 6.14 g L^{-1}, which was 69.61% superior to the fed-batch process.

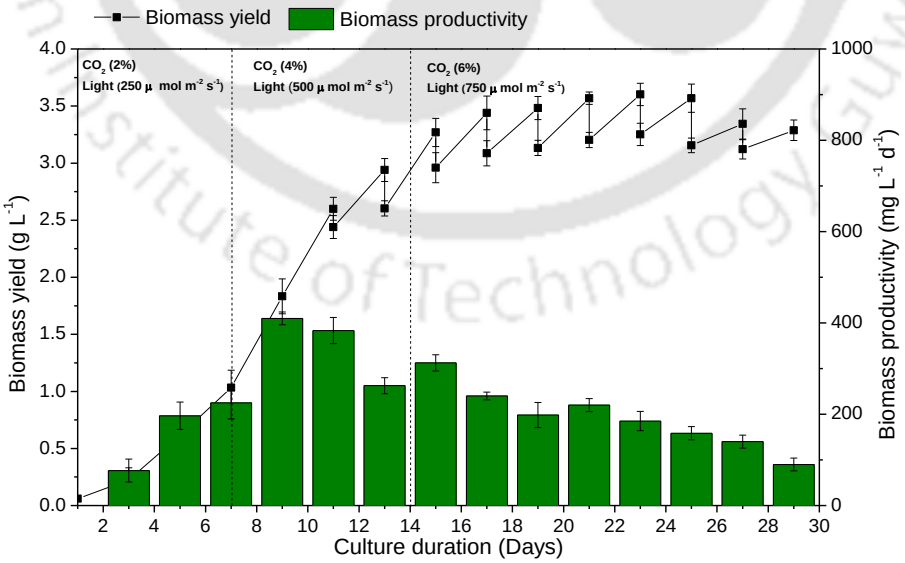

Fig. 4.18. KMC4 growth profile obtained from semi-continuous mode of cultivation.

4.3.2.2. Nutrient uptake

The nutrient consumption profile depicted in Fig.19a shows that nitrate assimilation during the semi-continuous mode was found comparable to the fed-batch study. A higher nitrate uptake was observed up to the 13th day of culture; after that, reduced biomass productivity affected the nitrate assimilation rate. An increased CO_2 and light in the 3rd phase initially supported for higher nitrate removal. However, after the 16th day of culture, no significant change in nitrate removal was recorded. In contrast to nitrate, Fig.19b shows higher phosphate content, as observed during the fed-batch study. Optimal phosphate assimilation (40-60%) was observed until the 17th day of culture. It was later maintained until microalgal growth reaches the early stationary phase on the 22nd day of culture.

The above study suggests that both fed-batch and semi-continuous mode of cultivation was sustainable for biomass production. Whereas, to achieve maximum nutrient removal efficiency, significant optimization is required.

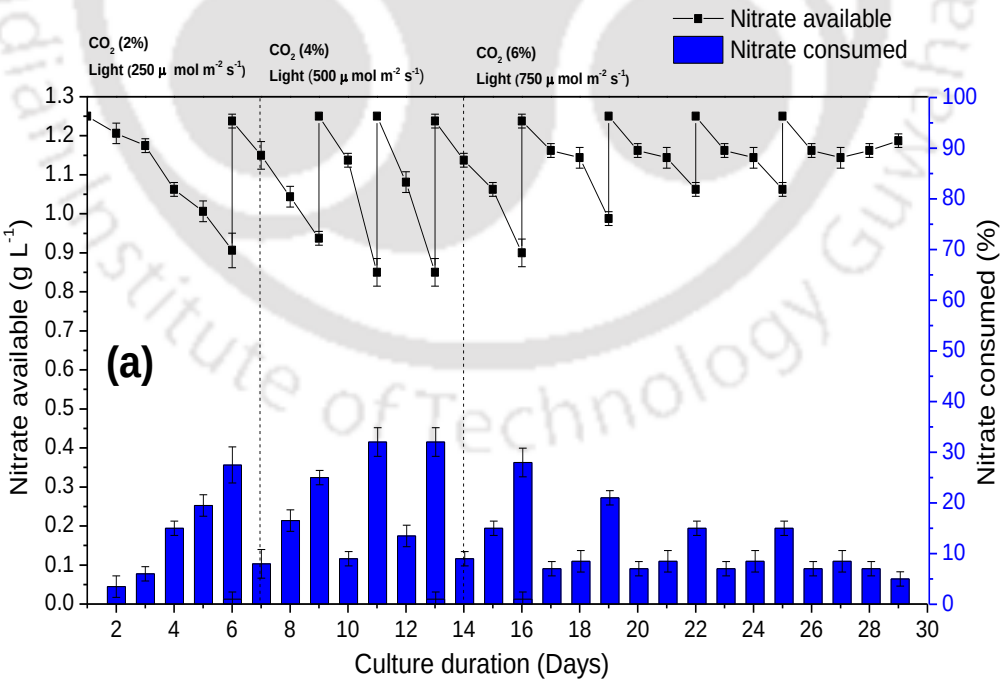

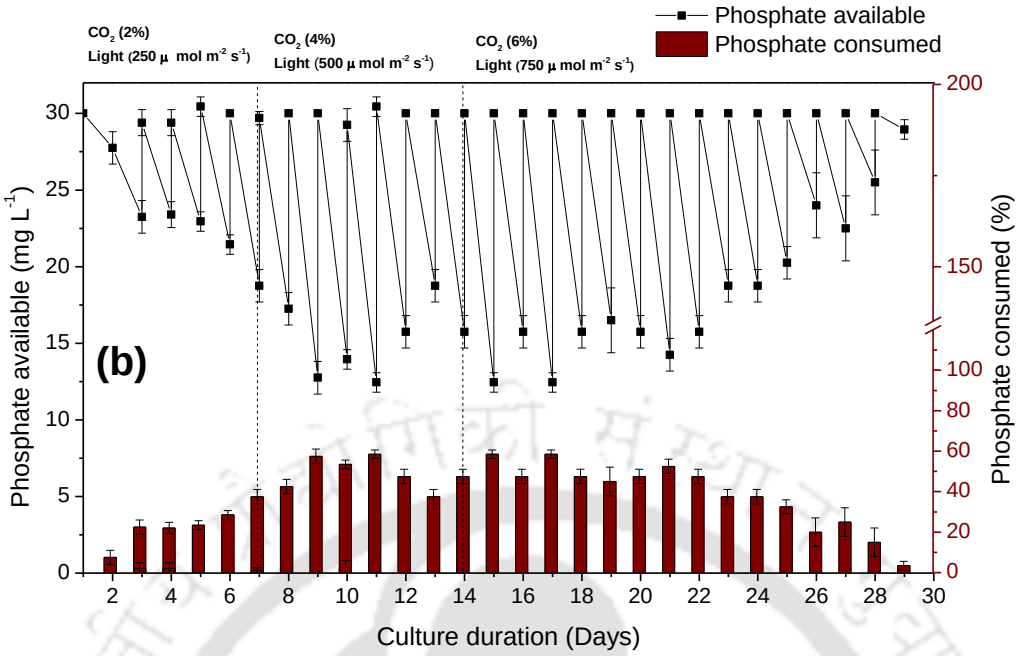

Fig. 4.19. (a) Nitrate and (b) phosphate consumption profile of KMC4 obtained from the semi-continuous mode of cultivation.

4.3.3. Characterization of biomass

4.3.3.1. Biomass composition

The biomass harvested after fed-batch and semi-continuous mode of culture was lyophilized. The biomass was further characterized for its compositional study, and the results are presented in Table. 4.9. The proximate analysis showed that both biomass had increased volatile matters content (75-78 wt%) than the unoptimized flask study (72-73 wt%). Whereas, the fixed carbon content was significantly reduced (12-16 wt%) in comparison to the unoptimized flask study (19-21 wt%). This suggests that the biomass derived from the present study can be used for combustion, but reduced fixed carbon will lead to unstable combustion. This was also observed for the biomass derived from the optimized flask and PBR. However, no significant change in ash content suggests that both biomass can be used for bioenergy production through the various thermochemical conversion process.

In consistent with the previous batch optimization study, biomass harvested from the present study had the least change in its ultimate composition. Both biomass had a superior carbon (48-50 wt%) and hydrogen (7-8 wt%) content. The presence of

nitrogen (<6.5 wt%) and sulfur (<0.2%) suggest possible SOx and NOx emission, which require pretreatment to reduce its effect. However, the superior energy content in terms of HHV (~21.3 MJ Kg^{-1}) ascertains that harvested biomass had the potential for bioenergy applications.

The biochemical composition suggests that lipid content in semi-continuous mode biomass (29.71 ± 1.4 wt%) was reduced in comparison to the biomass derived from the fed-batch (32.4 ± 1.6). This was due to the nitrogen presence in growth medium at a substantial quantity, whereas in fed-batch cells were grown under nutrient-deficient state before harvesting. This had also resulted in increased carbohydrate content in semi-continuous derived biomass. However, the carbohydrate-rich biomass after lipid extraction can be a potential feedstock for fermentation. In addition, the protein (~35 wt%) in biomass can be considered for nutraceuticals production.

Table. 4.9. Physicochemical characteristics of KMC4 biomass derived from fed-batch and semi-continuous mode of cultivation

Components	Fed-batch	Semi-continuous
Proximate composition		
Moisture (wt%)	5 ± 0.2	5 ± 0.1
Volatile matter (wt%)	79.23 ± 1.3	75.95 ± 0.9
Fixed carbon (wt%)	12.36 ± 0.2	15.95 ± 0.2
Ash (wt%)	3.41 ± 0.1	3.1 ± 0.1
Ultimate composition		
C (wt%)[a]	48.72 ± 0.3	49.14 ± 0.2
H (wt%)[a]	7.64 ± 0.1	7.55 ± 0.1
N (wt%)[a]	6.4 ± 0.2	6.02 ± 0.1
S (wt%)[a]	0.15 ± 0.1	0.19 ± 0.1
O (wt%)[b]	33.68 ± 0.3	34 ± 0.4
HHV (MJ Kg^{-1})[a]	21.35 ± 0.3	21.31 ± 0.2
Biochemical composition [a]		
Carbohydrate (wt%)	27.91 ± 0.7	31.16 ± 0.5
Protein (wt%)	35.27 ± 1.4	35.33 ± 1.1
Lipid (wt%)	32.4 ± 1.6	29.71 ± 1.4

[a]Dry basis

[b]By difference (O = 100 - (C+H+S+N+Ash))

4.3.3.2. TGA profile

The thermal decomposition behavior of fed-batch and semi-continuous mode derived biomass was studied using TGA, and the TG graphs are presented in Fig. 4.20. Due to no significant change in the biomass composition, the pyrolytic profile of the present study was found comparable to the biomass derived from the optimization process.

The TG graphs in Fig. 4.20a suggests that both biomass had an initial weight loss of 5% due to the removal of moisture (up to 120 ℃). In the second stage (120-500 ℃), a higher volatile matter in the fed-batch biomass resulted in maximum weight loss (78%) through devolatilization than the semi-continuous biomass (75%). The low-ash content and reduced fixed carbon in both biomass had resulted in less char as a residue (14-17.5%). However, a higher char in semi-continuous biomass signifies the potential of bioenergy production through the combustion process. In addition, the char has several applications such as adsorption, energy storage, catalyst, soil amendment etc. The TG profile for combustion study (Fig. 4.20b) had shown 3-5% initial weight loss for moisture removal followed by 91-93% of weight loss due to the devolatilization and combustion (120-500 °C). This had resulted in a limited residue (3-3.5%) of ash, which was comparable to the biomass derived from the optimization process. Near-complete combustion of both biomass with limited ash ascertains the potential of biomass for bioenergy production through various thermochemical conversion.

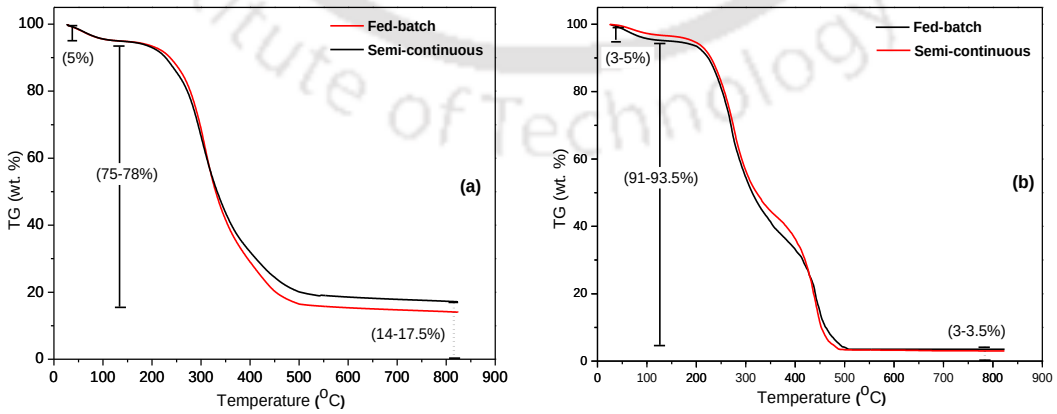

Fig. 4.20. TG profile (a, Pyrolysis; b, combustion) of biomass derived from fed-batch and semi-continuous mode of cultivation

4.3.4. FAME analysis

The FAME composition of lipids derived from the biomass of fed-batch and semi-continuous mode of cultivation is presented in Fig. 4.21. The results suggest that maximum FAMEs were of SFA that accounted for 58-60% of the total FAMEs. However, the semi-continuous (58.78 wt%) had comparatively higher SFA than the fed-batch (59.75 wt%). The SFA of the present study and the optimized PBR, all were found superior to the flask studies. The MUFA content in the present study was found comparable to the optimization study. However, the C16 and C18 content in MUFA was at a higher content in fed-batch (21.14 wt%) than the semi-continuous (20.4 wt%) and optimized PBR (18 wt%). Additionally, the present study had significantly reduced PUFA content in fed-batch (8.75 wt%) and semi-continuous (9.85 wt%) than the previous PBR and flask studies (11-14 wt%).

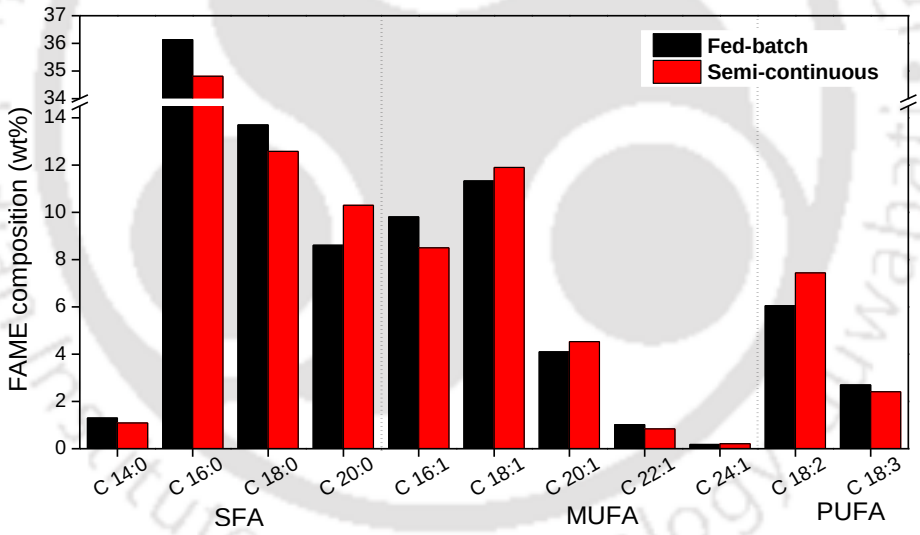

Fig 4.21. FAME profile (SAF: Saturated fatty acid, MUFA: Monounsaturated fatty acid, and PUFA: Polly unsaturated fatty acid) of KMC4 lipid obtained from fed-batch and semi-continuous mode of cultivation.

4.4. HTL and Co-HTL of microalgal biomass and domestic sewage sludge for biocrude production

4.4.1. HTL of individual feedstock

4.4.1.1. HTL of KMC4

Prior to the Co-HTL study, HTL of individual feedstocks (KMC4 and DSS) were performed to comprehend the product distribution profile (biocrude, aqueous phase, and solid residue). Recent studies suggested that reaction temperature is one of the influential parameters that had a significant effect on HTL product distribution [32,191]. Hence, the effect of reaction temperature on the HTL of KMC4 biomass was studied, and obtained results are illustrated in Fig. 4.22a. The study showed that an increase in reaction temperature from 275 °C to 325 °C resulted in increasing biocrude yield (12 wt% to 33 wt%). Whereas, the solid residue was decreased from 14 wt% to 8 wt% along with the aqueous phase (60 wt% to 43 wt%). That leads to a significant increase in conversion from 85 wt% to 92 wt%. A further increase in reaction temperature from 325 °C to 350 °C had not shown any significant change in the yield of biocrude and conversion. Whereas, a small decrease in the aqueous phase (45 wt%) was observed. In consideration to the maximum biocrude yield at a lower temperature, HTL of KMC4 at 325 °C was considered as an optimal reaction temperature. The present findings are comparable to previous studies, which suggests that an increase in reaction temperature promotes biocrude yield [32,107,192]. As reported by Feng et al. [32], a higher temperature could activate the energy required to break the bonds that intensify depolymerization and hydrolysis of biomolecules (lipid, protein, and carbohydrate) present in microalgal biomass. However, an increase in temperature beyond the optimal limit could also result in secondary cracking of biocrude that minimizes the biocrude yield and leads to the formation of coke and gaseous products [192,193].

Although no studies on HTL of DSW treatment derived *Monoraphidium* sp. was reported, the present findings are in agreement with previous reports on microalgal biomass for biocrude productions. Recently Xu et al. [26] reported that an optimal reaction temperature of 340 °C produced ~25 wt% biocrude yield from *Chlorella* sp.

A low biocrude yield in the aforementioned study could be due to the presence of high ash content (16.06 wt%) in the feedstock that resulted in a solid residue of ~17.5 wt%. Besides the optimization of reaction parameters, pre-treatment of feedstock also showed a significant increase in biocrude yield with limiting solid residue. In another study, HTL of *Chlorella pyrenoidosa* at 300 °C with a residence time of 60 min resulted in 38.06 wt% biocrude, which was significantly reduced during the Co-HTL process with starch-rich biomass waste (sweet potato residue) [113]. Zhang et al. [108], found that two minutes of ultrasonic pre-treatment (300 W power) leads to an improved biocrude yield of 50 wt% during HTL of *Spirulina platensis* at 340 °C with 35 min residence time. Hence, significant biocrude yield from KMC4 feedstock without any pretreatment confirmed its potential for sustainable bioenergy production.

4.4.1.2. HTL of DSS

In contrast to KMC4, HTL of DSS had a relatively different product distribution profile as summarized in Fig. 4.22b. An increase in reaction temperature resulted in an enhanced biocrude yield from 9 wt% to 22 wt%. However, the obtained maximum biocrude yield was 33.3% less as compared to the optimal biocrude achieved from KMC4. This could be due to the presence of low volatile matters (56 wt%) in the DSS feedstock (Table 3.2). Similarly, the aqueous phase was present in limited proportions (34–40 wt%), and the solid residue at the optimal reaction temperature (350 °C) was of 33 wt%. A significantly high solid residue was due to the high ash content (31%) of the feedstock, which further restricted the conversion within 57 wt%-67 wt%. A recent study reported that sewage sludge contains organic and inorganic compounds, microbiological pollutants, pathogens, and other hydrocarbons [47,194]. Due to the complex biochemical composition, HTL of wet sewage sludge often requires a moderately higher reaction temperature (340 °C) for optimal biocrude production [47,193].

The biocrude obtained from DSS was found to be comparable to the previous study that achieved a maximum biocrude yield of 22.9 wt% from HTL of sewage sludge at 340 °C [47]. In another study, non-catalytic HTL of sewage sludge at 340 °C and 30 min residence time resulted in a biocrude yield of ~23 wt% [26]. However, Kapusta [195] reported an increased biocrude yield from 22 wt% to 27 wt% due to

ultrasonic pre-treatment. Similarly, HTL of sewage sludge with a mixed organic solvent (MeOH-H_2O) achieved a remarkably high biocrude yield of 46.5 wt%, which had 38.1% of esters and 37.4% of methyl esters with limited solid residue (11 wt%) [193]. Thus, DSS with a considerable biocrude yield (without any pretreatment) was found to be a potential candidate for co-liquefaction with other bioenergy feedstocks. Nonetheless, high ash content in sewage sludge was a critical challenge that may restrict optimum biocrude production. Thus, it is recommended to carry out further studies to evaluate the interaction of DSS with co-feedstock during Co-HTL.

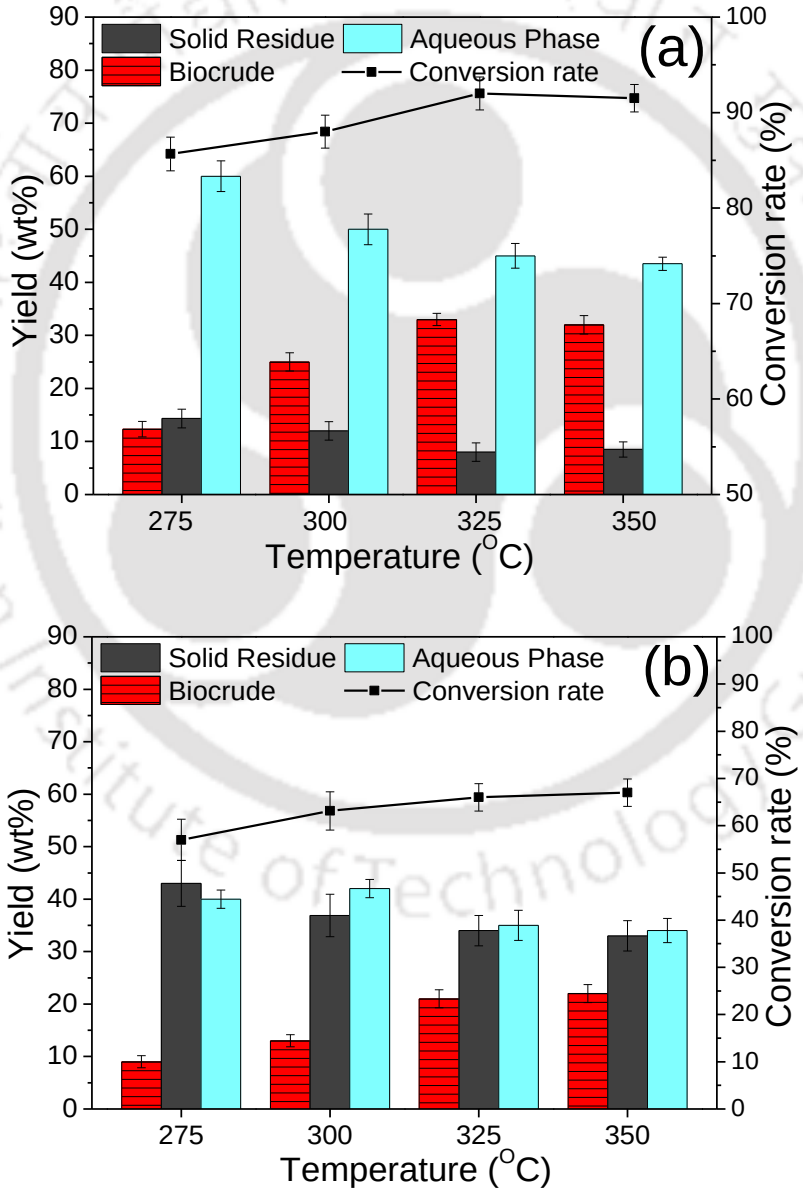

Fig. 4.22. Effect of temperature on HTL products distribution (wt%) and conversion rate (%) of (a) KMC4 (b) DSS (residence time 30 min).

4.4.2. Co-HTL of KMC4 and DSS

4.4.2.1. Effect of temperature

The present study explores the effect of various reaction parameters on Co-HTL of KMC4 and DSS, and the obtained results are presented in Fig. 4.23. The effect of different reaction temperatures on Co-HTL product distribution was the initial study performed with a feedstock ratio of 50:50 (wt%) (KMC4:DSS) (Fig. 4.23a). The study showed an increase in biocrude yield with an increase in reaction temperature from 275 °C to 325 °C, which was comparable to HTL of both feedstocks. A temperature of 325 °C was determined to be optimal for the Co-HTL process, as at this temperature a maximum biocrude yield of 29.47 wt% was achieved. However, the biocrude yield was 10.7% less compared to the HTL of KMC4 (33 wt%). This was due to significant differences in volatile matters concentration in the individual feedstocks (Table 4.8). Therefore, the integration of both feedstocks resulted in a 12% decrease in volatile matters that subsequently hindered the biocrude yield.

In contrast to biocrude, a rise in reaction temperature from 275 °C to 350 °C resulted in a decreased aqueous phase from 50 wt% to 38 wt%. A similar outcome was reported in a recent study that suggested, HTL at low temperatures results in higher aqueous phase fractions due to biomass hydrolysis [33]. However, water acts like an acid and base catalyst owing to high ionic products due to its dissociation into H^+ and OH^- ions when the reaction temperature is further increased near to a critical point. Subsequently, a low dielectric constant triggers isomerization, depolymerization, and repolymerization resulting in the conversion of organic matters into biocrude [192]. This was in agreement with the present study, where a decrease in aqueous phase leads to an increase in biocrude yield.

The present study also exhibited a significantly higher percentage of solid residue (21 wt%) at the optimal reaction temperature of 325 °C. This can be attributed to the fact that feedstock composition in a ratio of 50:50 (wt%) comprised of an ash content of nearly 19%. Subsequently, an increase in solid residue resulted in a maximum conversion of 79 wt% (at 325 °C), which was 14.13% less when compared to the KMC4 (at 325 °C). The obtained results are in agreement with the previous study on Co-HTL of *Chlorella pyrenoidosa* and rice husk (50:50 wt%) where biocrude

yield increased from 15.5% at 200 °C to 37.6% at 300 °C, and then decreased slightly to 33.1% at 350 °C. A similar trend was reported for its solid residues and aqueous phase [196]. Feng et al. [32] performed Co-HTL of *Spirulina* and *Spartina alterniflora*. They reported an increased biocrude yield up to 45.63 wt% at 340 °C, whereas a further rise in temperature led to a decrease in yield. However, to enhance biocrude yield and conversion with limiting solid residue in the present study, the effect of different feedstock ratios on the Co-HTL process was evaluated.

4.4.2.2. Effect of feedstock ratio

The present study investigated the effects of different feedstocks ratios of KMC4 and DSS on Co-HTL product distributions at an optimal reaction temperature of 325 °C. Among the three different feedstock ratios, 75:25 wt% (KMC4:DSS) had the maximum biocrude yield of 34.6 wt% compared to the 50:50 wt% and 25:75 wt% (Fig. 4.23b). This was due to increased volatile matter and a decreased ash content compared to the other feedstock ratios. In addition, the 75:25 wt% feedstock ratio had 4.84% and 64.76% superior biocrude yield compared to the HTL of KMC4 and DSS, respectively.

Similarly, an increased biocrude simultaneously showed a reduced solid residue of 16.6 wt% at 75:25 wt% feedstock ratio compared to 50:50 wt% (21 wt%) and 25:75 wt% (27.5 wt%) respectively. However, an insignificant change in the aqueous phase suggested that an increase in DSS mass ratio had the least effect on its yield. Thus, 75:25 wt% (KMC4:DSS) feedstock ratio was considered optimal for the Co-HTL process that had a maximum conversion of 83.4 wt% with a limited solid residue. This further suggests, positive synergistic effect existed in the Co-HTL of two feedstocks in terms of better quantity bio-crude produced. Thus, selection of KMC4 and DSS was found potential for Co-HTL feedstocks as compared to the previous reports where Co-HTL resulted in a significantly less synergistic effect for biocrude yield [113–115].

An increase in biocrude yield and reduced solid residue during Co-HTL at optimal feedstock ratio (75:25 wt%, KMC4:DSS) could be attributed to the presence of mineral elements in DSS that supported the maximum conversion of organic matters

(further discussed in Section 3.3.5). However, an increased DSS ratio resulted in decreased organic matters in the feedstock that leads to a significant reduction in biocrude yield.

4.4.2.3. Effect of residence time

The HTL and Co-HTL studies were performed with a residence time of 30 min in the preceding experiments for maximum biocrude yield [26,107,197]. However, residence time was also suggested as one of the crucial parameters in Co-HTL due to independent feedstock compositions [193,198]. Thus, the effect of residence time (15 min to 60 min) on Co-HTL was studied at optimal reaction temperature (325 °C) and feedstock ratio of 75:25 wt% (KMC4:DSS). The present study showed a positive effect on biocrude yield with an increase in residence time from 15 min to 45 min (Fig. 4.23c). A maximum biocrude yield of 39.38 wt% was achieved at a residence time of 45 min. That was 16% and 79% superior to the biocrudes obtained from individual HTL of KMC4 and DSS respectively. An improved biocrude yield subsequently limited solid residue content, thus achieved a maximum conversion of 83.96 wt%, which was 25.31% higher than the HTL of DSS. Hence, a residence time of 45 min was considered as optimal with a 13.81% increase in the biocrude yield when compared to 30 min residence time. However, a longer residence time of 60 min increased the aqueous phase and the solid residue, which could be attributed to the subsequent repolymerization of biocrude.

The optimal results of the present study were found comparatively superior to several other reported literature on HTL and Co-HTL of different feedstocks. The biocrude yield (39.38 wt%) from the present Co-HTL study was found higher than the biocrude yield (33.9 wt%) obtained from HTL of *Chlorella* sp. [199]. The present result was also found comparable to the HTL of wastewater treatment derived Chlorella sp. biomass performed at 320 °C, 60 min residence time, and 15% solid loading [198]. The presence of low DSS loading in the present optimal Co-HTL reaction condition resulted in a significantly higher biocrude yield than that reported by Xu et al. [26] (24 wt%). In another study, co-liquefaction of swine manure (SW) and mixed algae culture (AW) was studied at different ratios. A 75%:25% (SW:AW) exhibited an optimal biocrude yield of 35.7 wt%, whereas further increase AW resulted

in decreased biocrude yield [114]. Similarly, Co-HTL of low-lipid microalgae and starch-rich biomass waste resulted in a maximum biocrude yield of ~34 wt% (5:1 feedstock ratio) that was significantly reduced with effect to increase in solid loading of starch-rich biomass [113]. Co-liquefaction of *C. pyrenoidosa* (CP) and rice husk (RH) had a similar trend that followed decreased biocrude yield with an increased RH mass ratio. The biocrude yield constantly increased from 13.9% at the combination of 0% CP with 100% RH to 43.6% at the combination of 100% CP with 0% RH [196]. However, results from the present study suggest that KMC4 and DSS were the potential feedstocks to explore commercial biocrude production via Co-HTL due to an increased biocrude yield. This was because of the minerals presence in DSS that supported synergistic effect on biocrude yield and can mitigate the harmful pathogen in the waste. Further scale-up study will help to explore the physicochemical property of biofuel fractions obtained through fractional distillation and subsequent engine applications. Additionally, the integration of Co-HTL plant operation near the wastewater treatment site may significantly reduce logistics costs associated with the collection and transportation of feedstocks.

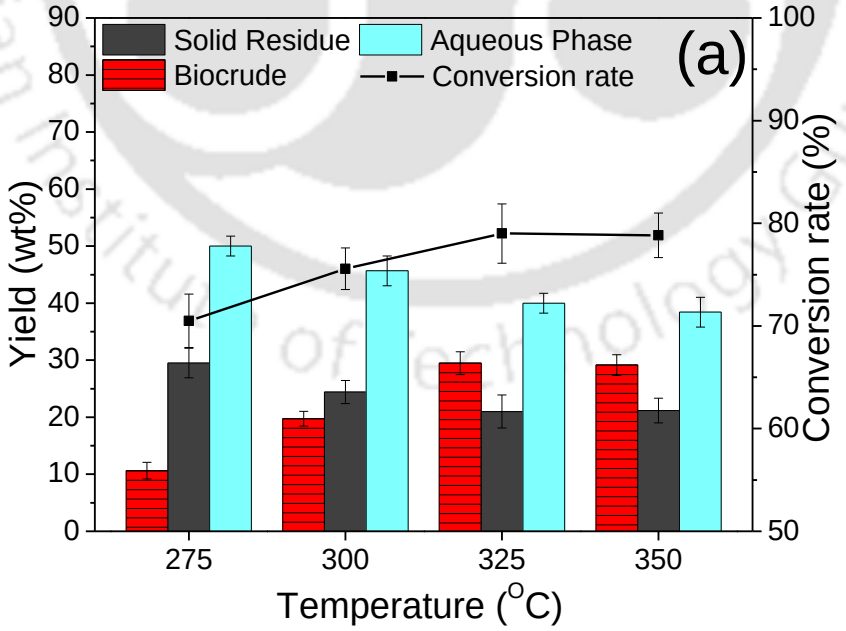

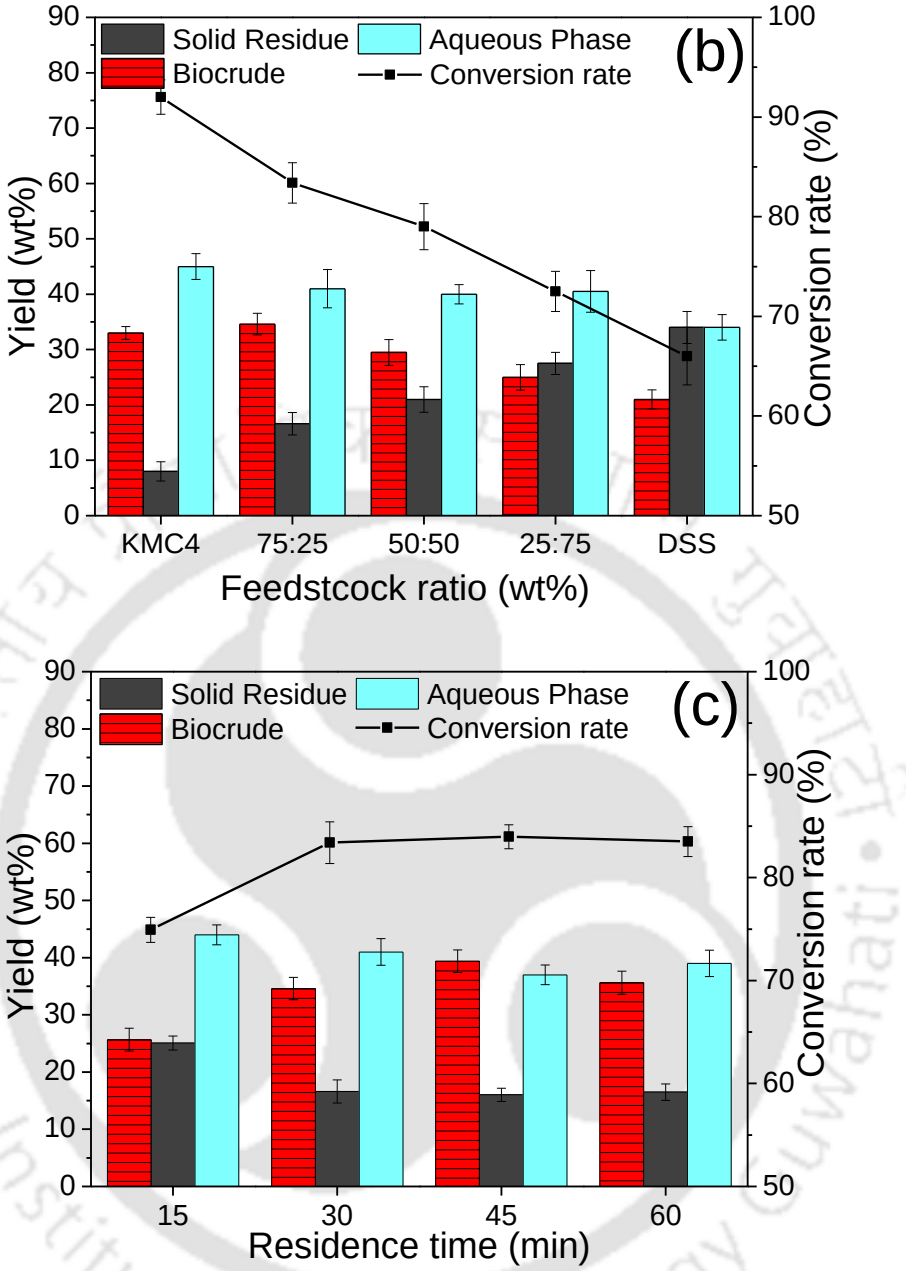

Fig. 4.23. Effect of (a) temperature (50:50 wt% KMC4:DSS, 30 min residence time); (b) feedstock ratio (at 325 °C, 30 min residence time); and (c) residence time (at 325 °C, 75:25 wt% KMC4:DSS) on Co-HTL product distribution (wt%) and conversion rate (%).

4.4.3. Characterization of biocrude

4.4.3.1. Elemental composition and ER of biocrudes

In the present study, the elemental compositions of biocrudes were analyzed to evaluate the energy density and their potential as a substitute for fossil fuel. All three

biocrudes derived from HTL and Co-HTL process were rich in C (73%-77%) and H (9%-11%) (Table 4.10) which was higher than previously reported literature [26,132,199]. The Co-HTL of KMC4 and DSS resulted in an increased atomic H/C ratio in the biocrude (1.65) as compared to biocrude derived from HTL of KMC4 (1.45) and DSS (1.55). In addition, a decrease in oxygen content (8.85%) was recorded in Co-HTL biocrude. A lower O/C and increased H/C in the Co-HTL biocrude was due to deoxygenation and decarboxylation mechanism of feedstock during the liquefaction process [197]. This further implies an intensification of energy density in biofuel, which is an essential factor for the sustainable energy conversion process. The present study exhibited a significant reduction in nitrogen content during Co-HTL, which was much lesser than previous reports [26,192,199]. This could be due to the deamination and decarboxylation of protein present in the feedstock [197].

A decrease in atomic O/C and an increase in the atomic H/C ratio resulted in a 10.12% and 4.5% higher HHV in the Co-HTL biocrude as compared to the biocrude derived from HTL of KMC4 and DSS respectively. Also, HHV of Co-HTL biocrude (39.47 MJ Kg^{-1}) was much higher than the biocrude derived from *Chlorella* sp. [199] and pretreated municipal secondary sludge [132]. However, the present findings are comparable to previous studies where catalytic HTL improved the HHV of biocrude [192,200]. This suggests that the presence of catalytic elements such as Al, Ca, Fe, and Mg in adequate concentrations in the DSS must have triggered deoxygenation and decarboxylation reaction for enhanced biofuel property. The superior HHV further resulted in an energy recovery of 77.73%, which was 30.5% and 50.7% higher, compared to the KMC4 and DSS, respectively. Recently Aguiar et al. [33] reported, higher biocrude yield influenced energy recovery in addition to the heating value. Though the biocrude yield in the present study was higher compared to previous studies, optimizing the liquefaction process further could result in a superior biocrude yield with limiting solid residues. This will also lead to improved energy recovery, as reported earlier [32].

The composition of biocrude was further compared with petro-crude that suggested the atomic H/C ratio of the Co-HTL biocrude (1.64) was at par with the petroleum crude oils (1.5-2). The oxygen and nitrogen content were at a much higher

limit that implies possible NOx emissions during combustion. However, low sulfur in biocrude suggests limited SOx emission that establishes its potential as a biofuel. The overall comparative study of Co-HTL biocrude to the petro-crude revealed a relatively similar profile, except for the high nitrogen and oxygen content. In this context, a catalytic upgradation of biocrude can be recommended for denitrogenation and deoxygenation with simultaneous improvement of the H/C ratio in biocrude [192].

Table 4.10. Elemental composition of biocrudes obtained from HTL and Co-HTL process.

Properties[a]	KMC4	DSS	KMC4:DSS	Petro-crude [192]
Biocrude yield (%)	33 ± 1.15	23 ± 1.73	39.26 ± 2.45	-
C (wt%)	73.82 ± 1.03	75.3 ± 0.9	76.77 ± 1.05	83-87
H (wt%)	9.01 ± 0.3	9.82 ± 0.37	10.6 ± 0.2	10-14
N (wt%)	5.8 ± 0.1	4.71 ± 0.18	3.38 ± 0.1	0.1-2.0
S (wt%)	0.43 ± 0.03	0.74 ± 0.03	0.4 ± 0.06	0.05-6.0
O[b] (wt%)	10.94 ± 0.09	9.43 ± 0.5	8.85 ± 0.3	0.05-1.5
H/C (mol/mol)	1.45	1.55	1.65	1.5-2
O/C (mol/mol)	0.11	0.09	0.09	<0.02
N/C (mol/mol)	0.07	0.05	0.04	<0.02
HHV (MJ Kg^{-1})	35.84 ± 0.86	37.76 ± 1.1	39.47 ± 1.75	42-49
ER (%)	57.6 ± 1.4	46.2 ± 1.18	76.8 ± 1.48	-

[a]Dry basis.
[b]By difference.

4.4.3.2. Distillation profiles of biocrudes

Recently distillation profiles of biocrudes were successfully studied using TGA, which is considered as a miniature distillation process [108,191,197]. In the present study, the distillation profile of biocrudes obtained from HTL and Co-HTL of KMC4 and DSS were studied in TGA and depicted in Fig. 4.24. Additionally, the boiling point distribution was estimated and presented in (Table 4.11). All three biocrudes had shown relatively different distillation profiles with respect to boiling

point distributions. The presence of higher volatile matters with limited ash content in KMC4 feedstock resulted in higher fractions of heavy naphtha (8.53%), kerosene (19.1%), and gas oil (27.23%). Whereas, the presence of low volatile and high ash contents resulted in a reduced distillation profile of DSS derived biocrude with 16.47% of vacuum residue. However, Co-HTL of 75:25 wt% (KMC4:DSS) resulted in 18.76% and 25.23% enhanced yield of heavy naphtha and kerosene fractions as compared to the KMC4 fractions (Table 4.11). Hence, an improved distillation profile could be due to the presence of mineral elements (Al, Ca, Fe, Mg, etc.) in DSS that exhibit significant catalytic properties. However, a high vacuum residue content (13.48%) in Co-HTL derived biocrude was recorded due to the leaching of mineral elements (such as Si and Fe) in DSS. The results of this work is found to be comparable to previous studies that had also reported high vacuum residues [108,111]. However, the Co-HTL biocrude had 74.4% light biocrude fractions (distillation range of 30-400 °C), which was significantly higher than previous reports [26,198]. In this context, Co-HTL derived biocrude was found to be feasible for bioenergy applications. However, future studies on pretreatments and catalytic upgradations could result in enhanced low boiling point fractions [193].

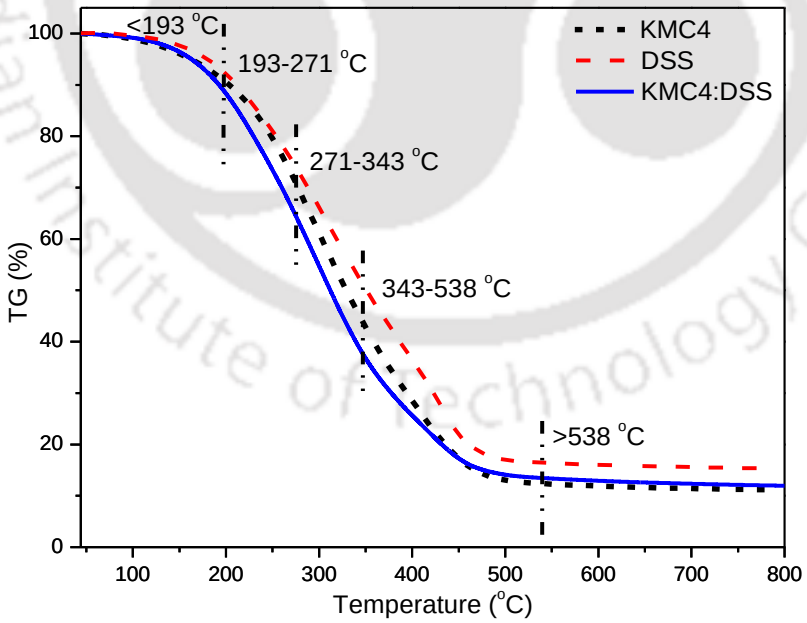

Fig. 4.24. Distillation profile (wt%) of biocrudes derived from HTL and Co-HTL.

Table 4.11. Boiling point distribution (wt%) of biocrudesa obtained from HTL and Co-HTL of KMC4 and DSS.

Distillation range	KMC4	DSS	KMC4:DSS
<193 (Heavy naphtha)	8.53	6.77	10.13
193-271 (Kerosene)	19.1	18.07	23.92
271-343 (Gas oil)	27.23	22.74	27.09
343-538 (Vac. gas oil)	32.75	35.95	25.38
>538 (Vac. residue)	12.39	16.47	13.48

[a] Moisture free and DCM free.

4.4.3.3. FTIR analysis of biocrudes

Different functional groups present in the HTL and Co-HTL derived biocrudes were analyzed using FTIR and presented in Fig. 4.25. The study showed that the functional groups were almost similar in all three different biocrudes that confirmed the presence of comparable chemical structures within the biocrude samples. The absorption peak at 3280 cm^{-1} was from O-H/N-H stretching vibrations of hydroxyl and amino group compounds (water, phenols, fatty acid amides, and N-containing heterocyclic compounds) [108]. The broad and strong absorption peaks in the range of 3000-2800 cm^{-1} and 1460-1350 cm^{-1} were due to the C-H stretching of $-CH_2$ and $-CH_3$ (methyl and methylene) groups that suggested the presence of long-chain aliphatic hydrocarbons [193]. The band from 1800-1590 cm^{-1} are assigned to CO functional groups that indicated the presence of carboxylic acids, ketones, aldehydes and esters in biocrude [32]. Absorption peaks in the range of 1300-1200 cm^{-1} and 1100-1050 cm^{-1} marked the presence of alcohol and phenolic compounds due to C-O stretching vibrations [108]. Additionally, the presence of aromatic compounds and corresponding alternate derivatives in the biocrude is evident from the peaks between 800-730 cm^{-1} [32]. Despite similar functional groups, increased peak intensity due to C-H stretching

and decrease in O-H/N-H, CO, and C-O intensity suggested a reduction in nitrogen and oxygen group. This resulted in increased calorific value and energy recovery, as discussed in the elemental profile of Co-HTL biocrude (Section 3.3.1).

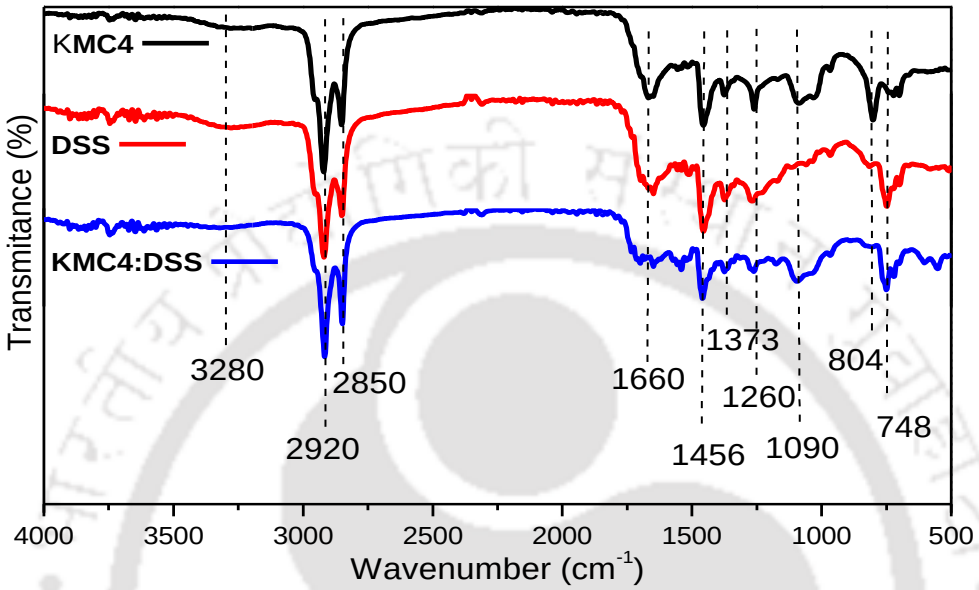

Fig. 4.25. FTIR analysis of biocrudes derived from HTL and Co-HTL.

4.4.3.4. GC–MS analysis of biocrudes

The biocrude derived from the optimal Co-HTL reaction conditions of 325 °C, 75:25 wt% (KMC4:DSS), and 45 min residence time was analyzed by GC-MS along with the HTL biocrudes from KMC4 and DSS to identify the major chemical constituents. The corresponding compounds for individual peaks were identified and depicted in Table 4.12. The study suggests that all three samples had the major compounds in the range of C6 to C28 groups. These compounds were further classified as alcohol, esters, phenols, hydrocarbons, and N and O heterocyclic compounds that were in the concentrations of 11.14%, 58.01%, 8.48%, 11.07%, and 11.3%, in the Co-HTL biocrude (Fig. 4.26). The corresponding values for the biocrude derived from KMC were 5.96%, 21.61%, 4.873%, 4.61%, 7.637%, and for DSS were 5.82%, 23.491%, 4.71%, 5.39%, 0.91%, respectively. The study showed that concentrations of esters, hydrocarbons were relatively increased during the Co-HTL process. The esters compounds in Co-HTL were fumaric acid, ethyl phenyl ester; Carbonic acid,

dodecyl vinyl ester; 2-Propenoic acid, tridecyl ester; Carbonic acid, tridecyl vinyl ester; 2-Propenoic acid, pentadecyl ester; Carbonic acid, tetradecyl vinyl ester; 2-Pentadecanone, 6,10,14-trimethyl-; 3,7,11,15-Tetramethyl-2-hexadecene-1-ol-; dibutyl phalate; hexadecanoic acid, methyl ester; phthalic acid, butyl hept-4-yl ester; 6-Octadecenoic acid, methyl ester; 3,7,11,15-tetramethylhexadec-2-en-1-yl acetate; phthalic acid, di(oct-3-yl) ester. The long-chain fatty acids and esters had resulted from the hydrolysis of the lipids present in the feedstock. The Co-HTL biocrude with high esters content suggests that the biofuel had improved ignition properties [191,192]. The Co-HTL had a substantial quantity of alcohol and hydrocarbons (Isophytol; Cyclohexadecane; 3-Octadecyne; and Neophytadiene) with a molecular weight in the range of 200-400, which were produced due to the hydrolysis of lipids and decarboxylation of fatty acids [192]. A higher proportion of low molecular weight esters along with alcohols and hydrocarbons resulted in an increased yield of low-boiling point fractions (heavy naphtha, kerosene, and gas oil). The biocrude also shown the presence of the phenols and its derivatives (Phenol and 2,4-Di-tert-butylphenol) may likely be due to the breakdown of the cell membrane and cell wall [108]. The N containing heterocyclic compounds (2-Pyrrolidinone, 5-(ethoxymethyl)-; Quinoline, 3-methyl-; Pyrrolo[1,2-a]pyrazine-1,4-dione,hexahydro-3-(2-methylpropyl)-; Pyrrolo[1,2-a]pyrazine-1,4-dione, hexahydro-3-(phenylmethyl)-) may be derived from the decomposition and dehydration of proteins and amides [197,198]. A low phenol in Co-HTL biocrude suggests it was less toxic and hazardous. Whereas, low N containing heterocyclic compounds in Co-HTL biocrude compared to the biocrudes derived from KMC4 and DSS suggests, comparatively low NOx emissions. However, the biocrude requires further upgradation to enhance low volatile fractions and reduced nitrogen content. The present compounds distribution was found comparable to previous reports that also found a high proportion of esters and hydrocarbons with low phenols and N containing heterocyclic compounds [192,197]. However, future studies on the identification of several unidentified compounds will provide insights into fuel property and required an upgradation pathway that can significantly improve the distillation profile of biocrude.

Table 4.12. Tentative compounds and relative peak areas of biocrude derived from HTL (KMC4 and DSS) and Co-HTL (KMC4:DSS) at 325 °C for 45 min with a feedstock ration (75:25 wt%).

RT (min.)	Compound name	Formula	Area (%)		
			KMC4	DSS	Co-HTL
4.062	Phenol	C_6H_6O	0.973	1.01	0.94
4.588	2-Pyrrolidinone, 5-(ethoxymethyl)-	$C_7H_{13}NO_2$	0.79	-	0.7
5.986	2-Cyclopenten-1-one, 2,3-trimethyl-	$C_8H_{12}O$	-	0.64	-
6.261	Pentanamide, 4-methyl-	$C_6H_{13}NO$	0.56	-	-
11.171	Quinoline, 3-methyl-	$C_{10}H_9N$	0.81	-	0.79
13.623	2,4-Di-tert-butylphenol	$C_{14}H_{22}O$	3.9	3.7	3.60
15.106	Fumaric acid, ethyl phenyl ester	$C_{12}H_{12}O_4$	-	2.13	1.88
15.499	Cyclohexadecane	$C_{16}H_{32}$	0.33	0.85	0.45
15.649	Carbonic acid, dodecyl vinyl ester	$C_{15}H_{28}O_3$	0.64	-	0.59
17.881	2-Propenoic acid, tridecyl ester	$C_{16}H_{30}O_2$	0.51	1.39	0.66
18.01	Carbonic acid, tridecyl vinyl ester	$C_{16}H_{30}O_3$	2.19	1.94	2.37
19.179	2-Propenoic acid, pentadecyl ester	$C_{18}H_{34}O_2$	1.73	-	1.50
20.406	Carbonic acid, tetradecyl vinyl ester	$C_{17}H_{32}O_3$	0.44	0.88	0.64
21.262	3-Octadecyne	$C_{18}H_{34}$	0.98	1.13	1.08
21.428	2-Pentadecanone, 6,10,14-trimethyl-	$C_{18}H_{36}O$	-	1.27	1.53
21.777	Neophytadiene	$C_{20}H_{38}$	3.3	3.41	4.40
22.284	3,7,11,15-Tetramethyl-2-hexadecene-1-ol-	$C_{20}H_{40}O$	-	1.66	1.87
22.822	1-Dodecanol, 2-octyl	$C_{20}H_{42}O$	0.372	-	-
23.032	Dibutyl phalate	$C_{16}H_{22}O_4$	1.71	2.18	2.03
23.425	Hexadecanoic acid, methyl ester	$C_{17}H_{34}O_2$	0.96	0.39	0.78
23.726	Pyrrolo[1,2-a]pyrazine-1,4-dione,hexahydro-3-(2-methylpropyl)-	$C_{11}H_{18}N_2O_2$	4.51	-	3.85
23.94	Isophytol	$C_{20}H_{40}O$	4.06	3.81	4.41
24.171	Phthalic acid, butyl hept-4-yl ester	$C_{19}H_{28}O_4$	7.38	4.61	12.04
26.3	Tetrahydropyran Z-10-dodecenoate	$C_{17}H_{30}O_3$		2.03	1.04
27.408	6-Octadecenoic acid, methyl ester	C19H36O2	0.55	0.82	0.42
27.625	3,7,11,15-tetramethylhexadec-2-en-1-yl acetate	$C_{22}H_{42}O_2$	4.2	4.01	3.64
32.41	Pyrrolo[1,2-a]pyrazine-1,4-dione, hexahydro-3-(phenylmethyl)-	$C_{14}H_{16}N_2O_2$	0.96	0.91	0.71
36.392	Phthalic acid, di(oct-3-yl) ester	$C_{24}H_{38}O_4$	1.3	1.57	1.13
39.573	Octacosanol	$C_{28}H_{58}O$	1.9	2.01	1.56

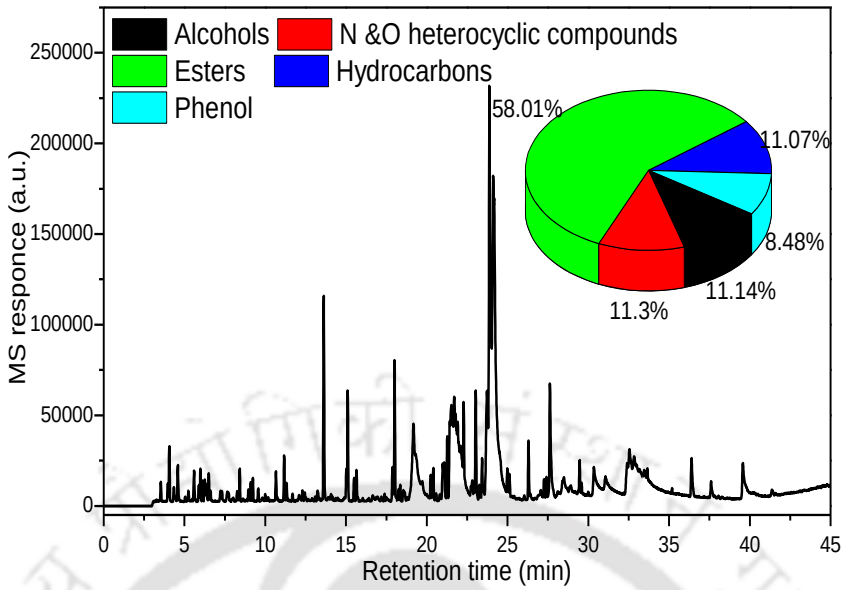

Fig. 4.26. GC-MS chromatogram obtained for biocrude from Co-HTL of 75:25 wt% (KMC4:DSS) at 325 °C and 45 min residence time.

4.4.3.5. Mineral elements in Co-HTL feedstock and derived biocrude

Sewage sludge contains several mineral elements, the direct disposal of which leads to severe environmental pollution. In this context, HTL of DSS has become a research hotspot for the simultaneous mitigation of mineral elements and the transformation of hydrocarbon-rich organic waste into energy-dense biocrude and biochar (solid residues) [201,202]. However, the shift of trace amounts of mineral elements into biocrude could reduce its quality causing interferences in the subsequent downstream process [132,203]. In the present study, the optimal Co-HTL feedstock (75:25 wt%; KMC4:DSS) was characterized by the ICP-AES technique that revealed the presence of Si, Fe, Al, Ca, and Mg in the range of 2500-8200 ppm. Whereas, the concentration of K, Zn, Ti, Mn, Na, Ba, Sr, Ag, Pb were in the range of 2-700 ppm (Fig. 4.27). The elemental distribution in feedstock was found to be comparable to previous reports [26,47,107,132]. The biocrude obtained from the optimal Co-HTL feedstock had shown a relatively lower concentration of mineral elements. The concentration of Al, Mg, K, Ti, Mn and Sr in the biocrude was in the range of 0.2-30 ppm, whereas the concentration of Ca was 100 ppm. However, all these elements were >95% of the concentration present in the feedstock. A few elements such as Si, Fe, Zn, and Na were at a comparatively higher concentration in Co-HTL biocrude that

suggests possible leaching of these elements. A similar observation was reported in a previous study that reported the transfer of heavy metals from sewage sludge to biocrude during fast HTL at 340 °C [47]. Similarly, leaching of heavy metals at low concentrations was observed during the Co-HTL of rice husk and sewage sludge [204]. Hence, an improved biocrude separation process can be recommended to limit the leaching of mineral elements into the biocrude.

The present study reports a higher biocrude yield at optimized Co-HTL reaction conditions, which could be attributed to the presence of aforementioned mineral elements at a substantial quantity in the feedstock [205]. These elements are widely considered for biofuel production through heterogeneous catalytic chemical and thermochemical reactions [29,36,206,207]. However, limited studies are reported to explore the effects of these heavy metals on Co-HTL product distribution. Xu et al. [26] reported that the addition of 20 wt% sewage sludge ash containing metallic compounds supported an enhanced biocrude yield during Co-HTL process was coherent to the present study. In another study, supplementation of sewage sludge-based activated carbons containing metallic compounds had significantly increased biocrude yield during liquefaction of sewage sludge at 350 °C [208]. However, a limited study was done to explore the detailed catalytic mechanism of heavy metals present in DSS for biocrude yield and subsequent Co-HTL product distribution. Hence, further exploration of DSS mineral elements can provide insights into the detailed catalytic mechanisms for improved product distribution profile.

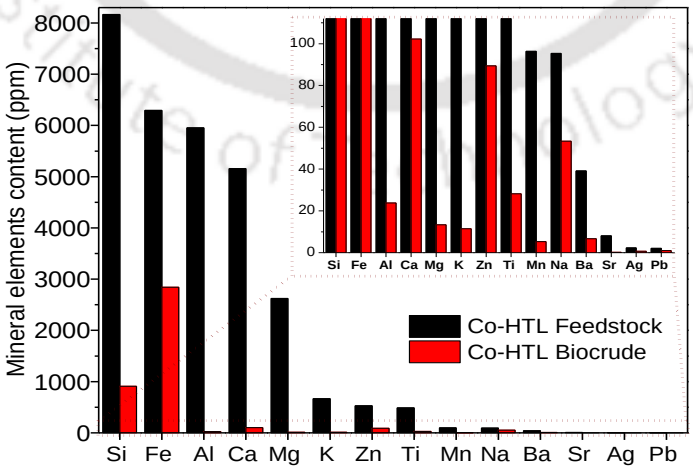

Fig. 4.27. Mineral elements composition (ppm) in the Co-HTL feedstock (75:25 wt%; KMC:DSS) and its biocrude.

4.5. Valorization of solid and liquid residues for value-added products

There is a need for detailed studies on the solid and liquid waste derived from the biofuel conversion process to make microalgal biorefinery energy-efficient and sustainable. The two different biofuel conversion processes that were exponentially studied in the present work are (i) biodiesel production via transesterification and (ii) biocrude production via HTL. The wastes which were derived from these processes include lipid-extracted microalgal biomass (LEMB) from biodiesel conversion, whereas solid residues and aqueous phase were derived from the HTL process. The present section focuses on the characterization and valorization of these waste for the production of value-added co-products.

4.5.1. Characterization of LEMB

Recent studies reported that a large amount of LEMB is generated and estimated to be three times the amount of biodiesel produced [24]. This contains unextracted lipid, carbohydrate, protein, nitrogen, phosphorous, and other micronutrients in substantial quantities that make it a potential biofuel feedstock [1,46]. In view of this, the feasibility of KMC4 LEMB derived from RDSW and control BG11 (section 4) was studied as a bioenergy feedstock.

4.5.1.1. Proximate and ultimate analysis

Proximate and ultimate analysis of biomass determines its potentiality as a bioenergy feedstock. In the present study, proximate analysis of LEMB derived from the RDSW and BG11 had near similar content of moisture (< 6 wt%), volatile matters (75-76 wt%), fixed carbon (16-19 wt%), and ash (2-3 wt%). Both biomass had comparatively less moisture and ash content (< 6wt%) with a higher volatile matter than the *Dunaliella tertiolecta* grown in a photobioreactor [209]. Moreover, it was comparable to various wood biomass conventionally used as bioenergy feedstocks [184]. This suggests that the biomass can be used as a potential feedstock for combustion and bio-oil production through various thermochemical conversion processes.

The ultimate composition of RDSW LEMB was found to contain carbon 47.04%, hydrogen 7.29%, nitrogen 6.6%, sulfur 0.16%, and oxygen 38.91%. The

corresponding values of the elemental composition for the control BG11 LEMB were 50.18%, 7.51%, 6.3%, 0.11%, and 35.9%, respectively. The Table 4.13 suggests, lipid extraction from both RDSW and BG11 biomass had the least effect on its ultimate composition. This could be due to the presence of other biomolecules such as carbohydrates, proteins, and pigments. Further, the composition was compared to other biomass feedstocks that suggest, LEMB had comparatively higher carbon and hydrogen content than other biomass feedstocks [184,209–211]. Further, LEMB with higher hydrogen and less oxygen content had resulted in a significantly high energy value in terms of HHV. Besides, the comparable H/C and O/C ratio define the potential of RDSW LEMB as promising bioenergy feedstock. However, the nitrogen content in LEMB suggests possible NOx emission, which can be resolved with the denitrogenation process.

A study by Guldhe et al. [1] suggested that the presence of carbon and nitrogen at a considerable amount in LEMB residue could make it a favorable feedstock for anaerobic digestion. Also, the produced energy can help to maintain energy balance that makes the integrated microalgal wastewater treatment and bioenergy production system self-sustainable [86]. Two separate studies suggested that carbohydrates present in the LEMB as cellulose, hemicellulose, and starch can be hydrolyzed to produce various biofuels [1,209]. Besides biofuel production, LEMB hydrolysate can also be supplemented to microalgal culture as a growth promoter and enhancer that will augment biomass and lipid yield [24]. In a recent study, an optimal composition of the lipid-free algal hydrolysate and waste glycerol was found to enhance the growth rate and lipid accumulation of *Scenedesmus obliquus* [46]. Another study suggested that the presence of glucose, arabinose, and xylose in lipid-free algal biomass extract resulted in two-fold *Chlorella minutissima* biomass productivity with 54.12% of lipid content [167].

Table 4.13. Ultimate composition of different biomass feedstock and its energy value (HHV).

Biomass feedstock	C	H	N	S	O*	H/C (mol/ mol)	O/C (mol/ mol)	N/C (mol/ mol)	HHV (Mj Kg^{-1})	Reference
Chlorella sp. (LMBRs)	28.36	4.75	5.81	0.27	60.81	1.99	1.6	0.17	5.54	[210]
Dunaliella Tertiolecta (Lipid extracted)	44.78	6.78	8.4	-	40.04	1.8	0.67	0.16	14.83	[209]
Chlorella sp. residual biomass	45.3	6.5	8.5	0.6	27	1.78	0.91	0.006	19.77	[211]
Algae residue after lipid extraction	48.33	6.12	9.12	0.61	35.82	1.6	0.77	0.0001	18.69	[212]
Jatropha wood	42.2	6.3	0.32	-	51.18	1.7	0.45	0.16	14.13	[184]
Pine Saw dust	46.14	6.27	0.006	-	47.23	1.5	0.56	0.16	16.13	
Monoraphidium sp. KMC4 (WL) [a]	48.22	7.66	5.91	0.13	38.08	1.89	0.59	0.1	20.33	Present
Monoraphidium sp. KMC4 (WL) [b]	51.04	7.94	5.5	0.08	35.44	1.85	0.52	0.09	22.14	study
Monoraphidium sp. KMC4 (LEMB) [a]	47.04	7.29	6.6	0.16	38.91	1.85	0.62	0.12	19.36	
Monoraphidium sp. KMC4 (LEMB) [b]	50.18	7.51	6.3	0.11	35.9	1.78	0.54	0.1	21.27	

* Oxygen content estimated by difference; LMBRs: Lipid extracted microalgal biomass residues; [a] RDSW derived biomass; [b] BG11 derived biomass

4.5.1.2. Thermogravimetric analysis

TGA study of KMC4 LEMB derived from RDSW and BG11 was carried out, and the results showed similar trends of thermal degradation profile due to their comparable proximate and ultimate composition. However, it was significantly different from the biomass "with-lipid (WL)". During the pyrolysis study, weight loss was observed in three different stages (Fig. 4.28a). Initial weight loss up to 150 ℃ was due to the release of moisture and light volatile matters (~2-3%) through dehydration. The second stage (200-550 ℃) had the maximum weight loss of 69-71% that represents decomposition of volatile matters such as carbohydrates, proteins, pigments, and leftover lipids in the biomass. This was comparatively less to the WL biomass (73% weight loss). The third stage had 2-3% weight loss that suggests the presence of minimal higher volatile compounds, thus resulted in 20-23% char as residues. The present study had shown the presence of a significantly high volatile matter in KMC4 LEMB compared to the de-oiled biomass of *Chlorella variabilis* [213]. Further, it was also found consistent with the previous studies that reported de-oiled *Chlamydomonas* sp. JSC4, *Chlorella sorokiniana*, and *Dunaliella tertiolecta* had enough potential for bio-oil production by pyrolysis [209,214].

The combustion profile showed four major stages of weight loss (Fig. 4.28b). The first stage (up to 200 ℃) weight loss, expressed dehydration of the biomass. The second stage from 200-280 ℃ had shown early combustion of LEMB due to the absence of lipid and resulted in 88%-91% weight loss. This was significantly different from the WL biomass, which had the second stage of degradation profile ranging from a temperature of 200 ℃ to 440 ℃. However, in contrast to WL, LEMB had 2-3% weight loss between 260-460℃ (third stage) that could be due to the degradation of leftover lipids in the cells. Lastly, in the fourth stage, from 460 ℃ onwards, a negligible weight loss was observed that could be due to the oxidation of char. The combustion profile of LEMB was found to be superior to previous reports [160,161]. Thus, the results suggest that LEMB can be used for bioenergy production through the combustion process, and it will release < 5% of ash as residue. Additionally, low-temperature combustion will also make process energy efficient. The above characterization demonstrates the feasibility of biofuel production from the LEMB

through chemical, biochemical, and thermochemical processes. However, estimation of energy recovery, scale-up potential, technoeconomic analysis, and life-cycle analysis will validate the sustainability of the process.

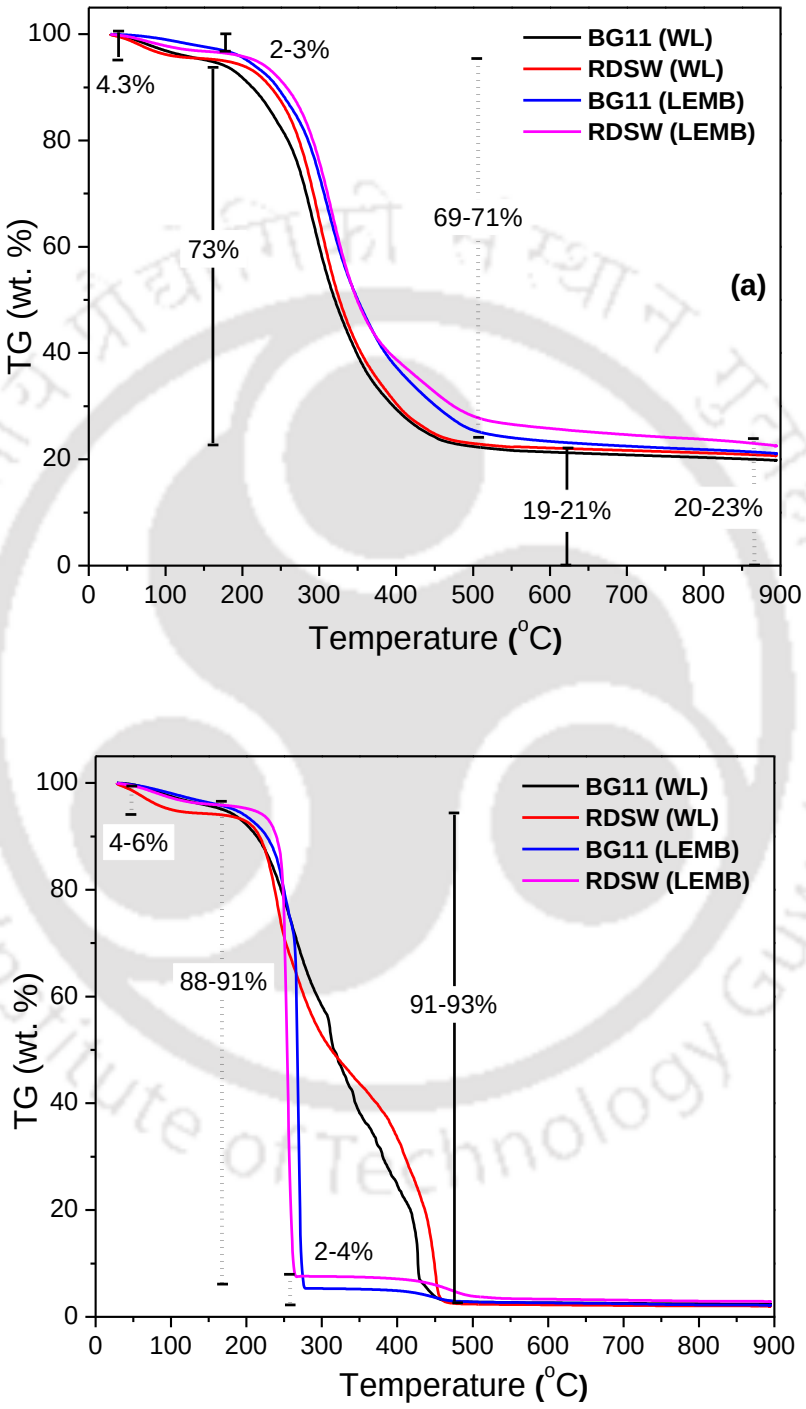

Fig. 4.28. (a) Pyrolysis and (b) combustion profile of KMC4 WL (with-lipid) and LEMB biomass derived from RDSW and BG11.

4.5.2. Conversion of LEMB to hydrochar

Among several solid waste-derived biofuel conversion processes, the present study was focused on hydrochar production via hydrothermal carbonization (HTC) of LEMB. During this, the effect of reaction parameters (temperature and residence time) on hydrochar yield and its property was explored. Considering the need for a large quantity of biomass to conduct multiple experiments, LEMB was collected from KMC4 biomass after the lipid extraction that was obtained from the batch process in PBR (section 4.2.2). The composition of biomass feedstock is shown in Table 4.14.

4.5.2.1. Hydrochar yield

The reaction temperature and residence time are the two critical parameters in HTC that determine hydrochar yield and its property [37]. Recently several researchers studied HTC of biomass with a reaction temperature ranging from 150 ℃ to 280 ℃, and residence time from 15 min to 4 hr [38,215–217]. The studies found that the optimal reaction parameters depend on the feedstock composition. However, the hydrochar yield from temperature and residence time of 200-250 ℃ and 30-60 min had a significantly high energy content. In consideration to that, the present experiments are performed, and the obtained results are shown in Fig. 4.29. The study showed that with an increase in reaction temperature and residence time, hydrochar yield was decreased. Among all, the highest and lowest hydrochar yield was obtained from HC200-30 and HC250-60, which was of 67.81 wt% and 47.36 wt%, respectively. In contrast, increasing temperature (200-225 ℃) resulted in a superior calorific value (HHV) obtained from HC250-60 (29.82 MJ Kg^{-1}), which was later decreased at a reaction temperature of 250 ℃.

The present result was in accordance to the previous studies that suggest, increasing reaction temperature and residence time results in decreased hydrochar yield and increased calorific value [37,215,216]. A recent study reported that higher temperature supports the breakdown of biomass through the process of hydrolysis, dehydration, decarboxylation, aromatization, and re-condensation mechanism. However, the supply of additional energy delivered through temperature resulted in the increased production of an aqueous and gaseous fraction instead of hydrochar [37].

The hydrochar yield from the present study was found comparable to the previous reports [215,216,218].

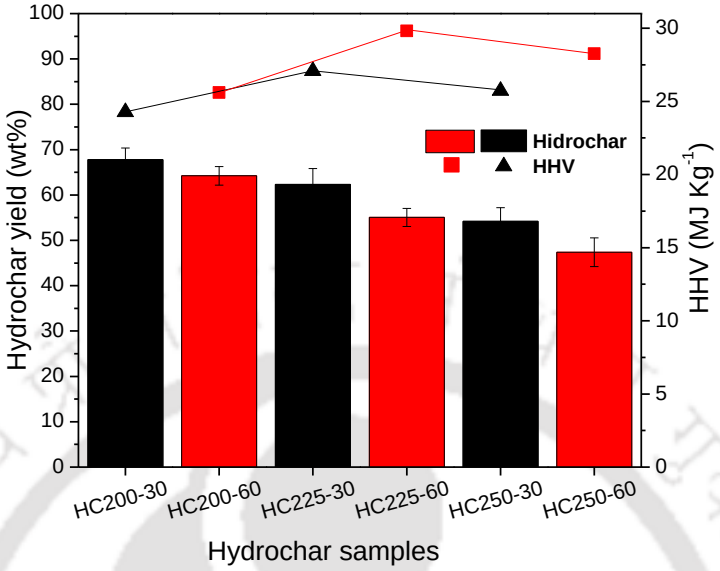

Fig. 4.29. Effect of reaction temperature and time on hydrochar yield (wt%) and its corresponding calorific value in terms of HHV (MJ Kg^{-1}).

4.5.2.2. Characterization of hydrochar

The elemental compositions of the hydrochar samples and their energy content are presented in Table 4.14. Compared to the biomass, all hydrochar samples had a higher proportion of carbon, hydrogen, and a lower proportion of nitrogen, sulfur, and oxygen. It was mainly due to dehydration and decarboxylation processes [219]. In context to the effect of reaction parameters on hydrochar composition, an increase in reaction temperature from 200-225 ℃ supported for an increased carbon (57.23% to 65.8%) and hydrogen content (7.2% to 7.98%). In contrast, the oxygen, nitrogen, and sulfur content was significantly decreased. However, a further increase in temperature to 250 ℃ resulted in decreased carbon and hydrogen content. Lee et al. [215] reported, higher temperature (220 ℃ and 240 ℃) breaks carbon bond in biomass and emits CO and CO_2, which leads to the reduced carbon content in hydrochar. Whereas dehydration and decarboxylation resulted in reduced oxygen content [216]. The nitrogen and sulfur oxides formed during HTC are dissolved in the aqueous phase [219]. Thus, nitrogen and sulfur content in hydrochar were in accordance with the

potential risk of airborne pollutant formation (i.e., SOx and NOx), which can be emitted into the atmosphere during hydrochar combustion [215]. Additionally, the elemental composition of the present hydrochars was found comparable to the previous studies [121,215,216,220].

The calorific value (HHV) was increased with an increase in reaction temperature (from 200℃ to 225 ℃), and 29.77 MJ Kg^{-1} was the maximum in HC225-60. However, a further increase in temperature to 250 ℃ showed reduced calorific value. The calorific value of HC225-60 was found significantly higher than the hydrochars obtained from various feedstocks such as lipid extracted algae (*Chlorella vulgaris*), *Scenedesmus* sp. (after pretreatment) and other microalgal biomass [38,215,216]. Additionally, increased calorific value in the present study supported a higher energy density (ED) in HC225-60 (1.53). However, reduced hydrochar yield resulted in reduced energy yield due to the enhanced transfer of the organic matter to aqueous and gaseous phase [221].

Recently, several studies estimated the coalification degree of hydrochar for commercial coals using the Van Krevelen diagram [38,215,216]. In that context, the H/C and O/C ratio of biomass and hydrochars were estimated to study the effect of HTC reaction parameters on the coalification degree and presented in Fig. 4.30. The study showed that all hydrochar samples were in the range of lignite (low-rank coal), whereas HC-225-60 had the least H/C and O/C ratio. A reduction in the H/C ratio was due to dehydration and increased degree of aromatization, while O/C reduced through the process of dehydration and decarboxylation. Recently Liu et al. [216] reported, low H/C and O/C have superior combustion potential with limiting energy loss through fumes and steam, which was observed in HC225-60. The present results are in agreement with the previous study that suggests, optimal reaction temperature and retention time lead to a least H/C and O/C ratio [38,215,216]. Thus, the above study found, HTC225-60 had the maximum energy content for superior calorific value, energy density (ED), and energy yield (EY) that defines its potential for solid fuel.

Table 4.14. Effect of HTC reaction condition on hydrochar yield, and its property.

Sample	T (°C)	Time (min.)	Yield (wt%)	C	H	N	S	O*	H/C	O/C	N/C	ED	EY (%)	HHV (MJ Kg^{-1})
Biomass[a]	-	-	-	48.16	6.9	7.11	0.19	37.64	1.7	0.6	0.13	-	-	19.41
HC200-30	200	30	68 ± 3	57.23	7.2	5.3	0.25	30.02	1.49	0.39	0.07	1.24	84.74	24.26
HC200-60	200	60	64 ± 2	59.03	7.49	4.9	0.21	28.36	1.51	0.36	0.07	1.31	84.63	25.58
HC225-30	225	30	62 ± 3	61.39	7.67	4.8	0.19	25.94	1.49	0.31	0.06	1.39	86.92	27.07
HC225-60	225	60	55 ± 2	65.80	7.98	4.42	0.18	21.60	1.44	0.24	0.05	1.53	84.43	29.77
HC250-30	250	30	54 ± 3	60.39	7.17	4.54	0.17	27.71	1.41	0.34	0.06	1.32	71.77	25.7
HC250-60	250	60	47 ± 3	63.38	7.82	4.41	0.16	24.22	1.47	0.28	0.05	1.45	68.93	28.25

[a] LEMB derived from the PBR; HC: Hydrochar; T: Temperature; *O: Estimated by difference; ED: Energy densification ratio; EY : Energy yield

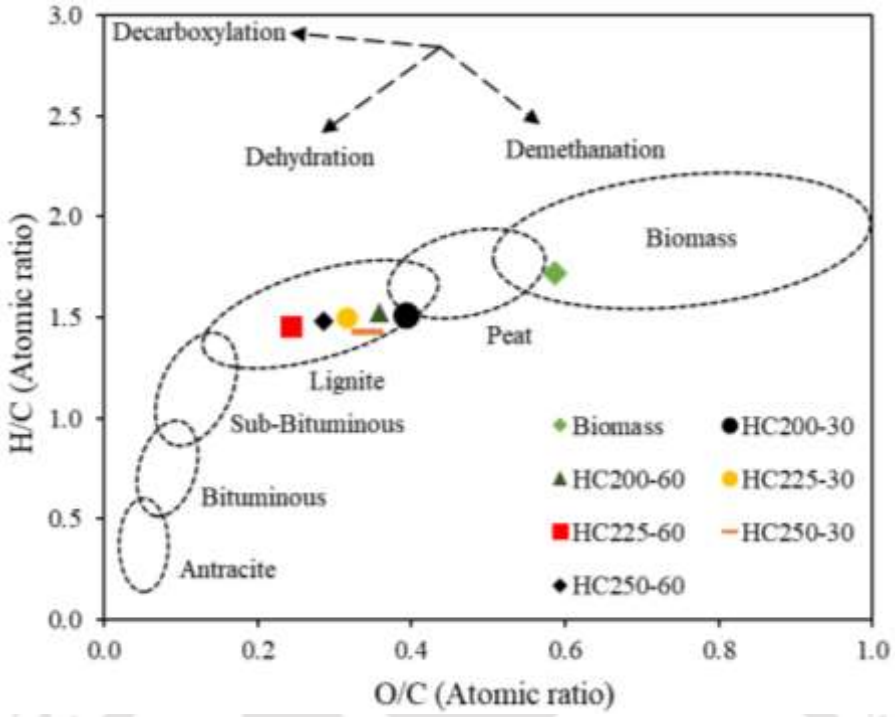

Fig. 4.30. The Van Krevelen diagrams of biomass and hydrochar samples.

To evaluate combustion potential of the optimal hydrochar, thermogravimetric analysis (TGA) of HC225-60 was performed under an air atmosphere, and the obtained thermogravimetric (TG) profile is presented in Fig. 4.31. During the combustion, weight loss follows moisture removal, volatile removal, volatile ignition, char ignition, and char burnout, respectively [215]. The overall weight loss in the present study was completed in three stages. In the first stage (up to 120 ℃), dehydration resulted in the removal of moisture content that accounted for a nominal weight loss of (3.7 %). The second stage (200 ℃ to 550 ℃) had the maximum weight loss (83.25%) due to the devolatilization and combustion of hydrochar. The third stage (550 ℃ onwards) had the least weight loss (2%), which occurred due to the combustion of char. The above study suggests maximum weight loss defines the potential of HC225-60 as solid biofuel for combustion purposes that will have a high energy output with SOx and NOx release under the permissible limit (as per elemental composition). The present results were found comparable to the hydrochar derived from the lipid extracted biomass of *Chlorella vulgaris* [215], pretreated *Scenedesmus* sp. [216], and *Chlorella* sp. [222].

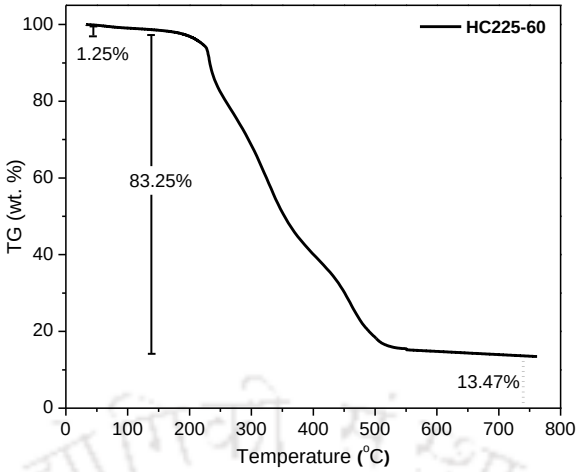

Fig. 4.31. Combustion profile of hydrochar (HC225-60) obtained from the HTC at 225 °C with 60 min residence time.

4.5.3. Valorization of waste derived from Co-HTL

Solid and liquid waste derived from the HTL process contain sufficient nutrients and energy values. Reduce, recycle, and reuse of these waste can significantly turn bioenergy conversion to an energy-efficient process. In the present study, Co-HTL of KMC4 and DSW was optimized and achieved significantly high biocrude yield in comparison to the HTL of individual feedstock. Furthermore, the optimal reaction condition released 53.03 wt% of residue in the form of aqueous phase and solid residue that can be recycled and reused under biorefinery approach. After all, comprehensive characterization is essential that will decide its potential application. In this context, aqueous phase and solid residues obtained from the optimal Co-HTL reaction condition was characterized to explore its potential application.

4.5.3.1. Characterization of aqueous phase

The optimal Co-HTL (KMC4:DSS) at 325 °C for 45 min with 75:25 wt% feedstock ratio resulted in an aqueous phase yield of 37 wt%. Table 4.15 depicts detailed composition of the aqueous phase. The pH of aqueous phase was found slightly alkaline (pH-8.2) that was due to the release of ammonia through hydrolysis and deamination [223]. This can also be validated through nitrogen contents in the form of ammonia (1.9 g L^{-1}) and nitrate (0.13 g L^{-1}) in the sample. The phosphate content (0.22 g L^{-1}) in aqueous phase was relatively less than nitrogen content that

could be due to transfer of organophosphates such as phospholipids to the solvent (DCM) [130]. Among all nutrients, TOC had the maximum concentration (12.87 g L^{-1}), which are comparable to previous studies [223]. Recently, several applications of these nutrients rich aqueous phase samples were studied for heterotrophic microalgal growth, biogas production through anaerobic digestion, and also reused in HTC and HTL [223]. Moreover, presence of phenol and carboxylic acid rich compounds has applications in pharmaceutical and chemical industries [112].

4.5.3.2. Characterization of solid residues

The optimal reaction condition of Co-HTL process resulted in solid residue of 16.03 wt%, which has significant applications in various sectors due to its energy density as estimated from elemental analysis (Table 4.15). The carbon (47.8 wt%), hydrogen (6.1 wt%), and HHV (17.23 MJ Kg^{-1}) content was comparable to several biomass feedstocks [35]. Hence, it can be used as a potential bioenergy feedstock. The solid residues from the HTL process are also considered as biochar that has applications in soil amendment, construction materials, catalysts for bioenergy conversion processes, and storage material for hydrogen [133]. Additionally, the solid residues can also be considered as biosorbent and carbon supplement in anaerobic digestion [48]. Hence, the characterization of aqueous phase and solid residues confirmed their potential as value-added products which has several applications under biorefinery approach.

Table 4.15. Composition of aqueous phase and solid residue derived from co-HTL (KMC4:DSS) at 325 °C for 45 min with 75:25 wt% feedstock ratio.

Aqueous phase[a]					
pH	TDS (gL^{-1})	NH_4^+ (gL^{-1})	NO_3^- (gL^{-1})	PO_4^{3-} (gL^{-1})	TOC (gL^{-1})
8.2	19.6	1.9	0.13	0.22	12.87
Solid residue[b]					
C (wt%)	H (wt%)	N (wt%)	S (wt%)	HHV (MJ Kg^{-1})	
47.8	6.1	3.1	0.19	17.23	

[a]Solvent free
[b]Dry basis

4.6. Scale-up feasibility and mass balance of the biorefinery

The results obtained from the optimized experimental conditions had shown significant potential for large scale cultivation of KMC4 using domestic sewage wastewater. In addition, the obtained biofuels such as biodiesel and biocrude fractions (petrol, kerosene and diesel) had sustainable commercial applications. In that context a theoretical conversion yield and mass balance of the developed biorefinery was estimated at a scalled up conditions and the obtained results are depicted in Fig. 4.3.

To perform mass cultivation of microalgae, DSW can be collected from the campus sewage treatment plant (STP) of IIT Guwahati, which has a wastewater treatment capacity of 1.3 million litre per day. The present estimation shows that, to use of one million litre of DSW for batch cultivation of KMC4 will require nitrate and phosphate supplement of 2,520 kg and 30 kg, respectively. This will further generate 2,490 kg biomass (dry cell weight) followed by 4,822 kg CO_2 sequestration. The biomass conversion to biofuel will result in production of 632 kg of biodiesel and 980 kg of biocrude with a petrol, kerosene and diesel fractions of 99 kg, 234 kg, and 266 kg, respectively. In addition, the biorefinery process will generate hydrochar of 974 kg and solid residue (char) of 398 kg. The commercial application of the biofuel suggests that around 600 kg biodiesel can support a city bus to run ten return trips (60 km) for 26 days with 20% blending (B20) with commercial diesel.

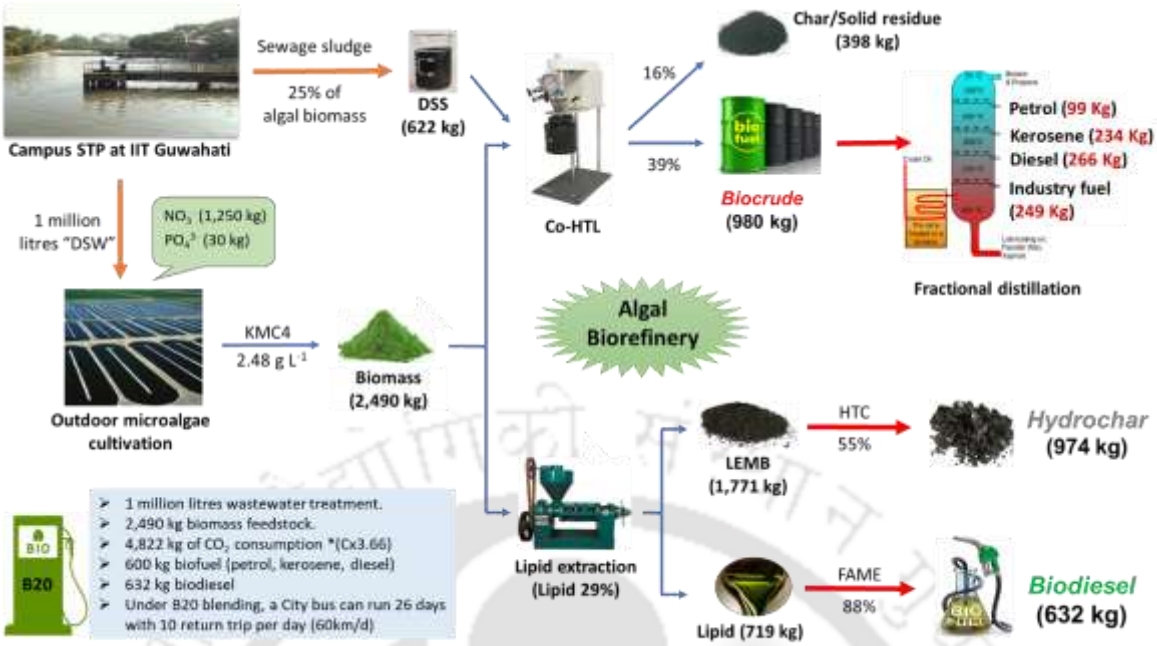

Fig. 4.32. Theoretical conversion yield and mass balance of the developed microalgal biorefinery

Chapter 5

Conclusion and Future Scope

5.1. Concluding Remark

The initial screening study shown, RDSW was a promising microalgal growth medium that can significantly reduce freshwater dependency. Among eight microalgal strains, *Monoraphidium* sp. KMC4 was attributed as the potential strain that produced higher biomass and lipid yield along with superior bioremediation ability. The elemental, biochemical, and thermochemical characterization of RDSW derived KMC4 biomass was comparable to control BG11 biomass.

To enhance the biomass yield, KMC4 culture condition was optimized in the flask. The optimization study in RDSW with KMC4 concludes with the following conditions: supplement of 1.25 g L^{-1} nitrate and 30 mg L^{-1} phosphate followed by culture condition of 25 ℃ temperature, 15%, v/v inoculum, and 115 µmol m^{-2} s^{-1} light intensity. The optimized study resulted in a significantly improved biomass yield of 2.28 ± 0.07 g L^{-1} compared to the initial unoptimized flask study with 1.47 ± 0.09 g L^{-1}. Further, the process optimization was performed in 25 L flat panel indoor PBR. The optimization study found 1.25 g L^{-1} (nitrate), 30 mg L^{-1} (phosphate), and 25 ℃ (culture temperature), 15% (inoculum), a combination of 250-500 µmol m^{-2} s^{-1} (light intensity), and a combination of 2-4% of CO_2 optimal for KMC4 growth in indoor-photobioreactor with RDSW as a growth medium. The optimized condition in PBR resulted in 2.49 ± 0.07 g L^{-1} of biomass yield. The optimized batch process in PBR was further studied under fed-batch and semi-continuous mode that had resulted in biomass yield of 3.62 ± 0.1 g L^{-1} and 6.14 g L^{-1}, respectively. At the end of both experiments, the nutrient removal profile of KMC4 suggests a need for further optimization that will result in maximum nutrient removal.

Biocrude production via Co-HTL of wastewater treatment derived *Monoraphidium* sp. KMC4 biomass and domestic sewage sludge were reported in this work. An optimal reaction condition of 325 °C, 75:25 wt % (KMC4:DSS), and 45 min residence time resulted in a biocrude yield of 39.6 wt% with a conversion 83.96 wt%. The biocrude from Co-HTL was found to be superior to the individual biocrudes derived from KMC4 and DSS. The Co-HTL biocrude had higher C (76.77%), H (10.6%), and its atomic H/C ratio was close to the petro-crude (1.5-2.0). Additionally, reduced O and N content resulted in an improved HHV (39.47 MJ Kg^{-1}) with energy recovery of 76.8%. The distillation profile suggested that Co-HTL significantly enhanced the production of low-boiling biocrude fractions (heavy naphtha, kerosene, and gas oil) with a nominal vacuum residue. The functional groups and chemical constituents further confirmed significant hydrocarbons in the biocrude with limited N and O heterocyclic compounds. Improved physicochemical and thermal properties of Co-HTL biocrude, followed by an enhanced biocrude yield, was possibly due to the mineral elements distribution in DSS (feedstock). Whereas, separation of these minerals after the completion of Co-HTL reaction, resulted in significantly enhanced fuel property of biocrude.

The final objective of the present work was to perform a comprehensive characterization of solid residues and liquid effluents generated through the biofuel conversion process to facilitate the circular bioeconomy model. The optimization of HTC used solid residue LEMB as feedstock that had resulted in 55 ± 2 wt% hydrochar yield. The optimal hydrochar had H/C and O/C profile comparable to lignite coal, along with superior biofuel potential. Additionally, characterization of the aqueous phase and solid residue had shown significant nutrients content and energy value for potential applications under the biorefinery approach.

Thus, the above study concludes that native microalgal strain *Monoraphidium* sp. KMC4 had significant scalability and bioremediation potential. The biocrude production using DSS as one of co-feedstock was found promising for sustainable waste assimilation, followed by biofuel production. Additionally, valorization of solid and liquid waste towards producing value-added co-products will make microalgae biorefinery self-sustainable, energy-efficient, and cost-effective.

5.2. Future scope

The present findings had significantly addressed critical challenges involved in microalgal biorefinery. However, the above study was limited to a lab-scale. Therefore, much scope for future studies is proposed to support the commercial implementation of the present biorefinery model. This includes (i) mass cultivation for bioremediation followed by biomass production; (ii) continuous pilot-scale biofuel conversion; (iii) recycle of solid and liquid waste; (iv) TEA and LCA of pilot-scale microalgal biorefinery model.

Scale-up studies in outdoor raceway ponds and low-cost outdoor PBRs will generate significant biomass and provide a platform to evaluate the sustainability of the process. Implementation of the outdoor cultivation systems near industries or sewage treatment plants can support convenient accessibility of wastewater. At the same time, HTL operation under continuous mode will generate sufficient biocrude that can be transferred to existing petroleum refineries for fractional distillation. Valorization of solid residues and liquid effluents in the present study had shown potential biorefinery applications. However, the recovery of waste from each stage is a major challenge that needs to be addressed during pilot-scale operations. Additionally, repetitive recycling of solid and liquid waste on quality and quantity of products needs to be explored. Finally, techno-economic evaluation and life cycle analysis of pilot-scale microalgal biorefinery model is required that will suggest sustainability of the overall process. In addition, revision of government policies may be proposed to provide subsidies and tax exemption on the capital and operational cost of microalgal biorefinery to encourage commercialization of the process.

The present study also proposes a futuristic microalgal biorefinery approach (Fig. 5.1). During this, solid and liquid waste collected from different sectors (domestic, municipal, agricultural, and industrial) will be valorized for bioenergy feedstocks. Moreover, the integrated process will treat respective wastewater from each sector and recycle it. The proposed model will address feedstock limitations (comparatively less microalgal biomass productivity in winter and rainy) and waste mitigation followed by productions of value-added biorefinery products.

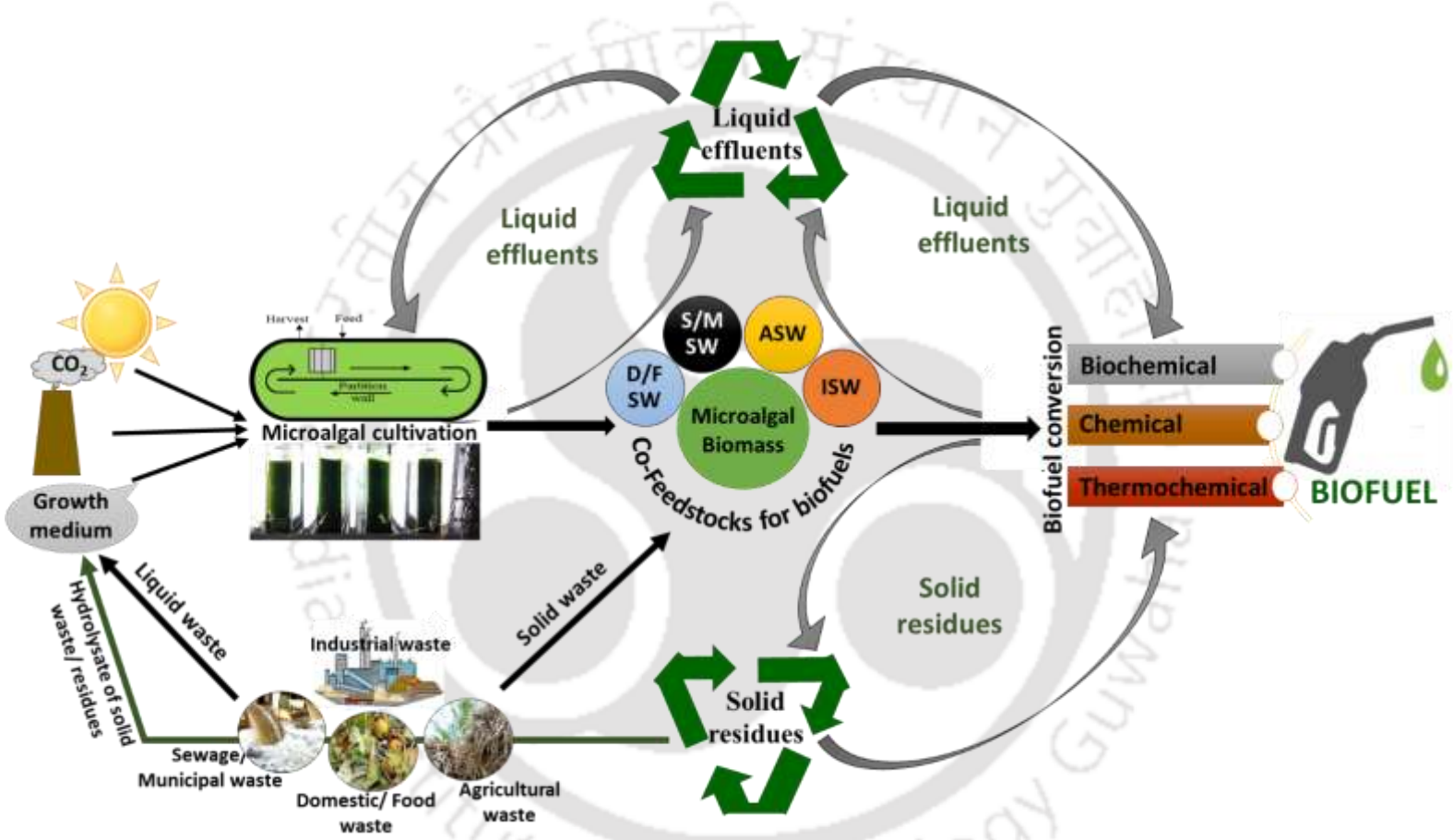

Fig.5.1. A sustainable microalgal biorefinery approach for mitigation and conversion of waste feedstocks to bioenergy under a circular bioeconomy (D/FSW – Domestic/food solid-waste; S/MSW – Sewage/municipal solid-waste; ASW – Agricultural solid-waste; ISW – Industrial solid-waste).

References

[1] Guldhe A, Kumari S, Ramanna L, Ramsundar P, Singh P, Rawat I, et al. Prospects , recent advancements and challenges of different wastewater streams for microalgal cultivation. J Environ Manage 2017;203:299–315. doi:10.1016/j.jenvman.2017.08.012.

[2] Bajpai P, Dash V. Hybrid renewable energy systems for power generation in stand-alone applications: A review. Renew Sustain Energy Rev 2012;16:2926–39. doi:10.1016/j.rser.2012.02.009.

[3] Panwar NL, Kaushik SC, Kothari S. Role of renewable energy sources in environmental protection: A review. Renew Sustain Energy Rev 2011;15:1513–24. doi:10.1016/j.rser.2010.11.037.

[4] Fischer G, Schrattenholzer L. Global bioenergy potentials through 2050. Biomass and Bioenergy 2001;20:151–9. doi:10.1016/S0961-9534(00)00074-X.

[5] Shu K, Schneider UA, Scheffran J. Optimizing the bioenergy industry infrastructure: Transportation networks and bioenergy plant locations. Appl Energy 2017;192:247–61. doi:10.1016/j.apenergy.2017.01.092.

[6] Saidur R, Abdelaziz EA, Demirbas A, Hossain MS, Mekhilef S. A review on biomass as a fuel for boilers. Renew Sustain Energy Rev 2011;15:2262–89. doi:10.1016/j.rser.2011.02.015.

[7] Maity JP, Bundschuh J, Chen CY, Bhattacharya P. Microalgae for third generation biofuel production, mitigation ofgreenhouse gas emissions and wastewater treatment: Present andfuture perspectives - A mini review. Energy 2014;78:104–13. doi:10.1016/j.energy.2014.04.003.

[8] Mathimani T, Pugazhendhi A. Utilization of algae for biofuel, bio-products and bio-remediation. Biocatal Agric Biotechnol 2019;17:326–30. doi:10.1016/j.bcab.2018.12.007.

[9] Costa JAV, de Morais MG. The role of biochemical engineering in the production of biofuels from microalgae. Bioresour Technol 2011;102:2–9. doi:10.1016/j.biortech.2010.06.014.

[10] Wijffels RH, Barbosa MJ. An outlook on microalgal biofuels. Science (80-) 2010;329:796–9. doi:10.1126/science.1189003.

[11] Brennan L, Owende P. Biofuels from microalgae—A review of technologies for production, processing, and extractions of biofuels and co-products. Renew Sustain Energy Rev 2010;14:557–77. doi:10.1016/j.rser.2009.10.009.

[12] Nagarajan D, Lee DJ, Chen CY, Chang JS. Resource recovery from wastewaters using microalgae-based approaches: A circular bioeconomy perspective. Bioresour Technol 2020;302:122817. doi:10.1016/j.biortech.2020.122817.

[13] Chisti Y. Biodiesel from microalgae. Biotechnol Adv 2007;25:294–306. doi:10.1016/j.biotechadv.2007.02.001.

[14] Mata TM, Martins AA, Caetano NS. Microalgae for biodiesel production and other applications: A review. Renew Sustain Energy Rev 2010;14:217–32. doi:10.1016/j.rser.2009.07.020.

[15] Venkata Mohan S, Nikhil GN, Chiranjeevi P, Nagendranatha Reddy C, Rohit M V., Kumar AN, et al. Waste biorefinery models towards sustainable circular bioeconomy: Critical review and future perspectives. Bioresour Technol 2016;215:2–12. doi:10.1016/j.biortech.2016.03.130.

[16] Li K, Liu Q, Fang F, Luo R, Lu Q, Zhou W, et al. Microalgae-based wastewater treatment for nutrients recovery: A review. Bioresour Technol 2019;291:121934. doi:10.1016/j.biortech.2019.121934.

[17] Hemalatha M, Venkata Mohan S. Microalgae cultivation as tertiary unit operation for treatment of pharmaceutical wastewater associated with lipid production. Bioresour Technol 2016;215:117–22. doi:10.1016/j.biortech.2016.04.101.

[18] Gonçalves AL, Pires JCM, Simões M. A review on the use of microalgal consortia for wastewater treatment. Algal Res 2017;24:403–15. doi:10.1016/j.algal.2016.11.008.

[19] Abargues MR, Ferrer J, Bouzas A, Seco A. Removal and fate of endocrine disruptors chemicals under lab-scale postreatment stage. Removal assessment using light, oxygen and microalgae. Bioresour Technol 2013;149:142–8. doi:10.1016/j.biortech.2013.09.051.

[20] de Wilt A, Butkovskyi A, Tuantet K, Leal LH, Fernandes T V., Langenhoff A, et al. Micropollutant removal in an algal treatment system fed with source separated wastewater streams. J Hazard Mater 2016;304:84–92. doi:10.1016/j.jhazmat.2015.10.033.

[21] Xiong JQ, Kurade MB, Jeon BH. Can Microalgae Remove Pharmaceutical Contaminants from Water? Trends Biotechnol 2018;36:30–44. doi:10.1016/j.tibtech.2017.09.003.

[22] Makut BB, Das D, Goswami G. Production of microbial biomass feedstock via co-cultivation of microalgae-bacteria consortium coupled with effective wastewater treatment: A sustainable approach. Algal Res 2019;37:228–39. doi:10.1016/j.algal.2018.11.020.

[23] Mohd Udaiyappan AF, Abu Hasan H, Takriff MS, Sheikh Abdullah SR. A review of the potentials, challenges and current status of microalgae biomass applications in industrial wastewater treatment. J Water Process Eng 2017;20:8–21. doi:10.1016/j.jwpe.2017.09.006.

[24] Maurya R, Paliwal C, Chokshi K, Pancha I, Ghosh T, Satpati GG, et al. Hydrolysate of lipid extracted microalgal biomass residue: An algal growth promoter and enhancer. Bioresour Technol 2016;207:197–204. doi:10.1016/j.biortech.2016.02.018.

[25] Pittman JK, Dean AP, Osundeko O. The potential of sustainable algal biofuel production using wastewater resources. Bioresour Technol 2011;102:17–25. doi:10.1016/j.biortech.2010.06.035.

[26] Xu D, Wang Y, Lin G, Guo S, Wang S, Wu Z. Co-hydrothermal liquefaction of microalgae and sewage sludge in subcritical water: Ash effects on bio-oil production. Renew Energy 2019;138:1143–51. doi:10.1016/j.renene.2019.02.020.

[27] Guldhe A, Ansari FA, Singh P, Bux F. Heterotrophic cultivation of microalgae using aquaculture wastewater : A biorefinery concept for biomass production and nutrient remediation. Ecol Eng 2017;99:47–53. doi:10.1016/j.ecoleng.2016.11.013.

[28] Chew KW, Yap JY, Show PL, Suan NH, Juan JC, Ling TC, et al. Microalgae biorefinery: High value products perspectives. Bioresour Technol 2017;229:53–62. doi:10.1016/j.biortech.2017.01.006.

[29] Mardhiah HH, Ong HC, Masjuki HH, Lim S, Lee H V. A review on latest developments and future prospects of heterogeneous catalyst in biodiesel production from non-edible oils. Renew Sustain Energy Rev 2017;67:1225–36. doi:10.1016/j.rser.2016.09.036.

[30] Kumar V, Muthuraj M, Palabhanvi B, Ghoshal AK, Das D. Evaluation and optimization of two stage sequential in situ transesterification process for fatty acid methyl ester quantification from microalgae. Renew Energy 2014;68:560–9. doi:10.1016/J.RENENE.2014.02.037.

[31] Mishra S, Singh N, Sarma AK. Assessment of a Novel Algal Strain Chlamydomonas debaryana NIREMACC03 for Mass Cultivation, Biofuels Production and Kinetic Studies. Appl Biochem Biotechnol 2015;176:2253–66. doi:10.1007/s12010-015-1714-z.

[32] Feng H, Zhang B, He Z, Wang S, Salih O, Wang Q. Study on co-liquefaction of Spirulina and Spartina alterniflora in ethanol-water co-solvent for bio-oil. Energy 2018;155:1093–101. doi:10.1016/j.energy.2018.02.146.

[33] Aguiar E, Pinto F, Varela F, Reis A, Costa P, Lúcia M. Hydrothermal liquefaction of biomass produced from domestic sewage treatment in high-rate ponds. Renew Energy 2018;118:644–53. doi:10.1016/j.renene.2017.11.041.

[34] Mathimani T, Mallick N. A review on the hydrothermal processing of microalgal biomass to bio-oil - Knowledge gaps and recent advances. J Clean Prod 2019;217:69–84. doi:10.1016/j.jclepro.2019.01.129.

[35] Gollakota ARK, Kishore N, Gu S. A review on hydrothermal liquefaction of biomass. Renew Sustain Energy Rev 2018;81:1378–92. doi:10.1016/j.rser.2017.05.178.

[36] Chen W-H, Lin B-J, Huang M-Y. Thermochemical conversion of microalgal biomass into biofuels: A review. Bioresour Technol 2015;184:314–27. doi:10.1016/J.BIORTECH.2014.11.050.

[37] Nizamuddin S, Baloch HA, Griffin GJ, Mubarak NM, Bhutto AW, Abro R, et al. An overview of effect of process parameters on hydrothermal carbonization of biomass. Renew Sustain Energy Rev 2017;73:1289–99. doi:10.1016/J.RSER.2016.12.122.

[38] Marin-Batista JD, Villamil JA, Rodriguez JJ, Mohedano AF, de la Rubia MA. Valorization of microalgal biomass by hydrothermal carbonization and anaerobic digestion. Bioresour Technol 2019;274:395–402. doi:10.1016/j.biortech.2018.11.103.

[39] Wang T, Zhai Y, Zhu Y, Li C, Zeng G. A review of the hydrothermal carbonization of biomass waste for hydrochar formation: Process conditions, fundamentals, and physicochemical properties. Renew Sustain Energy Rev 2018;90:223–47. doi:10.1016/J.RSER.2018.03.071.

[40] Chandra R, Iqbal HMN, Vishal G, Lee HS, Nagra S. Algal biorefinery: A sustainable approach to valorize algal-based biomass towards multiple product recovery. Bioresour Technol 2019;278:346–59. doi:10.1016/j.biortech.2019.01.104.

[41] Maurya R, Paliwal C, Ghosh T, Pancha I, Chokshi K, Mitra M, et al. Applications of de-oiled microalgal biomass towards development of sustainable biorefinery. Bioresour Technol 2016;214:787–96. doi:10.1016/j.biortech.2016.04.115.

[42] Gifuni I, Pollio A, Safi C, Marzocchella A, Olivieri G. Current Bottlenecks and Challenges of the Microalgal Biorefinery. Trends Biotechnol 2019;37:242–52. doi:10.1016/j.tibtech.2018.09.006.

[43] Farooq W, Suh WI, Park MS. Water use and its recycling in microalgae cultivation for biofuel application. Bioresour Technol 2015;184:73–81. doi:10.1016/J.BIORTECH.2014.10.140.

[44] Wang W, Sha J, Lu Z, Shao S, Sun P, Hu Q, et al. Implementation of UV-based advanced oxidation processes in algal medium recycling. Sci Total Environ 2018;634:243–50. doi:10.1016/J.SCITOTENV.2018.03.342.

[45] Roy M, Mohanty K. A comprehensive review on microalgal harvesting strategies: Current status and future prospects. Algal Res 2019;44:101683. doi:10.1016/j.algal.2019.101683.

[46] Abomohra AEF, Eladel H, El-Esawi M, Wang S, Wang Q, He Z, et al. Effect of lipid-free microalgal biomass and waste glycerol on growth and lipid production of Scenedesmus obliquus: Innovative waste recycling for extraordinary lipid production. Bioresour Technol 2018;249:992–9. doi:10.1016/j.biortech.2017.10.102.

[47] Xu D, Lin G, Liu L, Wang Y, Jing Z, Wang S. Comprehensive evaluation on product characteristics of fast hydrothermal liquefaction of sewage sludge at different temperatures. Energy 2018;159:686–95. doi:10.1016/j.energy.2018.06.191.

[48] Arun J, Varshini P, Prithvinath PK, Priyadarshini V, Gopinath KP.

Enrichment of bio-oil after hydrothermal liquefaction (HTL) of microalgae C. vulgaris grown in wastewater: Bio-char and post HTL wastewater utilization studies. Bioresour Technol 2018;261:182–7. doi:10.1016/J.BIORTECH.2018.04.029.

[49] Van Wagenen J, Pape ML, Angelidaki I. Characterization of nutrient removal and microalgal biomass production on an industrial waste-stream by application of the deceleration-stat technique. Water Res 2015;75:301–11. doi:10.1016/j.watres.2015.02.022.

[50] Salama ES, Kurade MB, Abou-Shanab RAI, El-Dalatony MM, Yang IS, Min B, et al. Recent progress in microalgal biomass production coupled with wastewater treatment for biofuel generation. Renew Sustain Energy Rev 2017;79:1189–211. doi:10.1016/j.rser.2017.05.091.

[51] Zhang C, Zhang Y, Zhuang B, Zhou X. Strategic enhancement of algal biomass, nutrient uptake and lipid through statistical optimization of nutrient supplementation in coupling Scenedesmus obliquus-like microalgae cultivation and municipal wastewater treatment. Bioresour Technol 2014;171:71–9. doi:10.1016/j.biortech.2014.07.060.

[52] Mohammadi M, Mowla D, Esmaeilzadeh F, Ghasemi Y. Cultivation of microalgae in a power plant wastewater for sulfate removal and biomass production: A batch study. J Environ Chem Eng 2018;6:2812–20. doi:10.1016/j.jece.2018.04.037.

[53] Chen R, Li R, Deitz L, Liu Y, Stevenson RJ, Liao W. Freshwater algal cultivation with animal waste for nutrient removal and biomass production. Biomass and Bioenergy 2012;39:128–38. doi:10.1016/j.biombioe.2011.12.045.

[54] Wang XX, Wu YH, Zhang TY, Xu XQ, Dao GH, Hu HY. Simultaneous nitrogen, phosphorous, and hardness removal from reverse osmosis concentrate by microalgae cultivation. Water Res 2016;94:215–24. doi:10.1016/j.watres.2016.02.062.

[55] Abou-Shanab RAI, Hwang JH, Cho Y, Min B, Jeon BH. Characterization of microalgal species isolated from fresh water bodies as a potential source for biodiesel production. Appl Energy 2011;88:3300–6. doi:10.1016/j.apenergy.2011.01.060.

[56] Bhola V, Desikan R, Santosh SK, Subburamu K, Sanniyasi E, Bux F. Effects of parameters affecting biomass yield and thermal behaviour of Chlorella vulgaris. J Biosci Bioeng 2011;111:377–82. doi:10.1016/j.jbiosc.2010.11.006.

[57] Suali E, Sarbatly R. Conversion of microalgae to biofuel. Renew Sustain Energy Rev 2012;16:4316–42. doi:10.1016/j.rser.2012.03.047.

[58] Basu S, Roy AS, Mohanty K, Ghoshal AK. CO2 biofixation and carbonic anhydrase activity in Scenedesmus obliquus SA1 cultivated in large scale open system. Bioresour Technol 2014;164:323–30.

doi:10.1016/j.biortech.2014.05.017.

[59] Chaichalerm S, Pokethitiyook P, Yuan W, Meetam M, Sritong K, Pugkaew W, et al. Culture of microalgal strains isolated from natural habitats in Thailand in various enriched media. Appl Energy 2012;89:296–302. doi:10.1016/j.apenergy.2011.07.028.

[60] Çakmak ZE, Ölmez TT, Çakmak T, Menemen Y, Tekinay T. Induction of triacylglycerol production in Chlamydomonas reinhardtii: Comparative analysis of different element regimes. Bioresour Technol 2014;155:379–87. doi:10.1016/j.biortech.2013.12.093.

[61] Xu Y, Boeing WJ. Modeling maximum lipid productivity of microalgae: Review and next step. Renew Sustain Energy Rev 2014;32:29–39. doi:10.1016/j.rser.2014.01.002.

[62] Rodolfi L, Zittelli GC, Bassi N, Padovani G, Biondi N, Bonini G, et al. Microalgae for oil: Strain selection, induction of lipid synthesis and outdoor mass cultivation in a low-cost photobioreactor. Biotechnol Bioeng 2009;102:100–12. doi:10.1002/bit.22033.

[63] Cai T, Park SY, Li Y. Nutrient recovery from wastewater streams by microalgae: Status and prospects. Renew Sustain Energy Rev 2013;19:360–9. doi:10.1016/j.rser.2012.11.030.

[64] Sydney EB, da Silva TE, Tokarski A, Novak AC, de Carvalho JC, Woiciecohwski AL, et al. Screening of microalgae with potential for biodiesel production and nutrient removal from treated domestic sewage. Appl Energy 2011;88:3291–4. doi:10.1016/j.apenergy.2010.11.024.

[65] Wang L, Min M, Li Y, Chen P, Chen Y, Liu Y, et al. Cultivation of green algae Chlorella sp. in different wastewaters from municipal wastewater treatment plant. Appl Biochem Biotechnol 2010;162:1174–86. doi:10.1007/s12010-009-8866-7.

[66] Hodaifa G, Sánchez S, Eugenia M, Órpez R. Biomass production of Scenedesmus obliquus from mixtures of urban and olive-oil mill wastewaters used as culture medium. Appl Energy 2013;104:345–52. doi:10.1016/j.apenergy.2012.11.005.

[67] Levine RB, Costanza-Robinson MS, Spatafora GA. Neochloris oleoabundans grown on anaerobically digested dairy manure for concomitant nutrient removal and biodiesel feedstock production. Biomass and Bioenergy 2011;35:40–9. doi:10.1016/j.biombioe.2010.08.035.

[68] Yang J, Li X, Hu H, Zhang X, Yu Y, Chen Y. Growth and lipid accumulation properties of a freshwater microalga, Chlorella ellipsoidea YJ1, in domestic secondary effluents. Appl Energy 2011;88:3295–9. doi:10.1016/j.apenergy.2010.11.029.

[69] Rawat I, Ranjith Kumar R, Mutanda T, Bux F. Dual role of microalgae: Phycoremediation of domestic wastewater and biomass production for sustainable biofuels production. Appl Energy 2011;88:3411–24.

doi:10.1016/j.apenergy.2010.11.025.

[70] Li Y, Chen YF, Chen P, Min M, Zhou W, Martinez B, et al. Characterization of a microalga Chlorella sp. well adapted to highly concentrated municipal wastewater for nutrient removal and biodiesel production. Bioresour Technol 2011;102:5138–44. doi:10.1016/j.biortech.2011.01.091.

[71] Mitra D, van Leeuwen J (Hans), Lamsal B. Heterotrophic/mixotrophic cultivation of oleaginous Chlorella vulgaris on industrial co-products. Algal Res 2012;1:40–8. doi:10.1016/j.algal.2012.03.002.

[72] Kong QX, Li L, Martinez B, Chen P, Ruan R. Culture of microalgae chlamydomonas reinhardtii in wastewater for biomass feedstock production. Appl Biochem Biotechnol 2010;160:9–18. doi:10.1007/s12010-009-8670-4.

[73] Amit, Chandra R, Ghosh UK, Nayak JK. Phycoremediation potential of marine microalga Tetraselmis indica on secondary treated domestic sewage for nutrient removal and biodiesel production. Environ Sci Pollut Res 2017;24:20868–75. doi:10.1007/s11356-017-9734-6.

[74] Kumar PK, Krishna SV, Naidu SS, Verma K, Bhagawan D, Himabindu V. Biomass production from microalgae Chlorella grown in sewage, kitchen wastewater using industrial CO2 emissions: Comparative study. Carbon Resour Convers 2019;2:126–33. doi:10.1016/j.crcon.2019.06.002.

[75] Farooq W, Lee YC, Ryu BG, Kim BH, Kim HS, Choi YE, et al. Two-stage cultivation of two Chlorella sp. strains by simultaneous treatment of brewery wastewater and maximizing lipid productivity. Bioresour Technol 2013;132:230–8. doi:10.1016/j.biortech.2013.01.034.

[76] Cho S, Lee N, Park S, Yu J, Luong TT, Oh Y, et al. Microalgae cultivation for bioenergy production using wastewaters from a municipal WWTP as nutritional sources. Bioresour Technol 2013;131:515–20. doi:10.1016/j.biortech.2012.12.176.

[77] Chinnasamy S, Bhatnagar A, Hunt RW, Das KC. Microalgae cultivation in a wastewater dominated by carpet mill effluents for biofuel applications. Bioresour Technol 2010;101:3097–105. doi:10.1016/j.biortech.2009.12.026.

[78] Wu LF, Chen PC, Huang AP, Lee CM. The feasibility of biodiesel production by microalgae using industrial wastewater. Bioresour Technol 2012;113:14–8. doi:10.1016/j.biortech.2011.12.128.

[79] Cheah WY, Show PL, Juan JC, Chang JS, Ling TC. Enhancing biomass and lipid productions of microalgae in palm oil mill effluent using carbon and nutrient supplementation. Energy Convers Manag 2018;164:188–97. doi:10.1016/j.enconman.2018.02.094.

[80] Van Wagenen J, Holdt SL, De Francisci D, Valverde-Pérez B, Plósz BG, Angelidaki I. Microplate-based method for high-throughput screening of microalgae growth potential. Bioresour Technol 2014;169:566–72. doi:10.1016/j.biortech.2014.06.096.

[81] Shen L, Damascene Ndayambaje J, Murwanashyaka T, Cui W, Manirafasha E, Chen C, et al. Assessment upon heterotrophic microalgae screened from wastewater microbiota for concurrent pollutants removal and biofuel production. Bioresour Technol 2017;245:386–93. doi:10.1016/j.biortech.2017.07.177.

[82] Wen Y, He Y, Ji X, Li S, Chen L, Zhou Y, et al. Isolation of an indigenous Chlorella vulgaris from swine wastewater and characterization of its nutrient removal ability in undiluted sewage. Bioresour Technol 2017;243:247–53. doi:10.1016/j.biortech.2017.06.094.

[83] Piligaev A V., Sorokina KN, Shashkov M V., Parmon VN. Screening and comparative metabolic profiling of high lipid content microalgae strains for application in wastewater treatment. Bioresour Technol 2018;250:538–47. doi:10.1016/j.biortech.2017.11.063.

[84] Renuka N, Sood A, Ratha SK, Prasanna R, Ahluwalia AS. Evaluation of microalgal consortia for treatment of primary treated sewage effluent and biomass production. J Appl Phycol 2013;25:1529–37. doi:10.1007/s10811-013-9982-x.

[85] Ferro L, Gentili FG, Funk C. Isolation and characterization of microalgal strains for biomass production and wastewater reclamation in Northern Sweden. Algal Res 2018;32:44–53. doi:10.1016/j.algal.2018.03.006.

[86] García D, Posadas E, Blanco S, Acién G, García-Encina P, Bolado S, et al. Evaluation of the dynamics of microalgae population structure and process performance during piggery wastewater treatment in algal-bacterial photobioreactors. Bioresour Technol 2018;248:120–6. doi:10.1016/j.biortech.2017.06.079.

[87] Bohutskyi P, Kligerman DC, Byers N, Nasr LK, Cua C, Chow S, et al. Effects of inoculum size, light intensity, and dose of anaerobic digestion centrate on growth and productivity of Chlorella and Scenedesmus microalgae and their poly-culture in primary and secondary wastewater. Algal Res 2016;19:278–90. doi:10.1016/j.algal.2016.09.010.

[88] Kanaga K, Pandey A, Kumar S, Geetanjali. Multi-objective optimization of media nutrients for enhanced production of algae biomass and fatty acid biosynthesis from Chlorella pyrenoidosa NCIM 2738. Bioresour Technol 2016;200:940–50. doi:10.1016/j.biortech.2015.11.017.

[89] Lau PS, Tam NFY, Wong YS. Effect of algal density on nutrient removal from primary settled wastewater. Environ Pollut 1995;89:59–66. doi:https://doi.org/10.1016/0269-7491(94)00044-E.

[90] Nayak M, Karemore A, Sen R. Performance evaluation of microalgae for concomitant wastewater bioremediation, CO2 biofixation and lipid biosynthesis for biodiesel application. Algal Res 2016;16:216–23. doi:10.1016/j.algal.2016.03.020.

[91] Chaudhary R, Dikshit AK, Tong YW. Carbon-dioxide biofixation and

phycoremediation of municipal wastewater using Chlorella vulgaris and Scenedesmus obliquus. Environ Sci Pollut Res 2018;25:20399–406. doi:10.1007/s11356-017-9575-3.

[92] Binnal P, Babu PN. Optimization of environmental factors affecting tertiary treatment of municipal wastewater by Chlorella protothecoides in a lab scale photobioreactor. J Water Process Eng 2017;17:290–8. doi:10.1016/j.jwpe.2017.05.003.

[93] Ryu BG, Kim EJ, Kim HS, Kim J, Choi YE, Yang JW. Simultaneous treatment of municipal wastewater and biodiesel production by cultivation of Chlorella vulgaris with indigenous wastewater bacteria. Biotechnol Bioprocess Eng 2014;19:201–10. doi:10.1007/s12257-013-0250-3.

[94] Singh SP, Singh P. Effect of temperature and light on the growth of algae species: A review. Renew Sustain Energy Rev 2015;50:431–44. doi:10.1016/j.rser.2015.05.024.

[95] Raeesossadati MJ, Ahmadzadeh H, McHenry MP, Moheimani NR. CO2 bioremediation by microalgae in photobioreactors: Impacts of biomass and CO2 concentrations, light, and temperature. Algal Res 2014;6:78–85. doi:10.1016/j.algal.2014.09.007.

[96] Ruangsomboon S. Effect of light, nutrient, cultivation time and salinity on lipid production of newly isolated strain of the green microalga, Botryococcus braunii KMITL 2. Bioresour Technol 2012;109:261–5. doi:10.1016/j.biortech.2011.07.025.

[97] Basu S, Roy AS, Mohanty K, Ghoshal AK. Enhanced CO2 sequestration by a novel microalga: Scenedesmus obliquus SA1 isolated from bio-diversity hotspot region of Assam, India. Bioresour Technol 2013;143:369–77. doi:10.1016/j.biortech.2013.06.010.

[98] Cheah WY, Show PL, Chang JS, Ling TC, Juan JC. Biosequestration of atmospheric CO2 and flue gas-containing CO2 by microalgae. Bioresour Technol 2015;184:190–201. doi:10.1016/j.biortech.2014.11.026.

[99] Juneja A, Ceballos RM, Murthy GS. Effects of environmental factors and nutrient availability on the biochemical composition of algae for biofuels production: A review. Energies 2013;6:4607–38. doi:10.3390/en6094607.

[100] Basu S, Sarma Roy A, Ghoshal AK, Mohanty K. Operational strategies for maximizing CO2 utilization efficiency by the novel microalga Scenedesmus obliquus SA1 cultivated in lab scale photobioreactor. Algal Res 2015;12:249–57. doi:10.1016/j.algal.2015.09.010.

[101] Nayak M, Karemore A, Sen R. Sustainable valorization of flue gas CO 2 and wastewater for the production of microalgal biomass as a biofuel feedstock in closed and open reactor systems. RSC Adv 2016;6:91111–20. doi:10.1039/C6RA17899E.

[102] Lam MK, Lee KT. Microalgae biofuels: A critical review of issues, problems and the way forward. Biotechnol Adv 2012;30:673–90.

doi:10.1016/j.biotechadv.2011.11.008.

[103] Park J, Kim B, Chang YK, Lee JW. Wet in situ transesterification of microalgae using ethyl acetate as a co-solvent and reactant. Bioresour Technol 2017;230:8–14. doi:https://doi.org/10.1016/j.biortech.2017.01.027.

[104] Muthuraj M, Kumar V, Palabhanvi B, Das D. Evaluation of indigenous microalgal isolate Chlorella sp. FC2 IITG as a cell factory for biodiesel production and scale up in outdoor conditions. J Ind Microbiol Biotechnol 2014;41:499–511. doi:10.1007/s10295-013-1397-9.

[105] Chauhan DS, Goswami G, Dineshbabu G, Palabhanvi B, Das D. Evaluation and optimization of feedstock quality for direct conversion of microalga Chlorella sp. FC2 IITG into biodiesel via supercritical methanol transesterification. Biomass Convers Biorefinery 2019. doi:10.1007/s13399-019-00432-2.

[106] Teo SH, Islam A, Taufiq-Yap YH. Algae derived biodiesel using nanocatalytic transesterification process. Chem Eng Res Des 2016;111:362–70. doi:https://doi.org/10.1016/j.cherd.2016.04.012.

[107] Dandamudi KPR, Muppaneni T, Markovski JS, Lammers P, Deng S. Hydrothermal liquefaction of green microalga Kirchneriella sp. under sub- and super-critical water conditions. Biomass and Bioenergy 2019;120:224–8. doi:10.1016/j.biombioe.2018.11.021.

[108] Zhang B, Feng H, He Z, Wang S, Chen H. Bio-oil production from hydrothermal liquefaction of ultrasonic pre-treated Spirulina platensis. Energy Convers Manag 2018;159:204–12. doi:10.1016/j.enconman.2017.12.100.

[109] Jarvis JM, Billing JM, Corilo YE, Schmidt AJ, Hallen RT, Schaub TM. FT-ICR MS analysis of blended pine-microalgae feedstock HTL biocrudes. Fuel 2018;216:341–8. doi:10.1016/j.fuel.2017.12.016.

[110] Brilman DWF, Drabik N, W\kadrzyk M. Hydrothermal co-liquefaction of microalgae, wood, and sugar beet pulp. Biomass Convers Biorefinery 2017;7:445–54. doi:10.1007/s13399-017-0241-2.

[111] Hu Y, Feng S, Bassi A, Xu CC. Improvement in bio-crude yield and quality through co-liquefaction of algal biomass and sawdust in ethanol-water mixed solvent and recycling of the aqueous by-product as a reaction medium. Energy Convers Manag 2018;171:618–25. doi:10.1016/j.enconman.2018.06.023.

[112] Chen X, Peng X, Ma X, Wang J. Investigation of Mannich reaction during co-liquefaction of microalgae and sweet potato waste. Bioresour Technol 2019;284:286–92. doi:10.1016/j.biortech.2019.03.136.

[113] Wang J, Peng X, Chen X, Ma X. Co-liquefaction of low-lipid microalgae and starch-rich biomass waste: The interaction effect on product distribution and composition. J Anal Appl Pyrolysis 2019;139:250–7. doi:10.1016/j.jaap.2019.02.013.

[114] Chen W, Zhang Y, Zhang J, Schideman L, Yu G, Zhang P, et al. Co-liquefaction of swine manure and mixed-culture algal biomass from a wastewater treatment system to produce bio-crude oil. Appl Energy 2014;128:209–16. doi:10.1016/j.apenergy.2014.04.068.

[115] Huang H jun, Chang Y chao, Lai F ying, Zhou C fei, Pan Z qian, Xiao X feng, et al. Co-liquefaction of sewage sludge and rice straw/wood sawdust: The effect of process parameters on the yields/properties of bio-oil and biochar products. Energy 2019;173:140–50. doi:10.1016/j.energy.2019.02.071.

[116] Saber M, Golzary A, Hosseinpour M, Takahashi F, Yoshikawa K. Catalytic hydrothermal liquefaction of microalgae using nanocatalyst. Appl Energy 2016;183:566–76. doi:10.1016/j.apenergy.2016.09.017.

[117] Zainan NH, Srivatsa SC, Li F, Bhattacharya S. Quality of bio-oil from catalytic pyrolysis of microalgae Chlorella vulgaris. Fuel 2018;223:12–9. doi:https://doi.org/10.1016/j.fuel.2018.02.166.

[118] Hu Z, Zheng Y, Yan F, Xiao B, Liu S. Bio-oil production through pyrolysis of blue-green algae blooms (BGAB): Product distribution and bio-oil characterization. Energy 2013;52:119–25. doi:https://doi.org/10.1016/j.energy.2013.01.059.

[119] Liu G, Liao Y, Wu Y, Ma X, Chen L. Characteristics of microalgae gasification through chemical looping in the presence of steam. Int J Hydrogen Energy 2017;42:22730–42. doi:https://doi.org/10.1016/j.ijhydene.2017.07.173.

[120] Hu Z, Jiang E, Ma X. The effect of oxygen carrier content and temperature on chemical looping gasification of microalgae for syngas production. J Energy Inst 2019;92:474–87. doi:https://doi.org/10.1016/j.joei.2018.05.001.

[121] Lee J, Sohn D, Lee K, Park KY. Solid fuel production through hydrothermal carbonization of sewage sludge and microalgae Chlorella sp. from wastewater treatment plant. Chemosphere 2019;230:157–63. doi:10.1016/j.chemosphere.2019.05.066.

[122] Zhang C, Wang C, Cao G, Chen W-H, Ho S-H. Comparison and characterization of property variation of microalgal biomass with non-oxidative and oxidative torrefaction. Fuel 2019;246:375–85. doi:https://doi.org/10.1016/j.fuel.2019.02.139.

[123] Laurens LML, Markham J, Templeton DW, Christensen ED, Van Wychen S, Vadelius EW, et al. Development of algae biorefinery concepts for biofuels and bioproducts; a perspective on process-compatible products and their impact on cost-reduction. Energy Environ Sci 2017;10:1716–38. doi:10.1039/c7ee01306j.

[124] Xu C, Lad N. Production of Heavy Oils with High Caloric Values by Direct Liquefaction of Woody Biomass in Sub/Near-critical Water. Energy & Fuels 2008;22:635–42. doi:10.1021/ef700424k.

[125] Fernandez S, Srinivas K, Schmidt AJ, Swita MS, Ahring BK. Anaerobic digestion of organic fraction from hydrothermal liquefied algae wastewater byproduct. Bioresour Technol 2018;247:250–8.

[126] Chen L, Zhu T, Fernandez JSM, Chen S, Li D. Recycling nutrients from a sequential hydrothermal liquefaction process for microalgae culture. Algal Res 2017;27:311–7. doi:https://doi.org/10.1016/j.algal.2017.09.023.

[127] Zhang X, Scott J, Sharma BK, Rajagopalan N. Advanced treatment of hydrothermal liquefaction wastewater with nanofiltration to recover carboxylic acids. Environ Sci Water Res Technol 2018;4:520–8.

[128] Du Z, Hu B, Shi A, Ma X, Cheng Y, Chen P, et al. Cultivation of a microalga Chlorella vulgaris using recycled aqueous phase nutrients from hydrothermal carbonization process. Bioresour Technol 2012;126:354–7.

[129] Usman M, Chen H, Chen K, Ren S, Clark JH, Fan J, et al. Characterization and utilization of aqueous products from hydrothermal conversion of biomass for bio-oil and hydro-char production: a review. Green Chem 2019;21:1553–72.

[130] Cherad R, Onwudili JA, Biller P, Williams PT, Ross AB. Hydrogen production from the catalytic supercritical water gasification of process water generated from hydrothermal liquefaction of microalgae. Fuel 2016;166:24–8. doi:10.1016/J.FUEL.2015.10.088.

[131] López Barreiro D, Prins W, Ronsse F, Brilman W. Hydrothermal liquefaction (HTL) of microalgae for biofuel production: State of the art review and future prospects. Biomass and Bioenergy 2013;53:113–27. doi:10.1016/j.biombioe.2012.12.029.

[132] Liu R, Tian W, Kong S, Meng Y, Wang H, Zhang J. Effects of inorganic and organic acid pretreatments on the hydrothermal liquefaction of municipal secondary sludge. Energy Convers Manag 2018;174:661–7. doi:10.1016/j.enconman.2018.08.058.

[133] Sharifzadeh M, Sadeqzadeh M, Guo M, Borhani TN, Murthy Konda NVSN, Garcia MC, et al. The multi-scale challenges of biomass fast pyrolysis and bio-oil upgrading: Review of the state of art and future research directions. Prog Energy Combust Sci 2019;71:1–80. doi:10.1016/j.pecs.2018.10.006.

[134] Yang C, Li R, Zhang B, Qiu Q, Wang B, Yang H, et al. Pyrolysis of microalgae: A critical review. Fuel Process Technol 2019;186:53–72. doi:10.1016/j.fuproc.2018.12.012.

[135] Fagbohungbe MO, Herbert BMJ, Hurst L, Ibeto CN, Li H, Usmani SQ, et al. The challenges of anaerobic digestion and the role of biochar in optimizing anaerobic digestion. Waste Manag 2017;61:236–49. doi:10.1016/j.wasman.2016.11.028.

[136] Masebinu SO, Akinlabi ET, Muzenda E, Aboyade AO. A review of biochar properties and their roles in mitigating challenges with anaerobic digestion. Renew Sustain Energy Rev 2019;103:291–307.

doi:10.1016/j.rser.2018.12.048.

[137] Chng LM, Chan DJC, Lee KT. Sustainable production of bioethanol using lipid-extracted biomass from Scenedesmus dimorphus. J Clean Prod 2016;130:68–73.

[138] Sialve B, Bernet N, Bernard O. Anaerobic digestion of microalgae as a necessary step to make microalgal biodiesel sustainable. Biotechnol Adv 2009;27:409–16.

[139] Yang Z, Guo R, Xu X, Fan X, Li X. Thermo-alkaline pretreatment of lipid-extracted microalgal biomass residues enhances hydrogen production. J Chem Technol Biotechnol 2011;86:454–60. doi:10.1002/jctb.2537.

[140] Cheng J, Huang R, Yu T, Li T, Zhou J, Cen K. Biodiesel production from lipids in wet microalgae with microwave irradiation and bio-crude production from algal residue through hydrothermal liquefaction. Bioresour Technol 2014;151:415–8. doi:https://doi.org/10.1016/j.biortech.2013.10.033.

[141] Vardon DR, Sharma BK, Blazina G V, Rajagopalan K, Strathmann TJ. Thermochemical conversion of raw and defatted algal biomass via hydrothermal liquefaction and slow pyrolysis. Bioresour Technol 2012;109:178–87. doi:https://doi.org/10.1016/j.biortech.2012.01.008.

[142] Gu H, Nagle N, Pienkos PT, Posewitz MC. Nitrogen recycling from fuel-extracted algal biomass: residuals as the sole nitrogen source for culturing Scenedesmus acutus. Bioresour Technol 2015;184:153–60.

[143] Rashid N, Rehman MSU, Han J-I. Recycling and reuse of spent microalgal biomass for sustainable biofuels. Biochem Eng J 2013;75:101–7.

[144] Yang F, Hanna MA, Sun R. Value-added uses for crude glycerol--a byproduct of biodiesel production. Biotechnol Biofuels 2012;5:13. doi:10.1186/1754-6834-5-13.

[145] Katiyar R, Gurjar BR, Bharti RK, Kumar A, Biswas S, Pruthi V. Heterotrophic cultivation of microalgae in photobioreactor using low cost crude glycerol for enhanced biodiesel production. Renew Energy 2017;113:1359–65. doi:https://doi.org/10.1016/j.renene.2017.06.100.

[146] Chang Y-M, Tsai W-T, Li M-H. Characterization of activated carbon prepared from chlorella-based algal residue. Bioresour Technol 2015;184:344–8. doi:https://doi.org/10.1016/j.biortech.2014.09.131.

[147] Neumann P, Torres A, Fermoso FG, Borja R, Jeison D. Anaerobic co-digestion of lipid-spent microalgae with waste activated sludge and glycerol in batch mode. Int Biodeterior Biodegradation 2015;100:85–8. doi:https://doi.org/10.1016/j.ibiod.2015.01.020.

[148] Manor ML, Kim J, Derksen TJ, Schwartz RL, Roneker CA, Bhatnagar RS, et al. Defatted microalgae serve as a dual dietary source of highly bioavailable iron and protein in an anemic pig model. Algal Res 2017;26:409–14. doi:https://doi.org/10.1016/j.algal.2017.07.018.

[149] Yang L, Tan X, Si B, Zhao F, Chu H, Zhou X, et al. Nutrients recycling and energy evaluation in a closed microalgal biofuel production system. Algal Res 2018;33:399–405. doi:https://doi.org/10.1016/j.algal.2018.06.009.

[150] Varshney P, Beardall J, Bhattacharya S, Wangikar PP. Isolation and biochemical characterisation of two thermophilic green algal species-Asterarcys quadricellulare and Chlorella sorokiniana, which are tolerant to high levels of carbon dioxide and nitric oxide. Algal Res 2018;30:28–37. doi:10.1016/j.algal.2017.12.006.

[151] Rahman MA, Aziz MA, Al-khulaidi RA, Sakib N, Islam M. Biodiesel production from microalgae S pirulina maxima by two step process: Optimization of process variable. J Radiat Res Appl Sci 2017;10:140–7. doi:10.1016/j.jrras.2017.02.004.

[152] Nazari L, Yuan Z, Ray MB, Xu C (Charles). Co-conversion of waste activated sludge and sawdust through hydrothermal liquefaction: Optimization of reaction parameters using response surface methodology. Appl Energy 2017;203:1–10. doi:10.1016/j.apenergy.2017.06.009.

[153] Bellou S, Aggelis G. Biochemical activities in Chlorella sp. and Nannochloropsis salina during lipid and sugar synthesis in a lab-scale open pond simulating reactor. J Biotechnol 2012;164:318–29. doi:10.1016/j.jbiotec.2013.01.010.

[154] Pruvost J, Van Vooren G, Le Gouic B, Couzinet-Mossion A, Legrand J. Systematic investigation of biomass and lipid productivity by microalgae in photobioreactors for biodiesel application. Bioresour Technol 2011;102:150–8. doi:10.1016/j.biortech.2010.06.153.

[155] Mishra RK, Mohanty K. Pyrolysis kinetics and thermal behavior of waste sawdust biomass using thermogravimetric analysis. Bioresour Technol 2018;251:63–74. doi:10.1016/j.biortech.2017.12.029.

[156] Singh Chouhan AP, Singh N, Sarma AK. A comparative analysis of kinetic parameters from TGDTA of Jatropha curcas oil, biodiesel, petroleum diesel and B50 using different methods. Fuel 2013;109:217–24. doi:10.1016/j.fuel.2012.12.059.

[157] Chokshi K, Pancha I, Ghosh A, Mishra S. Microalgal biomass generation by phycoremediation of dairy industry wastewater: An integrated approach towards sustainable biofuel production. Bioresour Technol 2016;221:455–60. doi:10.1016/j.biortech.2016.09.070.

[158] Ansari FA, Singh P, Guldhe A, Bux F. Microalgal cultivation using aquaculture wastewater: Integrated biomass generation and nutrient remediation. Algal Res 2017;21:169–77. doi:10.1016/j.algal.2016.11.015.

[159] Daneshvar E, Antikainen L, Koutra E, Kornaros M, Bhatnagar A. Investigation on the feasibility of Chlorella vulgaris cultivation in a mixture of pulp and aquaculture effluents: Treatment of wastewater and lipid extraction. Bioresour Technol 2018;255:104–10.

doi:10.1016/j.biortech.2018.01.101.

[160] Gautam R, Varma AK, Vinu R. Apparent Kinetics of Fast Pyrolysis of Four Different Microalgae and Product Analyses Using Pyrolysis-FTIR and Pyrolysis-GC/MS. Energy & Fuels 2017;31:12339–49. doi:10.1021/acs.energyfuels.7b02520.

[161] Miranda MT, Sepúlveda FJ, Arranz JI, Montero I, Rojas C V. Physical-energy characterization of microalgae Scenedesmus and experimental pellets. Fuel 2018;226:121–6. doi:10.1016/j.fuel.2018.03.097.

[162] Kirtania K, Bhattacharya S. Application of the distributed activation energy model to the kinetic study of pyrolysis of the fresh water algae Chlorococcum humicola. Bioresour Technol 2012;107:476–81. doi:10.1016/j.biortech.2011.12.094.

[163] Chiranjeevi P, Mohan SV. Critical parametric influence on microalgae cultivation towards maximizing biomass growth with simultaneous lipid productivity. Renew Energy 2016;98:64–71. doi:10.1016/j.renene.2016.03.063.

[164] Han L, Pei H, Hu W, Jiang L, Ma G, Zhang S, et al. Integrated campus sewage treatment and biomass production by Scenedesmus quadricauda SDEC-13. Bioresour Technol 2015;175:262–8. doi:10.1016/j.biortech.2014.10.100.

[165] Gai C, Liu Z, Han G, Peng N, Fan A. Combustion behavior and kinetics of low-lipid microalgae via thermogravimetric analysis. Bioresour Technol 2015;181:148–54. doi:10.1016/j.biortech.2015.01.045.

[166] Nautiyal P, Subramanian KA, Dastidar MG. Production and characterization of biodiesel from algae. Fuel Process Technol 2014;120:79–88. doi:10.1016/j.fuproc.2013.12.003.

[167] Arora N, Patel A, Pruthi PA, Pruthi V. Recycled de-Oiled Algal Biomass Extract as a Feedstock for Boosting Biodiesel Production from Chlorella minutissima. Appl Biochem Biotechnol 2016;180:1534–41. doi:10.1007/s12010-016-2185-6.

[168] Zhu L, Wang Z, Shu Q, Takala J, Hiltunen E, Feng P, et al. Nutrient removal and biodiesel production by integration of freshwater algae cultivation with piggery wastewater treatment. Water Res 2013;47:4294–302. doi:10.1016/j.watres.2013.05.004.

[169] Dhup S, Dhawan V. Effect of nitrogen concentration on lipid productivity and fatty acid composition of Monoraphidium sp. Bioresour Technol 2014;152:572–5. doi:10.1016/j.biortech.2013.11.068.

[170] Feng D, Chen Z, Xue S, Zhang W. Increased lipid production of the marine oleaginous microalgae Isochrysis zhangjiangensis (Chrysophyta) by nitrogen supplement. Bioresour Technol 2011;102:6710–6. doi:10.1016/j.biortech.2011.04.006.

[171] Conceição GR, Xavier LMBD, Matos JBTL, de Almeida PF, de Moura-Costa LF, Chinalia FA. Glucose and Nitrogen Amendments Can Mitigate Wastewater-Borne Bacteria Competition Effect Against Algal Growth in Wastewater-Based Systems. J Phycol 2019;55:1050–8. doi:10.1111/jpy.12902.

[172] Kiran B, Pathak K, Kumar R, Deshmukh D. Statistical optimization using Central Composite Design for biomass and lipid productivity of microalga : A step towards enhanced biodiesel production. Ecol Eng 2016;92:73–81. doi:10.1016/j.ecoleng.2016.03.026.

[173] Qu W, Zhang C, Zhang Y, Ho SH. Optimizing real swine wastewater treatment with maximum carbohydrate production by a newly isolated indigenous microalga Parachlorella kessleri QWY28. Bioresour Technol 2019;289:121702. doi:10.1016/j.biortech.2019.121702.

[174] Han F, Wang W, Li Y, Shen G, Wan M, Wang J. Changes of biomass, Lipid content and fatty acids composition under a light-dark cyclic culture of Chlorella pyrenoidosa in response to different temperature. Bioresour Technol 2013;132:182–9. doi:10.1016/j.biortech.2012.12.175.

[175] Cheng J, Xu J, Huang Y, Li Y, Zhou J, Cen K. Growth optimisation of microalga mutant at high CO2 concentration to purify undiluted anaerobic digestion effluent of swine manure. Bioresour Technol 2015;177:240–6. doi:10.1016/j.biortech.2014.11.099.

[176] Kim S, Moon M, Kwak M, Lee B, Chang YK. Statistical optimization of light intensity and CO2 concentration for lipid production derived from attached cultivation of green microalga Ettlia sp. Sci Rep 2018;8:15390. doi:10.1038/s41598-018-33793-1.

[177] Mishra A, Medhi K, Maheshwari N, Srivastava S, Thakur IS. Biofuel production and phycoremediation by Chlorella sp. ISTLA1 isolated from landfill site. Bioresour Technol 2018;253:121–9. doi:10.1016/j.biortech.2017.12.012.

[178] Gupta PL, Choi HJ, Pawar RR, Jung SP, Lee SM. Enhanced biomass production through optimization of carbon source and utilization of wastewater as a nutrient source. J Environ Manage 2016;184:585–95. doi:10.1016/j.jenvman.2016.10.018.

[179] Han F, Pei H, Hu W, Song M, Ma G, Pei R. Optimization and lipid production enhancement of microalgae culture by efficiently changing the conditions along with the growth-state. Energy Convers Manag 2015;90:315–22. doi:10.1016/j.enconman.2014.11.032.

[180] Hena S, Znad H, Heong KT, Judd S. Dairy farm wastewater treatment and lipid accumulation by Arthrospira platensis. Water Res 2018;128:267–77. doi:10.1016/j.watres.2017.10.057.

[181] Nayak M, Dhanarajan G, Dineshkumar R, Sen R. Artificial intelligence driven process optimization for cleaner production of biomass with co-

valorization of wastewater and flue gas in an algal biorefinery. J Clean Prod 2018;201:1092–100. doi:10.1016/j.jclepro.2018.08.048.

[182] Ge S, Qiu S, Tremblay D, Viner K, Champagne P, Jessop PG. Centrate wastewater treatment with Chlorella vulgaris: Simultaneous enhancement of nutrient removal, biomass and lipid production. Chem Eng J 2018;342:310–20. doi:10.1016/j.cej.2018.02.058.

[183] Feng H, Zhang B, He Z, Wang S, Salih O, Wang Q. Study on co-liquefaction of Spirulina and Spartina alterni fl ora in ethanol-water co-solvent for bio-oil. Energy 2018;155:1093–101. doi:10.1016/j.energy.2018.02.146.

[184] Danish M, Ahmad T. A review on utilization of wood biomass as a sustainable precursor for activated carbon production and application. Renew Sustain Energy Rev 2018;87:1–21. doi:10.1016/j.rser.2018.02.003.

[185] Chandra R, Castillo-Zacarias C, Delgado P, Parra-Saldívar R. A biorefinery approach for dairy wastewater treatment and product recovery towards establishing a biorefinery complexity index. J Clean Prod 2018;183:1184–96. doi:10.1016/j.jclepro.2018.02.124.

[186] Ho SH, Chen CNN, Lai YY, Lu W Bin, Chang JS. Exploring the high lipid production potential of a thermotolerant microalga using statistical optimization and semi-continuous cultivation. Bioresour Technol 2014;163:128–35. doi:10.1016/j.biortech.2014.04.028.

[187] Ferro L, Gojkovic Z, Muñoz R, Funk C. Growth performance and nutrient removal of a Chlorella vulgaris-Rhizobium sp. co-culture during mixotrophic feed-batch cultivation in synthetic wastewater. Algal Res 2019;44:101690. doi:10.1016/j.algal.2019.101690.

[188] Sun H, Ren Y, Lao Y, Li X, Chen F. A novel fed-batch strategy enhances lipid and astaxanthin productivity without compromising biomass of Chromochloris zofingiensis. Bioresour Technol 2020;308:123306. doi:10.1016/j.biortech.2020.123306.

[189] Cheirsilp B, Torpee S. Enhanced growth and lipid production of microalgae under mixotrophic culture condition: Effect of light intensity, glucose concentration and fed-batch cultivation. Bioresour Technol 2012;110:510–6. doi:10.1016/j.biortech.2012.01.125.

[190] Goswami G, Makut BB, Das D. Sustainable production of bio-crude oil via hydrothermal liquefaction of symbiotically grown biomass of microalgae-bacteria coupled with effective wastewater treatment. Sci Rep 2019;9:1–12. doi:10.1038/s41598-019-51315-5.

[191] Huang Z, Wufuer A, Wang Y, Dai L. Hydrothermal liquefaction of pretreated low-lipid microalgae for the production of bio-oil with low heteroatom content. Process Biochem 2018;69:136–43. doi:10.1016/j.procbio.2018.03.018.

[192] Koley S, Khadase MS, Mathimani T, Raheman H, Mallick N. Catalytic and non-catalytic hydrothermal processing of Scenedesmus obliquus biomass for

bio-crude production – A sustainable energy perspective. Energy Convers Manag 2018;163:111–21. doi:10.1016/j.enconman.2018.02.052.

[193] Li R, Ma Z, Yang T, Li B, Wei L, Sun Y. Sub–supercritical liquefaction of municipal wet sewage sludge to produce bio-oil: Effect of different organic–water mixed solvents. J Supercrit Fluids 2018;138:115–23. doi:10.1016/j.supflu.2018.04.011.

[194] Rizzardini C, Goi D. Sustainability of Domestic Sewage Sludge Disposal. Sustainability 2014;6:2424–34. doi:10.3390/su6052424.

[195] Kapusta K. Effect of ultrasound pretreatment of municipal sewage sludge on characteristics of bio-oil from hydrothermal liquefaction process. Waste Manag 2018;78:183–90. doi:10.1016/j.wasman.2018.05.043.

[196] Gai C, Li Y, Peng N, Fan A, Liu Z. Co-liquefaction of microalgae and lignocellulosic biomass in subcritical water. Bioresour Technol 2015;185:240–5. doi:10.1016/j.biortech.2015.03.015.

[197] Chen W, Lin Y, Liu H, Chen T, Hung C, Chen C, et al. A comprehensive analysis of food waste derived liquefaction bio-oil properties for industrial application. Appl Energy 2019;237:283–91. doi:10.1016/j.apenergy.2018.12.084.

[198] Li H, Wang M, Wang X, Zhang Y, Lu H, Duan N, et al. Biogas liquid digestate grown Chlorella sp. for biocrude oil production via hydrothermal liquefaction. Sci Total Environ 2018;635:70–7. doi:10.1016/j.scitotenv.2018.03.354.

[199] He Z, Xu D, Liu L, Wang Y, Wang S, Guo Y, et al. Product characterization of multi-temperature steps of hydrothermal liquefaction of Chlorella microalgae. Algal Res 2018;33:8–15. doi:10.1016/j.algal.2018.04.013.

[200] Xu D, Guo S, Liu L, Lin G, Wu Z, Guo Y, et al. Heterogeneous catalytic effects on the characteristics of water-soluble and water-insoluble biocrudes in chlorella hydrothermal liquefaction. Appl Energy 2019;243:165–74. doi:10.1016/j.apenergy.2019.03.180.

[201] Huang H, Yuan X. The migration and transformation behaviors of heavy metals during the hydrothermal treatment of sewage sludge. Bioresour Technol 2016;200:991–8. doi:10.1016/j.biortech.2015.10.099.

[202] Mulchandani A, Westerhoff P. Recovery opportunities for metals and energy from sewage sludges. Bioresour Technol 2016;215:215–26. doi:10.1016/j.biortech.2016.03.075.

[203] Leng L, Leng S, Chen J, Yuan X, Li J, Li K, et al. The migration and transformation behavior of heavy metals during co-liquefaction of municipal sewage sludge and lignocellulosic biomass. Bioresour Technol 2018;259:156–63. doi:10.1016/j.biortech.2018.03.019.

[204] Shi W, Liu C, Shu Y, Feng C, Lei Z, Zhang Z. Synergistic effect of rice husk addition on hydrothermal treatment of sewage sludge: Fate and

environmental risk of heavy metals. Bioresour Technol 2013;149:496–502. doi:10.1016/j.biortech.2013.09.114.

[205] Yang J, (Sophia)He Q, Yang L. A review on hydrothermal co-liquefaction of biomass. Appl Energy 2019;250:926–45. doi:10.1016/j.apenergy.2019.05.033.

[206] Saber M, Nakhshiniev B, Yoshikawa K. A review of production and upgrading of algal bio-oil. Renew Sustain Energy Rev 2016;58:918–30. doi:10.1016/j.rser.2015.12.342.

[207] Ong HC, Chen WH, Farooq A, Gan YY, Lee KT, Ashokkumar V. Catalytic thermochemical conversion of biomass for biofuel production: A comprehensive review. Renew Sustain Energy Rev 2019;113:109266. doi:10.1016/j.rser.2019.109266.

[208] Zhai Y, Chen H, Xu BB, Xiang B, Chen Z, Li C, et al. Influence of sewage sludge-based activated carbon and temperature on the liquefaction of sewage sludge: Yield and composition of bio-oil, immobilization and risk assessment of heavy metals. Bioresour Technol 2014;159:72–9. doi:10.1016/j.biortech.2014.02.049.

[209] Kim S-S, Ly HV, Kim J, Lee EY, Woo HC. Pyrolysis of microalgae residual biomass derived from Dunaliella tertiolecta after lipid extraction and carbohydrate saccharification. Chem Eng J 2015;263:194–9. doi:10.1016/j.cej.2014.11.045.

[210] Maurya R, Chokshi K, Ghosh T, Trivedi K, Pancha I, Kubavat D, et al. Lipid extracted microalgal biomass residue as a fertilizer substitute for Zea mays L. Front Plant Sci 2016;6:1–10. doi:10.3389/fpls.2015.01266.

[211] Lunprom S, Phanduang O, Salakkam A, Liao Q, Imai T, Reungsang A. Bio-hythane production from residual biomass of Chlorella sp. biomass through a two-stage anaerobic digestion. Int J Hydrogen Energy 2019;44:3339–46. doi:10.1016/j.ijhydene.2018.09.064.

[212] Kumari N, Singh RK. Biofuel and co-products from algae solvent extraction. J Environ Manage 2019;247:196–204. doi:10.1016/j.jenvman.2019.06.042.

[213] Maurya R, Ghosh T, Saravaia H, Paliwal C, Ghosh A, Mishra S. Non-isothermal pyrolysis of de-oiled microalgal biomass: Kinetics and evolved gas analysis. Bioresour Technol 2016;221:251–61. doi:10.1016/j.biortech.2016.09.022.

[214] Bui HH, Tran KQ, Chen WH. Pyrolysis of microalgae residues - A Kinetic study. Bioresour Technol 2015;199:362–6. doi:10.1016/j.biortech.2015.08.069.

[215] Lee J, Lee K, Sohn D, Kim YM, Park KY. Hydrothermal carbonization of lipid extracted algae for hydrochar production and feasibility of using hydrochar as a solid fuel. Energy 2018;153:913–20. doi:10.1016/j.energy.2018.04.112.

[216] Liu H, Chen Y, Yang H, Gentili FG, Söderlind U, Wang X, et al. Hydrothermal carbonization of natural microalgae containing a high ash content. Fuel 2019;249:441–8. doi:10.1016/j.fuel.2019.03.004.

[217] Akarsu K, Duman G, Yilmazer A, Keskin T, Azbar N, Yanik J. Sustainable valorization of food wastes into solid fuel by hydrothermal carbonization. Bioresour Technol 2019;292:121959. doi:10.1016/j.biortech.2019.121959.

[218] Park KY, Lee K, Kim D. Characterized hydrochar of algal biomass for producing solid fuel through hydrothermal carbonization. Bioresour Technol 2018;258:119–24. doi:10.1016/j.biortech.2018.03.003.

[219] Fang J, Zhan L, Ok YS, Gao B. Minireview of potential applications of hydrochar derived from hydrothermal carbonization of biomass. J Ind Eng Chem 2018;57:15–21. doi:10.1016/j.jiec.2017.08.026.

[220] Zhang Z, Zhao Y, Wang T. Spirulina hydrothermal carbonization: Effect on hydrochar properties and sulfur transformation. Bioresour Technol 2020;306. doi:10.1016/j.biortech.2020.123148.

[221] Belete YZ, Leu S, Boussiba S, Zorin B, Posten C, Thomsen L, et al. Characterization and utilization of hydrothermal carbonization aqueous phase as nutrient source for microalgal growth. Bioresour Technol 2019;290:121758. doi:10.1016/j.biortech.2019.121758.

[222] Leng S, Li W, Han C, Chen L, Chen J, Fan L, et al. Aqueous phase recirculation during hydrothermal carbonization of microalgae and soybean straw: A comparison study. Bioresour Technol 2020;298:122502. doi:10.1016/j.biortech.2019.122502.

[223] Leng L, Li J, Wen Z, Zhou W. Use of microalgae to recycle nutrients in aqueous phase derived from hydrothermal liquefaction process. Bioresour Technol 2018;256:529–42. doi:10.1016/j.biortech.2018.01.121.

List of Publications

Peer-reviewed Journal (From thesis)**:**

1. **Mishra, S.**, Mohanty, K., 2019. Comprehensive characterization of microalgal isolates and lipid-extracted biomass as zero-waste bioenergy feedstock: An integrated bioremediation and biorefinery approach. Bioresour. Technol. 177–184. https://doi.org/10.1016/j.biortech.2018.11.012

2. **Mishra, S.**, Mohanty, K., 2020. Co-HTL of domestic sewage sludge and wastewater treatment derived microalgal biomass – An integrated biorefinery approach for sustainable biocrude production. Energy Convers. Manag. 204, 112312. https://doi.org/10.1016/j.enconman.2019.112312

3. **Mishra, S.**, Roy, M., Mohanty, K., 2019. Microalgal bioenergy production under zero-waste biorefinery approach: Recent advances and future perspectives. Bioresour. Technol. 292, 122008. https://doi.org/10.1016/j.biortech.2019.122008

Manuscripts under preparation:

1. Batch optimization of microalgal growth parameters in flasks and scale-up in PBR.

2. Scale-up study on integrated bioremediation and production of biodiesel, bioethanol and hydrochar to facilitate a self-sustainable microalgal biorefinery model

Peer-reviewed Journal (Others)**:**

Gebremedhin, M., **Mishra, S.**, Mohanty, K., 2018. Augmentation of native microalgae based biofuel production through statistical optimization of campus sewage wastewater as low-cost growth media. J. Environ. Chem. Eng. 6, 6623–6632.

Book Chapter

Mishra S., Mohanty K. (2015) Growth Characteristics of Different Algal Species. In: Das D. (ed.) Algal Biorefinery: An Integrated Approach. Springer, Cham.

Conference Presentations

1. **S. Mishra**, K. Mohanty*, *Lipid-extracted microalgal biomass as a substrate for enhancing algal wastewater treatment followed by bioenergy production*, International conference on Biotechnoly for Sustainable Agriculture, Environment and Health (BSAEH-2021), 04th to 08th April 2021, Malaviya National Institute of Technology, India.
2. **S. Mishra**, K. Mohanty*, *Hydrothermal liquefaction of microalgal biomass for sustainable biocrude oil production*, 3rd International conference on waste management (RECYCLE 2020), 13th to 14th February 2020, Indian Institute of Technology Guwahati, India.
3. **Mishra, S.**, Hasin M., Mohanty, K., *A self-sustainable microalgal biorefinery model that facilitates integrated bioremediation and production of biodiesel, bioethanol and hydrochar*, International conference on New Horizons in Biotechnology (NHBT 2019), 20th to 24th November 2019, CSIR-NIST, Kerala, India.
4. **Mishra, S.**, Mohanty, K., *Hydrolysis of lipid-extracted microalgal biomass and its application to augment integrated algal wastewater treatment and biofuel production*, 9th International Conference of Algal Biomass, Biofuel, Bioproducts, 17th to 19th July 2019, Boulder, Colorado, USA.
5. **Mishra, S.**, Mohanty, K., *Co-hydrothermal liquefaction of sewage sludge and sewage wastewater treatment derived microalgae biomass for biocrude production*, International conference on biotechnological research and innovation for sustainable development (BiosD) (XV annual convention of BRSI), 22th to 25th November 2018, CSIR-IICT, Hyderabad, India.
6. **Mishra, S.**, Sahu H., Mohanty, K., *Transesterification of microalgae lipid using heterogeneous catalyst: Process optimization and kinetic study*, International conference on emerging trends in biotechnology for waste conversion (XIV annual convention of BRSI), 8th to 10th October 2017, CSIR-NEERI, Nagpur, India.
7. **Mishra, S.**, Dasu V.V., Mohanty, K., *Nutrient removal by chlorella pyrenoidosa from artificial wastewater with simultaneous biomass production*. CHEMCON-2015, Indian Institute of Technology Guwahati, Assam, India.

Bioresource Technology 273 (2019) 177–184

Contents lists available at ScienceDirect

Bioresource Technology

journal homepage: www.elsevier.com/locate/biortech

Comprehensive characterization of microalgal isolates and lipid-extracted biomass as zero-waste bioenergy feedstock: An integrated bioremediation and biorefinery approach

Sanjeev Mishra[a], Kaustubha Mohanty[a,b,*]

[a] Centre for Energy, Indian Institute of Technology Guwahati, Guwahati 781039, India
[b] Department of Chemical Engineering, Indian Institute of Technology Guwahati, Guwahati 781039, India

GRAPHICAL ABSTRACT

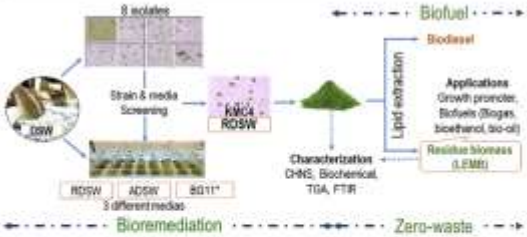

ARTICLE INFO

Keywords:
Microalgae
Wastewater treatment
Bioenergy feedstock
Lipid-extracted biomass
Biorefinery

ABSTRACT

The present study investigated the feasibility of domestic sewage wastewater (DSW) as an alternate to fresh-water microalgae growth media towards high-value bioenergy feedstock production. Eight native microalgal strains were screened from DSW and the effect of raw DSW (RDSW), and autoclaved DSW (ADSW) on growth and bioremediation potential were evaluated and compared with control BG11 medium. The study confirmed RDSW as a potential growth medium while *Monoraphidium* sp. KMC4 showed superior biomass ($1.47 \pm 0.08\ g\ l^{-1}$) and lipid yield ($436.01 \pm 0.06\ mg\ l^{-1}$). The corresponding values for bioremediation of ammonia, nitrate, phosphate, as well as COD remained within 88–100%. CHNS, biochemical, TGA, FTIR, FAME analysis of KMC4 confirmed it's potential as bioenergy feedstock. Additionally, a comprehensive characterization of lipid-extracted microalgae biomass (LEMB) was carried out which suggested that LEMB can be used as a growth promoter as well as feedstock for biogas, bioethanol, and bio-oil production.

1. Introduction

Bioenergy derived from microalgae is considered as one of the clean, green and sustainable energy resource and can be integrated into the biorefinery process (Guldhe et al., 2017a). However, high nutrients and fresh-water requirement are the critical constraints associated with the production of economically sustainable bioenergy feedstock from microalgae (Piligaev et al., 2018). In this context, wastewater with substantial pollutants such as nitrogen, phosphorous, and organic carbon is considered as potential growth media for microalgal growth. This approach can simultaneously address bioremediation and generate high-value biomass feedstock (García et al., 2018).

* Corresponding author at: Department of Chemical Engineering, Indian Institute of Technology Guwahati, Guwahati 781039, India.
E-mail address: kmohanty@iitg.ac.in (K. Mohanty).

https://doi.org/10.1016/j.biortech.2018.11.012
Received 17 September 2018; Received in revised form 31 October 2018; Accepted 4 November 2018
Available online 05 November 2018
0960-8524/

Energy Conversion and Management 204 (2020) 112312

Contents lists available at ScienceDirect

Energy Conversion and Management

journal homepage: www.elsevier.com/locate/enconman

Co-HTL of domestic sewage sludge and wastewater treatment derived microalgal biomass – An integrated biorefinery approach for sustainable biocrude production

Sanjeev Mishra[a], Kaustubha Mohanty[a,b,*]

[a] Centre for Energy, Indian Institute of Technology Guwahati, Guwahati 781039, India
[b] Department of Chemical Engineering, Indian Institute of Technology Guwahati, Guwahati 781039, India

ARTICLE INFO

Keywords:
Co-HTL
Microalgal biomass
Sewage sludge
Biocrude
Biorefinery

ABSTRACT

Microalgal biomass as bioenergy feedstock is gaining wide attention for biocrude production through hydrothermal liquefaction (HTL). However, the availability of feedstock in all seasons is a major challenge. Hence, to ensure a consistent supply of feedstock and transform waste to energy, the present study investigates co-HTL of domestic wastewater treatment derived microalgal biomass (*Monoraphidium* sp. KMC4) and domestic sewage sludge (DSS) as bioenergy feedstocks. The effects of temperature, feedstock ratio, and residence time were studied and optimised for maximum biocrude yield. The study showed that, co-HTL at optimum operating conditions of 325 °C, 75:25 wt% (KMC4:DSS), and 45 min produced 39.38 wt% biocrude yield at a conversion rate of 83.96 wt%. The optimum biocrude yield was 16% and 79% higher than the individual HTL of KMC4 and DSS respectively. The comprehensive characterizations of co-HTL biocrude showed 76.77%, 10.6%, 8.85%, 3.38% of C, H, N, O and 39.47 MJ Kg^{-1} of HHV with an energy recovery rate of 77.53%. Meanwhile, co-HTL enhanced the distillation profile of biocrude which had 10.13% of heavy naphtha, 23.92% of kerosene, and 27.09% of gas oil. The FTIR and GC–MS analysis confirmed that the co-HTL biocrude had superior hydrocarbons such as alcohols and esters with limited nitrogen and oxygen heterocyclic compounds. In addition, ICP-AES confirmed a significant decrease in transfer of mineral elements from the co-HTL feedstock to biocrude. This validates the sustainability of the co-HTL process to produce high energy density biocrude with the potential to substitute fossil fuels.

1. Introduction

Growing population and urbanization in the recent past has resulted in substantial consumption of carbon emitting fossil fuels, which are the primary sources of greenhouse gases, and its increased production has significantly affected the environment. Urbanization also produces a considerable amount of domestic sewage containing various organic and inorganic contaminants [1]. Therefore, it is necessary to develop a process that can resolve the escalating issues of energy security along with simultaneous wastewater treatment in a simple and efficient way. In this context, microalgal wastewater treatment is one of the clean, green, and sustainable process that can integrate with biofuel production under algal biorefinery approach [2–6]. Besides the traditional energy-intensive biodiesel and pyrolytic bio-oil; biocrude production through hydrothermal liquefaction (HTL) of wet microalgae slurry has gained attention in recent past [7–9]. Although, availability of feedstock in all seasons (comparatively less productivity in winter) is one of the major challenges for commercial HTL plant operation [10]. To resolve feedstock challenge, co-HTL of waste-derived biomass has potential for optimal plant operation along with enhanced biocrude productivity. However, selection of co-feedstock is vital to facilitate sustainable biorefinery approach [1,11].

Recently, co-HTL of microalgal biomass and various waste-derived biomass (lignocellulosic and food waste) feedstocks are studied that shown superior biocrude yield along with enhanced fuel property [8,12,13]. Co-liquefaction of microalgae and sweet potato waste (4:1 wt%) resulted in ~40% of biocrude yield and promoted energy recovery with high ester contents [14]. Another study achieved the maximum biocrude yield of ~34 wt% while the ratio was 5:1 wt% [15]. However, considering the above studies [14,15] and in addition to a few more reports on non-catalytic co-HTL had also shown relative less synergistic effects on biocrude yield [16,17]. Additionally, these

* Corresponding author.
E-mail address: kmohanty@iitg.ac.in (K. Mohanty).

https://doi.org/10.1016/j.enconman.2019.112312
Received 30 July 2019; Received in revised form 13 November 2019; Accepted 14 November 2019
Available online 21 November 2019
0196-8904/

Bioresource Technology 292 (2019) 122008

Contents lists available at ScienceDirect

Bioresource Technology

journal homepage: www.elsevier.com/locate/biortech

Review

Microalgal bioenergy production under zero-waste biorefinery approach: Recent advances and future perspectives

Sanjeev Mishra[a,1], Madonna Roy[a,1], Kaustubha Mohanty[a,b,*]

[a] Centre for Energy, Indian Institute of Technology Guwahati, Guwahati 781039, India
[b] Department of Chemical Engineering, Indian Institute of Technology Guwahati, Guwahati 781039, India

GRAPHICAL ABSTRACT

ARTICLE INFO

Keywords:
Microalgal biorefinery
Zero-waste
Circular economy
TEA
LCA

ABSTRACT

In view of the globalization and energy consumption, an economic and sustainable biorefinery model is essential to address the energy security and climate change. From this perspective, renewable biofuel production from microalgae along with a wide range of value-added co-products define its potential as a biorefinery feedstock. However, economic viability of microalgal biorefinery at its current state is not considered sustainable. Reduce, recycle, and reuse of waste derived from algal bioenergy conversion process will lead to an energy efficient and sustainable zero-waste microalgal biorefinery. This review focuses on three major aspects of zero-waste microalgal biorefinery approach; (1) recent advances on microalgal bioenergy conversion processes (chemical, biochemical and thermochemical); (2) mitigation and transformation of liquid and solid waste and (3) techno-economic analysis (TEA) and lifecycle assessment (LCA). In addition, the study also focuses on the challenges and future perspectives for an advanced microalgal biorefinery model.

1. Introduction

An ever-escalating global energy demand and global warming due to the burning of fossil fuels encourages the necessity for exploring and implementing alternate clean, green, and sustainable energy resources. Among several other renewable energy alternatives, bioenergy production from microalgae has acquired wide recognition over the last few years (Wijffels and Barbosa, 2010). However, commercialization of the process is a challenge considering current capital costs per unit of fuel production (Chandra et al., 2019). Given the background, high-value microalgal co-products should be explored for a sustainable bioefinery approach.

* Corresponding author at: Centre for Energy, Indian Institute of Technology Guwahati, Guwahati 781039, India.
E-mail address: kmohanty@iitg.ac.in (K. Mohanty).
[1] These authors contributed equally and should be regarded as co-first author.

https://doi.org/10.1016/j.biortech.2019.122008
Received 15 June 2019; Received in revised form 9 August 2019; Accepted 12 August 2019
Available online 16 August 2019
0960-8524/